

ผลของสภาพอากาศแบบเร่งต่อสมบัติเชิงกลและสัณฐานวิทยาของวัสดุเชิงประกอบ

เส้นใยหญ้าแฝก/พอลิเอไมด์-6



นางชนิษฐกัญญา หมั่นคิด

ศูนย์วิทยพัทยากร

วิทยานิพนธ์นี้เป็นส่วนหนึ่งของการศึกษาตามหลักสูตรปริญญาวิทยาศาสตรมหาบัณฑิต
สาขาวิชาปิโตรเคมีและวิทยาศาสตร์พอลิเมอร์ หลักสูตรปิโตรเคมีและวิทยาศาสตร์พอลิเมอร์

คณะวิทยาศาสตร์ จุฬาลงกรณ์มหาวิทยาลัย

ปีการศึกษา 2553

ลิขสิทธิ์ของจุฬาลงกรณ์มหาวิทยาลัย

ACCELERATED WEATHERING EFFECTS ON MECHANICAL
PROPERTIES AND MORPHOLOGY OF VETIVER GRASS
FIBER/POLYAMIDE-6 COMPOSITES

Mrs. Khanitthakanya Munkid



ศูนย์วิทยทรัพยากร
จุฬาลงกรณ์มหาวิทยาลัย

A Thesis Submitted in Partial Fulfillment of the Requirements
for the Degree of Master of Science Program in Petrochemistry and Polymer Science

Faculty of Science


Chulalongkorn University

Academic Year 2010

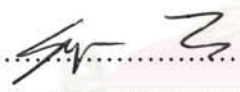
Copyright of Chulalongkorn University

Thesis Title ACCELERATED WEATHERING EFFECTS ON MECHANICAL
PROPERTIES AND MORPHOLOGY OF VERTIVER GRASS
FIBER/POLYAMIDE-6 COMPOSITES
By Mrs. Khanitthakanya Munkid
Field of Study Petrochemistry and Polymer Science
Thesis Advisor Professor Pattarapan Prasassarakich, Ph.D.


Accepted by the Faculty of Science, Chulalongkorn University in Partial
Fulfillment of the Requirements for the Master's Degree



..... Dean of the Faculty of Science
(Professor Supot Hannongbua, Dr.rer.nat.)

THESIS COMMITTEE


.....Chairman
(Associate Professor Supawan Tantayanon, Ph.D.)


.....Thesis Advisor
(Professor Pattarapan Prasassarakich, Ph.D.)


.....Examiner
(Associate Professor Wimonrat Trakarnpruk, Ph.D.)


.....External Examiner
(Dr. Suwadee Kongparakul, Ph.D.)

ขนิษฐกัญญา หมั่นคิด: ผลของสภาพอากาศแบบเร่งต่อสมบัติเชิงกลและสัณฐานวิทยาของ วัสดุเชิงประกอบเส้นใยหญ้าแฝก/พอลิเอไมด์-6 (ACCELERATED WEATHERING EFFECTS ON MECHANICAL PROPERTIES AND MORPHOLOGY OF VETIVER GRASS FIBER/POLYAMIDE-6 COMPOSITES) อ.ที่ปรึกษาวิทยานิพนธ์หลัก: ศ.ดร. ภัทรพรรณ ประศาสน์สารกิจ, 93 หน้า

ในงานวิจัยนี้ทำการประเมินผลการใช้เส้นใยธรรมชาติในวัสดุเชิงประกอบพอลิเอไมด์-6 เพื่อวัตถุประสงค์การแทนที่เส้นใยสังเคราะห์ การประยุกต์ใช้เส้นใยธรรมชาติสำหรับเสริมความแข็งแรงในวัสดุเชิงประกอบ ต้องการความแข็งแรงของการยึดติดระหว่างเส้นใยและเมทริกซ์สังเคราะห์ ในงานวิจัยนี้ทำการปรับปรุงพื้นผิวเส้นใยหญ้าด้วยวิธีเมอเซไรเซชัน และการใช้สารควบคู่โซเลน วัสดุเชิงประกอบพอลิเอไมด์-6 ที่เสริมความแข็งแรงด้วยเส้นใยหญ้าแฝก ในปริมาณเส้นใยหญ้าแฝก 15% และ 30% ทำการเตรียมโดยการใช้เครื่องหลอมพลาสติก 2 สกรู จากนั้นทำการศึกษาสมบัติเชิงกล สัณฐานวิทยา และความคงทนในระยะยาวของวัสดุเชิงประกอบพอลิเอไมด์-6 ที่เสริมความแข็งแรงด้วยเส้นใยหญ้า โดยเปรียบเทียบกับวัสดุเชิงประกอบทลคัม และวัสดุเชิงประกอบเส้นใยแก้ว วัสดุเชิงประกอบพอลิเอไมด์-6 ที่เสริมความแข็งแรงด้วยเส้นใยหญ้าแฝกที่ทำการปรับปรุงด้วยการใช้สารควบคู่โซเลน ปรับปรุงสมบัติได้ดีกว่าเมื่อเทียบกับเส้นใยหญ้าแฝกที่ปรับปรุงด้วยวิธีเมอเซไรเซชัน การเปรียบเทียบสมบัติการทนแรงดึงของวัสดุเชิงประกอบพอลิเอไมด์-6 ที่เสริมความแข็งแรงด้วยเส้นใยหญากับวัสดุเชิงประกอบที่ไม่ได้เสริมความแข็งแรง พบว่าการปรับปรุงเส้นใยหญ้าด้วยวิธีเมอเซไรเซชัน และการใช้สารควบคู่โซเลน ทำให้มีการเพิ่มขึ้นอย่างมีนัยสำคัญในค่าการทนแรงดึง จากผลการทดลองยังพบว่าการปรับปรุงเส้นใยหญ้าด้วยวิธีเมอเซไรเซชัน และการใช้สารควบคู่โซเลนทำให้มีการเพิ่มขึ้นอย่างมีนัยสำคัญของค่าการคดโค้งและค่ามอดูลัสคดโค้ง ของวัสดุเชิงประกอบพอลิเอไมด์-6 ที่เสริมความแข็งแรงด้วยเส้นใยหญ้า ภายหลังจากผ่านสภาพอากาศแบบเร่ง พบว่าวัสดุเชิงประกอบพอลิเอไมด์-6 ที่เสริมความแข็งแรงด้วยเส้นใยหญ้า สามารถรักษาอัตราส่วนในการลดลงของสมบัติเชิงกลตั้งต้นที่สูงกว่าวัสดุเชิงประกอบที่ไม่ได้ทำการเสริมแรง วัสดุเชิงประกอบทลคัม และวัสดุเชิงประกอบเส้นใยแก้ว

สาขาวิชา ปิโตรเคมีและวิทยาศาสตร์พอลิเมอร์ ลายมือชื่อนิติด.....

ปีการศึกษา 2553

ลายมือชื่ออ.ที่ปรึกษาวิทยานิพนธ์หลัก.....

5173409623 : MAJOR PETROCHEMISTRY AND POLYMER SCIENCE

KEYWORDS : ACCELERATED WEATHERING / VETIVER GRASS FIBER /
POLYAMIDE-6 COMPOSITES

KHANITTHAKANYA MUNKID: ACCELERATED WEATHERING
EFFECTS ON MECHANICAL PROPERTIES AND MORPHOLOGY OF
VETIVER GRASS FIBER/POLYAMIDE-6 COMPOSITES. ADVISOR:
PROF. PATTARAPAN PRASASSARAKICH, Ph.D., 93 pp.

This research evaluates the use of natural fiber in polyamide-6 composites aiming to synthetic fiber replacement. The application of natural fiber as reinforcement in composite materials requires a strong adhesion between fiber and the synthetic matrix. In this work, the surface treatments were mercerization and applying the silane coupling agent. The Vetiver grass fiber reinforced polyamide-6 composites at various contents of Vetiver grass fiber (15 and 30%) were prepared by using twin screw extruders. The mechanical properties, morphology and long term stability of Vetiver grass fiber reinforced polyamide-6 were investigated and compared with talc filled and glass fiber reinforced composites. Polyamide-6 composites reinforced with grass fiber treated with silane coupling agent had improved properties compared with grass fiber treated by mercerization. The comparison of tensile properties of the treated grass fiber reinforced polyamide-6 composites with unfilled composite showed that the mercerization and silane coupling agent of treated grass fiber gave a significant increase in tensile strength. The results also showed that the mercerization and silane coupling agent could significantly improved the flexural strength and modulus of grass fiber reinforced composites. After accelerated weathering, grass fiber reinforced polyamide-6 composites retained a higher fraction of the original mechanical properties than unfilled, talc filled and glass fiber reinforced composites.

Field of Study: Petrochemistry and Polymer Science Student's Signature

Academic Year: 2010

Advisor's Signature

ACKNOWLEDGMENTS

The author wishes to express her deepest gratitude to her advisor, Professor Dr. Pattarapan Prasassarakich for their guidance, encouragement and helpful suggestion throughout this research. In addition, the author is also grateful to the members of the thesis committee for their comments and suggestions.

The author also wish to express thanks for kind support from Nylon R&D Section of UBE Technical Center (Asia) Limited, R&D Section of IRPC PCL, Mettler-Toledo (Thailand) Limited, Program of Petrochemical and Polymer Science, Faculty of Science, NCE-PPAM, Chulalongkorn University.

Thanks go to her friends and everyone whose names are not mentioned here for their suggestions, assistances, advices concerning the experimental techniques and the encouragement during the period of this research.

Finally, and most of all, the author would like to express her deep gratitude to her family for their tender, love, care, inspiration and encouragement.



ศูนย์วิทยทรัพยากร
จุฬาลงกรณ์มหาวิทยาลัย

CONTENTS

	Page
ABSTRACT (IN THAI)	iv
ABSTRACT (ENGLISH)	v
ACKNOWLEDGMENTS	vi
CONTENTS.....	vii
LIST OF TABLES	x
LIST OF FIGURES	xi
CHAPTER I: INTRODUCTION.....	1
1.1 The Purpose of the Investigation	1
1.2 Objectives	1
1.3 Scope of the Investigation	2
CHAPTER II: THEORY AND LITERATURE REVIEW	3
2.1 Polyamide-6.....	3
2.2 Fibrous Reinforcement	5
2.2.1 Glass Fibers	5
2.2.2 Carbon/Graphite Fibers	5
2.2.3 Other Fibers	6
2.2.4 Mechanism of Reinforcement	7
2.3 Natural Fibers	10
2.3.1 Structure of Natural Fiber.....	10
2.3.2 Hydrophilic Character of Natural Fibers.....	11
2.3.3 Processing Techniques of Natural Fibers.....	11
2.4 Pretreatments of Natural Fibers.....	12
2.4.1 Mercerization of Natural Fibers	12
2.4.2 Silane Coupling Agent onto Natural Fibers	12

	Page
2.5 Degradation of Nylons	14
2.5.1 Hydrolysis	14
2.5.2 Thermal Degradation.....	16
2.5.3 Oxidative Degradation.....	21
2.5.3.1 Thermooxidative Degradation.....	21
2.5.3.2 Photooxidation.....	23
2.6 Literature Reviews.....	27
CHAPTER III: EXPERIMENTAL.....	30
3.1 Materials.....	30
3.2 Instruments	31
3.3 Fiber Preparation	31
3.4 Fiber Characterization	32
3.5 Composites Preparation.....	32
3.6 Accelerated Weathering Test	33
3.6.1 Xenon Weather Meter	33
3.6.2 Sunshine Weather Meter	34
3.7 Mechanical Properties Study.....	34
3.7.1 Tensile Properties	34
3.7.2 Flexural Properties.....	35
3.7.3 Charpy Impact Strength.....	35
3.8 Density.....	36
3.9 Morphological Study.....	36
CHAPTER IV: RESULTS AND DISCUSSION.....	37
4.1 Characterization of Vetiver Grass Fiber.....	37
4.2 Vetiver Grass Fiber/Polyamide-6 Composites	38
4.2.1 Mechanical Properties	38
4.2.2 Morphology	42

	Page
4.3 Accelerated Weathering: Xenon Weathering.....	44
4.3.1 Mechanical Properties	44
4.3.2 Retention	52
4.3.3 Morphology	58
4.4 Accelerated Weathering: Sunshine Weathering.....	62
4.4.1 Mechanical Properties	62
4.4.2 Retention.....	70
4.4.3 Comparison of Accelerated Weathering: Xenon Weathering Meter and Sunshine Weathering Meter	71
4.4.4 Morphology	77
CHAPTER V: CONCLUSION.	79
5.1 Conclusion.....	79
5.2 Suggestion for Future Work	80
REFERENCES.	81
APPENDICES	83
VITA.....	93

ศูนย์วิทยทรัพยากร
จุฬาลงกรณ์มหาวิทยาลัย

LIST OF TABLES

Table	Page
2.1 Worldwide PA-6 Fiber Production Capabilities (Estimated Capacities in 1,000 Metric Tons).....	4
3.1 Chemicals used in this study	30
3.2 Instrument used in this study	31
3.3 Composition of polyamide-6 composites (wt%).....	33
4.1 Mechanical properties and density of composites after conditioning at 23 °C and 50 %RH for 24 h.....	39
4.2 Tensile properties and retention of composites after accelerated weathering in Xenon weathering meter for 1000 h.....	46
4.3 Flexural properties, Charpy impact strength and retention of composites after accelerated weathering in Xenon weathering meter for 1000 h.....	47
4.4 Tensile properties and retention of composites after accelerated weathering in sunshine weathering meter for 1000 h.....	64
4.5 Flexural properties, Charpy impact strength and retention of composites after accelerated weathering in sunshine weathering meter for 1000 h.....	65
A-1 Density of composites	84
B-1 Tensile strength and elongation at break of composites.....	85
B-2 Tensile modulus of composites	86
B-3 Flexural properties of composites	87
B-4 Charpy Impact Strength of composites	88
C-1 Tensile strength and elongation at break of composites.....	89
C-2 Tensile modulus of composites	90
C-3 Flexural properties of composites	91
C-4 Charpy Impact Strength of composites	92

LIST OF FIGURES

Figure	Page
2.1 Structure of natural fiber	10
2.2 Photooxidation pathways for nylons	25
2.3 Photooxidation of N-alkyl amides.....	26
3.1 Vetiver grass fiber (a) Untreated (b) Mercerization treated and (c) Silane coupling agent treated.....	32
3.2 Tensile test specimen.....	34
3.3 Flexural test specimen	35
3.4 Charpy impact strength test specimen.....	35
4.1 TGA and DTG curves of Vetiver grass fiber	38
4.2 Mechanical properties composites after conditioning at 23 °C and 50 %RH for 24 h (a) tensile strength of PA, PA/V15-N, PA/V15-S, PA/V30-N, PA/V30-S and PA/T30 (b) tensile strength of PA/V15-S/GF15, PA/GF15 and PA/GF30 (c) flexural strength of PA, PA/V15-N, PA/V15-S, PA/V30-N, PA/V30-S and PA/T30 (d) flexural strength of PA/V15-S/GF15, PA/GF15 and PA/GF30 (e) Charpy impact strength of PA, PA/V15-N, PA/V15-S, PA/V30-N, PA/V30-S and PA/T30 (f) Charpy impact strength of PA/V15-S/GF15, PA/GF15 and PA/GF30.....	41
4.3 SEM micrographs of composites after conditioning at 23 °C and 50 %RH for 24 h: (a) PA/V15-N, (b) PA/V15-S, (c) PA/V30-N (d) PA/V30-S and (e) PA/V15-S/GF15 (X500 magnification, scale bar = 50 μm).....	43
4.4 Tensile strength of composites after accelerated weathering in Xenon weathering meter 1000 h (a) PA, PA/V15-N, PA/V15-S, PA/V30-N, PA/V30-S and PA/T30 (b) PA/V15-S/GF15, PA/GF15 and PA/GF30.....	48
4.5 Modulus of composites after accelerated weathering in Xenon weathering meter for 1000 h (a) tensile modulus (b) flexural modulus.....	49
4.6 Flexural strength of composites after accelerated weathering in Xenon weathering meter for 1000 h (a) PA, PA/V15-N, PA/V15-S, PA/V30-N, PA/V30-S and PA/T30 (b) PA/V15-S/GF15, PA/GF15 and PA/GF30.....	50

Figure	Page
4.7 Charpy impact strength of composites after accelerated weathering in Xenon weathering meter for 1000 h (a) PA, PA/V15-N, PA/V15-S, PA/V30-N, PA/V30-S and PA/T30 (b) PA/V15-S/GF15, PA/GF15 and PA/GF30.....	53
4.8 Tensile strength retention of composites after accelerated weathering in Xenon weathering meter for 1000 h (a) PA, PA/V15-N, PA/V15-S, PA/V30-N, PA/V30-S and PA/T30 (b) PA/V15-S/GF15, PA/GF15 and PA/GF30.....	54
4.9 Elongation at break retention of composites after accelerated weathering in Xenon weathering meter for 1000 h (a) PA, PA/V15-N, PA/V15-S, PA/V30-N, PA/V30-S and PA/T30 (b) PA/V15-S/GF15, PA/GF15 and PA/GF3.....	55
4.10 Flexural strength retention of composites after accelerated weathering in Xenon weathering meter for 1000 h (a) PA, PA/V15-N, PA/V15-S, PA/V30-N, PA/V30-S and PA/T30 (b) PA/V15-S/GF15, PA/GF15 and PA/GF30.....	56
4.11 Impact strength retention of composites after accelerated weathering in Xenon weathering meter for 1000 h (a) PA, PA/V15-N, PA/V15-S, PA/V30-N, PA/V30-S and PA/T30 (b) PA/V15-S/GF15, PA/GF15 and PA/GF30.....	57
4.12 SEM micrographs of composites accelerated weathering in Xenon weathering meter for 1000 h: (a) PA/V15-N, (b) PA/V15-S, (c) PA/V30-N, (d) PA/V30-S and (e) PA/V15-S/GF15 (X500 magnification, scale bar = 50 μ m).....	61
4.13 Tensile strength of composites after accelerated weathering in sunshine weathering meter 1000 h (a) PA, PA/V15-N, PA/V15-S, PA/V30-N, PA/V30-S and PA/T30 (b) PA/V15-S/GF15, PA/GF15 and PA/GF30.....	66
4.14 Modulus of composites after accelerated weathering in sunshine weathering meter 1000 h (a) tensile modulus (b) flexural modulus	67
4.15 Flexural strength of composites after accelerated weathering in sunshine weathering meter 1000 h (a) PA, PA/V15-N, PA/V15-S, PA/V30-N, PA/V30-S and PA/T30 (b) PA/V15-S/GF15, PA/GF15 and PA/GF30.....	68
4.16 Charpy impact strength of composites after accelerated weathering in sunshine weathering meter 1000 h (a) PA, PA/V15-N, PA/V15-S, PA/V30-N, PA/V30-S and PA/T30 (b) PA/V15-S/GF15, PA/GF15 and PA/GF30.....	69

Figure	Page
4.17 Tensile strength retention of composites after accelerated weathering in sunshine weathering meter for 1000 h (a) PA, PA/V15-N, PA/V15-S, PA/V30-N, PA/V30-S and PA/T30 (b) PA/V15-S/GF15, PA/GF15 and PA/GF30	73
4.18 Elongation at break retention of composites after accelerated weathering in sunshine weathering meter for 1000 h (a) PA, PA/V15-N, PA/V15-S, PA/V30-N, PA/V30-S and PA/T30 (b) PA/V15-S/GF15, PA/GF15 and PA/GF30	74
4.19 Flexural strength retention of composites after accelerated weathering in sunshine weathering meter for 1000 h (a) PA, PA/V15-N, PA/V15-S, PA/V30-N, PA/V30-S and PA/T30 (b) PA/V15-S/GF15, PA/GF15 and PA/GF30	75
4.20 Impact strength retention of composites after accelerated weathering in sunshine weathering meter for 1000 h (a) PA, PA/V15-N, PA/V15-S, PA/V30-N, PA/V30-S and PA/T30 (b) PA/V15-S/GF15, PA/GF15 and PA/GF30	76
4.21 SEM micrographs of composites accelerated weathering in sunshine weathering meter for 1000 h: (a) PA/V15-N, (b) PA/V15-S, (c) PA/V30-N, (d) PA/V30-S and (e) PA/V15-S/GF15 (X500 magnification, scale bar = 50 μ m).....	78

CHAPTER I

INTRODUCTION

1.1 The Purpose of the Investigation

Natural fibers, because of their low cost, low density and low abrasion, and excellent mechanical properties, are attractive alternatives to the more expensive glass fibers largely used to reinforce plastics. Natural fiber-based composites constitute a recent family of materials for industrial applications. Taking into account of the low density of these natural fibers, their specific stiffness and strength are comparable to those of glass fiber [1]. On the other hand, their disadvantages are: low degradation temperature; high moisture absorption; large volume (low apparent density); low compatibility with polymer matrices; manual and seasonal production [2]. However, lack of good interfacial adhesion, low melting point, and poor resistance towards moisture make the use of natural fiber reinforced composites less attractive. Pretreatments of the natural fiber can clean the fiber surface, chemically modify the surface, stop the moisture absorption process, and increase the surface roughness [3].

Vetiver grass is a tropical plant which grows naturally. In Thailand, Vetiver grass can be found growing in a wide range of area from highlands to lowlands in various soil conditions. The species which is most common in Thailand is referred to scientific term as *Vetiveria zizanioides*. This specie appears in a dense clump and grows fast through tillering. The clump diameter is about 30 cm and the height is 50 - 150 cm. The leaves are erect and rather stiff with 75 cm of length and 8 mm of width [4].

1.2 Objectives

The objectives of this research are as follows:

1. To prepare the Vetiver grass fiber reinforced polyamide-6 composites using twin screw extruder at various contents of Vetiver grass fibers (15 and 30%).
2. To investigate the mechanical properties and morphology of composites by scanning electron microscopy.

3. To investigate the long term stability of Vetiver grass fiber reinforced polyamide-6 composites compared with talc filled and glass fiber reinforced composites.

1.3 Scope of the Investigation

Vetiver grass fibers were improved by the chemical treatment, mercerization and silane coupling agent and the treated fiber reinforced polyamide-6 composites were prepared by twin screw extruder at various contents of Vetiver grass fibers. The effect of chemical treatment and fiber content on mechanical properties, morphology and long term stability by accelerated weathering were investigated.

The experimental procedures were carried out as follows:

1. Survey literature and study the research work.
2. Prepare the treated Vetiver grass fiber by mercerization (5 wt% NaOH) and applying silane coupling agent (1.0% w/w vinyltriethoxysilane and 0.5% w/w dicumyl peroxide).
3. Prepare the treated Vetiver grass fiber reinforced polyamide-6 composites by using twin screw extruder at various contents of Vetiver grass fiber.
4. Prepare test specimen of the treated Vetiver grass fiber reinforced polyamide-6 composites, unfilled composite, talc filled composite and the glass fiber reinforced composites by using injection molding machine.
5. Study the accelerated weathering effects by using sunshine weathering meter (Open flame carbon arc) and Xenon weathering meter (Xenon arc lamp) for 1000 hour.
6. Investigate the morphology of fracture test specimen after tensile test by scanning electron microscope (SEM).
7. Investigate the mechanical properties of grass fiber reinforced polyamide-6 composites, unfilled, talc filled composite and the glass fiber reinforced composites.
8. Summarize the results.

CHAPTER II

THEORY AND LITERATURE REVIEWS

2.1 Polyamide-6 [5]

Polyamide-6 is high performance semi-crystalline thermoplastics with attractive physical and mechanical properties that provide a wide range of end-use performances important in many industrial applications. Much of the recent growth in nylon has been found in automotive, where nylon made parts are gradually replacing metals (various steels and light alloys, aluminum and magnesium based), and in some case expensive plastics, including various Thermosets. All nylons are hygroscopic (moisture sensitive), which is an important factor to be considered during material pre-selection, parts design, mechanical performance prediction and optimization.

PA-6 occupies a prominent place in the engineering thermoplastics family because of its broad processing range and the relative ease with which the base polymer can be modified to achieve a wide spectrum of properties. Processing techniques include injection, blow and rotational molding, extrusion, and wire jacketing. Products have been formulated for applications requiring high load bearing capability at elevated temperatures or good low temperature toughness; very high or low levels of flexibility; resistance to wear, abrasion, and chemical attack.

The combination of property balances, enhanced processability, excellent surface appearance, and pigmentability creates for PA-6 a high level of product value

One of the earliest references to poly- ϵ -caproamide (PA-6) can be found in the investigative studies of S. Gabriel and T.A. Mass (1899) at the University of Berlin. They were studying seven-membered heterocyclic compounds and noted the formation of a thick, gelatinous, brownish mass on heating ϵ -caprolactam. Much later, Carothers, in his search for a synthetic polymer capable of being spun into fibers, studied various types of polyamides. He worked with ϵ -aminocaproic acid and noted that on heating it formed a high polymer. He focused his attention, however, on polyamides formed from dibasic acids and diamines that eventually led to the commercialization of PA-66. Paul Schlack and co-workers at I.G. Farben

demonstrated that caprolactam polymerizes on heating above 180°C in the presence of compounds with active hydrogen, especially water, alcohol, and carboxylic acids, and also with alkali hydroxides and amine bases. By 1938, I.G. Farben was spinning polycapramide fibers. Bristles of PA-6 were sold under the name “Perluran”.

The production of PA-6 did not expand much until after World War II and remained largely confined to Germany. Since the end of that war global production capability has multiplied several folds. Current global production capacity for PA-6 fiber is estimated at 3.3 million metric tons. Table 2.1 provides a regional breakdown of PA-6 capacities estimated for 1993 and projected to 2001. Allied Signal was the first company to manufacture PA-6 in the United States. Their plant commenced production in 1954 with an installed capacity of 10,900 mt (100% fiber until about 1958). Allied Signal’s 1993 nameplate capacity exceeds 270,000 mt per year. There are eight producers of PA-6 in the United States with 1993 total annual capacity in excess of 600,000 mt.

PA-6 and PA-66 together account for the major portion of nylons consumed as engineering plastics. The relative proportion of PA-6 to PA-66 used for plastics applications varies in different regions in the world. In the United States, the PA-66/PA-6 usage ratio is approximately 2:1, whereas in Japan it is 1:1.5, and in Europe and the rest of the world, it is approximately 1:1.

Table 2.1 Worldwide PA-6 Fiber Production Capabilities
(Estimated Capacities in 1,000 Metric Tons) [5]

	1993	2001
United States/Canada	576	576
Latin America	171	181
Western Europe	394	406
Eastern Europe	722	730
Japan	289	289
Asia (excluding Japan)	1,020	1,346
Middle East and Africa	84	97
	<u>3,256</u>	<u>3,625</u>

Asia (excluding Japan) is anticipated to show the highest growth rate in PA-6 capacity between 1993 and 2001.

2.2 Fibrous Reinforcement [5]

2.2.1 Glass Fibers [5]

The high tensile strength of glass fiber is preserved when they are coated immediately after fiber drawing. Thereafter, glass strength is reduced by abrasive contacts. “E” fiber glass is widely used because of its low cost. It provides a good combination of mechanical, chemical, and electrical properties. It is available as continuous strand, chopped to 3 mm (0.12 in.), 6 mm (0.24 in.), or 13 mm (0.51 in.) lengths, or milled to < 1 mm (0.039 in.). Specialty glasses including “S” glass for higher strength, “D” for lower dielectric loss, “A” for improved acid resistance, and fused silica for higher temperature resistance are costly alternatives. Specialty glasses are seldom used in nylon injection molding resins but are being used in nylon pultrusions. Chopper fiber glass is available in two standard filament diameters, G-filament at 9.5 μm and K-filament at 13 μm . Best reinforcements require a coating that bonds to the matrix and a sizing to maintain fiber bundles during feeding.

Long fiber glass reinforcement in PA-6, PA-66, and PA-46 is available via melt pultrusion, stranding, and long-cut pelletizing. Pellet lengths up to 13 mm are commercially available providing fiber aspect ratios over 1,000:1. Care in molding is necessary to avoid excessive fragmentation. Appropriately molded long glass nylons have higher tensile and impact strengths and exhibit less anisotropy. Ingression molding (a modified injection molding process) maintained up to 75% of original glass length.

Reinforced reaction injection molding (RRIM) uses milled glass fibers because they are easily processed, but they find limited use in injection molding because of minimal effect on key properties. Glass flakes are available for use in planar composites when reduced permeability is more important than tensile strength.

2.2.2 Carbon/Graphite Fibers [5]

Carbon and graphite fibers have a higher strength and modulus than glass fibers and yield correspondingly superior compositions. They are significantly more costly; for example, graphite fibers cost about 20 times as much as “E” glass. Early graphite fibers had no surface treatment to promote bonding to the resin matrix.

Some of the high strength and stiffness advantage over fiber glass was lost. Currently, graphite fibers are available with and without surface treatment. Composite properties are obviously affected by the surface treatment, so it, as well as the type of C-fiber, are important. Graphite fiber is typically made from a polyacrylonitrile (PAN) precursor that has been drawn and graphitized at high temperatures (2,000 °C to 3,000 °C). Carbon fiber is manufactured via a similar process, but the PAN is carbonized at lower temperature (1,200 °C to 1,800 °C) which results in a lower modulus, higher strength fiber.

Carbon fiber may also be made from a low-cost, coal-tar pitch, but the resulting product has a less regular size and shape and is a less effective reinforcement. Selection of a carbon (or graphite) fiber depends on the property profile desired in the nylon product and its value-in-use. Cost is partially offset by a “C” fiber/glass density ratio of 0.7:1. C-fiber production capacity grew rapidly in the 1980s to 8,600 metric tons worldwide but is still very small compared to that of the fiber glass (over 300,000 tones in the United States).

2.2.3 Other Fibers [5]

Other fibers sometimes used in nylon include ceramic, metal, and polymeric fibers, and these are discussed in the following paragraphs. A variety of ceramic fibers and whiskers are available but are not widely used. Calcium sulfate and aluminum silicate fibers are lower in cost (about half) than glass fibers but standard, unbundled fibers pose feeding problems. Potassium titanate fibers/whiskers serve as reinforcing pigments (white) by offering high stiffness and high refractive index at a cost premium. Processed mineral fibers, made from steel mill slag, offer low-cost reinforcement with intermediate mechanical properties compared to equal fiber glass content. Cermet (ceramic-metal) whiskers offer very high stiffness at a correspondingly high cost.

Metal fibers modify electrical, thermal, and mechanical properties. They are often used to produce slightly conductive, electrostatic discharge (ESD) compounds or more highly conductive electromagnetic interference (EMI) shielding materials. Stainless steel (S.S.) fibers are available for such applications. EMI shielding improves as volume resistivity is decreased by addition of low levels of S.S. fiber. Like glass fibers, stainless steel fibers require mild compounding to minimize

fiber attrition, which rapidly reduces shielding efficiency. Metal-coated glass or graphite fibers are available where combinations of good electrical, thermal, and mechanical properties are needed. Exotic fibers for extreme strength, stiffness, and high temperature performance include boron, Hastelloy, chromel, and tungsten, the latter costing several hundred times more than “E” glass. These exotic fibers are seldom employed in nylon.

To be a candidate for reinforcing nylon, a polymeric fiber must have a melting point above that of nylon. Aramid fibers meet this requirement and provide interesting reinforcing properties but need special processing to assure fully wetted surfaces and maximum reinforcing action. Polytetrafluoroethylene (PTFE) powder or fiber with a melt point of 327 °C is often used to modify the friction and wear characteristics of engineering resins. The super high molecular mass (over 10,000,000) and low modulus of PTFE fibers permit processing temperatures approaching 300 °C without sacrificing the physical structure. Liquid crystal polymers (LCP) may become useful candidates as their availability improves. Polyetheretherketone (PEEK) and polybenzimidazole (PBI) fibers have recently become available but at very high cost. PBI possesses unique high-temperature performance along with superior chemical resistance.

2.2.4 Mechanism of Reinforcement [5]

Basic factors in reinforcement are fiber strength, stiffness, aspect ratio, coupling to the matrix, orientation, and concentration. The “rule of mixtures” serves as a guide to the effect of filler or reinforcement on properties. The degree to which fillers and fibers can fill the volume of a composite, that is, the packing fraction, is also of interest and concludes the following discussion.

The rule of mixtures predicts a linear change in properties with volume fraction of reinforcement and is often used as a first estimate for filled/reinforced polymers. It states that the property of the composite is equal to the sum of the products of the volume fraction of each component multiplied by its value for that property. The rule of mixtures applies best to non-directional properties of composites such as specific volume, specific heat, refractive index, and dielectric constant. Mechanical properties exhibit nonlinearity at higher filler levels and with anisotropic (fiber-reinforced) composites. The tensile strength of injection molded nylon, for

example, increases with fiber glass content up to about 45 wt% and then asymptotically approaches a chopped fiber limit near 60 wt%. Compressive strength shows a similar response but moduli show a continuous increase. Tensile properties increase with fiber length; hence, continuous-fiber pultruded pellets extend strength limits to higher loadings. Nylon prepreg tape (pultruded) presents an upper limit guideline to reinforced nylon properties. Because of elastic interactions between matrix and filler, composite elastic properties differ from those predicted via the rule of mixtures. Physical model predictions require two independent elastic constants (e.g., shear modulus and bulk modulus) for the matrix resin and each additive. Two coupled equations involving bulk moduli and shear moduli give predictions for filled, isotropic composites.

Injection molding caused fiber attrition such that molded products have aspect ratios that are typically in the range of 20:1 to 40:1. The strengthening effects of fiber reinforcement increase with aspect ratio asymptotically approaching a limit near L/D of 400:1. A critical (minimum) aspect ratio can be defined as a function of interfacial bond strength and fiber characteristics. Perfect chemical coupling would provide interface bond strength equal to the matrix shear strength which is about 60 MPa for PA-66. This corresponds to a critical aspect ratio of 18:1 for glass-fiber-reinforced PA-66. For G-glass filaments, which have a 9.5 μm diameter, the critical fiber length is, therefore, 170 μm . Larger fibers obviously require a longer fiber length. For a K-glass fiber with a diameter of 13 μm the critical fiber length is 230 μm , and this has been confirmed for well-bonded fibers in PA-66. Incomplete wetting of individual fibers within bundles lowers the average interface bond strength and increases the critical aspect ratio. For this reason, a threefold increase in aspect ratio is often used as a guideline (i.e., 50:1 minimum aspect ratio).

Standard fiber reinforcements are cylindrical. New glass products with oval, bi-, and tri-bodal cross-sections, akin to polymeric fibers, are under development. They are expected to yield higher composite strengths because of higher surface-to-volume ratios with implications for revised critical aspect ratios.

Surface treatment of mineral fillers acts both as a coupling agent and as a processing aid by assisting dispersion, mixing, and breaking of agglomerates during compounding. One of the key factors determining the final properties of a reinforced material is the degree of coupling or bond strength of the fiber to the resin matrix. A certain minimal strength can be expected from a purely mechanical effect, the

shrinkage of matrix resin around the fiber. The strength of reinforcing fiber cannot be truly harnessed and transmitted to the composite unless the bond strength is high and of a chemical nature. NASA found pre-coating graphite fibers with a dilute solution of the matrix polymer increased strength and stiffness by over 20%. Polymers resistant to solvents can be impregnated onto continuous fibers as a low viscosity melts using a crosshead extruder. Coating powder impregnation permits wetting of the fiber strands prior to heating, pressurizing, and cooling.

Bifunctional coupling agents are used to bond the filler/reinforcement and the resin matrix. A typical bonding agent is characterized by an alkoxy silane at one end, which provides adhesion to the glass or highly polar filler, and a functional group at the other end that is capable of reaction with the nylon. Examples are 3-aminopropyltriethoxysilane, trimethoxysilylpropyldiethylenetriamine and N-(triethoxysilylpropyl) urea. The optimum level of aminosilane coupling agents lies in the 0.5 wt% to 1 wt% range for these fillers. Other organosilicon chemicals may be used with filler/reinforcements (such as talc and calcium carbonate) not suited to silane chemistry. Titanate coupling agents are available for use with a wide variety of fillers. Coupling to polymeric fibers (e.g., aramid fibers) creates a special challenge because silane chemistry does not apply. A fiber finish labeled "CS-805" has been used to successfully couple aramid fibers to resin matrices.

Uniform spherical particles have a maximum packing fraction of about 64 vol%. Agglomerated spherical particles have somewhat lower maximum packing fractions, 57 vol% for four-particle agglomerates of nearly spherical aluminum oxide. Wetting agents will help break up agglomerates to give packing fractions approaching the maximum. Fiber reinforcements have lower maximum packing fractions depending upon the fiber aspect ratio. A practical guideline for maximum packing of short glass fibers is 50 vol%. In nylons, 50 vol% fiber glass corresponds to about 70 wt% as a maximum level. Combinations of filler size and shape may increase packing fraction, for example, fibers plus spheres or fiber glass plus mineral filler. Micropacking of fillers and reinforcement can provide an increase in packing fraction.

2.3 Natural Fibers [3]

2.3.1 Structure of Natural Fiber [3]

Natural plant fibers are constituted of cellulose fibers, consisting of helically wound cellulose microfibrils, bound together by an amorphous lignin matrix. Lignin keeps the water in fibers; acts as a protection against biological attack and as a stiffener to give stem its resistance against gravity forces and wind. Hemicellulose found in the natural fibers is believed to be a compatibilizer between cellulose and lignin. The cell wall in a fiber is not a homogeneous membrane (see Figure 2.1)

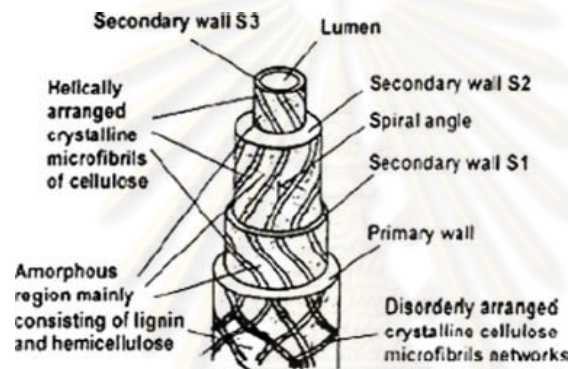


Figure 2.1 Structure of natural fiber [3].

Each fiber has a complex, layered structure consisting of a thin primary wall which is the first layer deposited during cell growth encircling a secondary wall. The secondary wall is made up of three layers and the thick middle layer determines the mechanical properties of the fiber. The middle layer consists of a series of helically wound cellular microfibrils formed from long chain cellulose molecules. The angle between the fiber axis and the microfibrils is called the microfibrillar angle. The characteristic value of microfibrillar angle varies from one fiber to another. These microfibrils have typically a diameter of about 10-30 nm and are made up of 30-100 cellulose molecules in extended chain conformation and provide mechanical strength to the fiber.

2.3.2 Hydrophilic Character of Natural Fibers [3]

Shortcomings associated with natural fibers have to overcome before using them in polymer composites. The most serious concerned problem with natural fibers is its hydrophilic nature, which causes the fiber to swell and ultimately rotting takes place through attack by fungi. Natural fibers are hydrophilic as they are derived from lignocellulose, which contain strongly polarized hydroxyl groups. These fibers, therefore, are inherently incompatible with hydrophobic thermoplastics, such as polyolefins. The major limitations of using these fibers as reinforcements in such matrices include poor interfacial adhesion between polar-hydrophilic fiber and nonpolar-hydrophobic matrix. Moreover, difficulty in mixing because of poor wetting of the fiber with the matrix is another problem that leads to composites with weak interface.

A possible solution to improve the fiber polymer interaction is by using compatibilizers and adhesion promoters which reduce the moisture absorption. Surface treatments of the fiber with silane make the fiber more hydrophobic.

To reduce the moisture absorption, the fiber has to be changed chemically and physically. Hydrothermal treatment is one of the approaches to reduce moisture absorption of natural fibers, which can increase the crystallinity of cellulose and therefore, contributes to a reduced moisture uptake. Moreover, on hydrothermal treatment, a part of hemicellulose is extracted thereby decreasing the moisture absorbance. Duralin process can be used to improve the quality of natural fibers. It has got a number of advantages such as no dew retting required, increased fiber yield, improved fiber quality consistency, reduced swelling and resistance from moisture, increased thermal stability, improved resistance to fungus and better mechanical properties.

2.3.3 Processing Techniques of Natural Fibers [3]

Fiber processing technology like microbial deterioration and system explosion plays an important role in improving the quality of fibers. Microbial deterioration of the material depends on the environmental conditions. The condition reached thereby are decisive for the energy necessary for delignification and fibrillation and thus also for the attainable fiber masses. To obtain a value gain, the

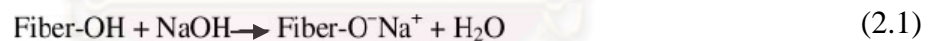
more important is to retain the super molecular structure of the fiber. The traditional microbial deterioration process is one of the most important prerequisite. However, this deterioration process can be partly replaced by the latest chemico-physical processes.

2.4 Pretreatments of Natural Fibers [3]

The interest in using natural fibers in composites has increased in recent years due their lightweight, nonabrasive, combustible, nontoxic, low cost and biodegradable properties. However, lack of good interfacial adhesion, low melting point and poor resistance to moisture absorption, make the use of natural fiber reinforced composites less attractive. Pretreatments of the fiber can clean the fiber surface, chemically modify the surface, stop the moisture absorption process and increase the surface roughness

2.4.1 Mercerization of Natural Fibers [3]

Alkali treatment of natural fibers, also called mercerization, is the common method to produce high-quality fibers (Eq. 2.1).



Mercerization leads to fibrillation which causes the breaking down of the composite fiber bundle into smaller fibers. Mercerization reduces fiber diameter, thereby increases the aspect ratio which leads to the development of a rough surface topography that results in better fibers-matrix interface adhesion and an increase in mechanical properties

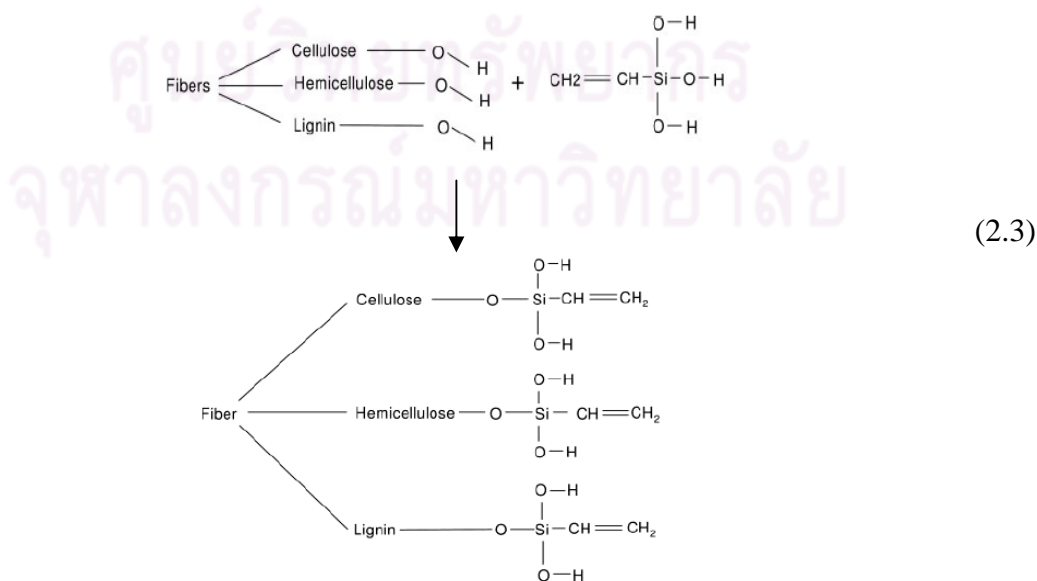
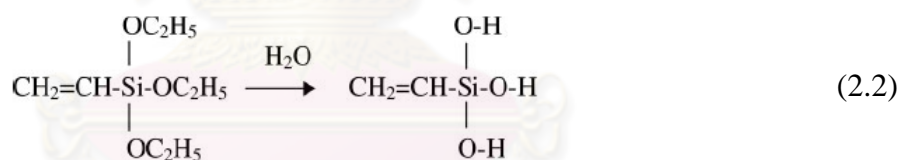
2.4.2 Silane Coupling Agent onto Natural Fibers [3]

Coupling agents usually improve the degree of cross-linking in the interface region and offer a perfect bonding. Among the various coupling agents, silane coupling agents were found to be effective in modifying the natural fiber-matrix interface. Efficiency of silane treatment was high for the alkaline treated fiber

than for the untreated fiber because more reactive site can be generated for silane reaction. Therefore, fibers were pretreated with NaOH for about half an hour before its coupling with silane. Fibers were then washed many times in distilled water and finally dried.

Silane coupling agents may reduce the number of cellulose hydroxyl groups in the fiber-matrix interface. In the presence of moisture, hydrolyzable alkoxy group leads to the formation of silanols. The silanol then reacts with the hydroxyl group of the fiber, forming stable covalent bonds to the cell wall that are chemisorbed onto the fiber surface. Therefore, the hydrocarbon chains provided by the application of silane restrain the swelling of the fiber by creating a cross-linked network because of covalent bonding between the matrix and the fiber.

Silanes were effective in improving the interface properties. Alkoxy silanes are able to form bonds with hydroxyl groups. Silanes after hydrolysis undergo condensation and bond formation stage and can form polysiloxane structures by reaction with hydroxyl group of the fibers. The reactions are given in Eq. 2.2 hydrolysis of silane and Eq. 2.3 Reaction of silane with -OH groups of natural fiber.



2.5 Degradation of Nylons [5]

The degradation of nylons is a complex subject that is still not fully understood. There are several reasons for this difficulty. First, the results of studies are often overlaid by other reactions, such as oxidation and hydrolysis, due to failure to rigorously exclude air or moisture. Second, the degradation is influenced greatly by impurities and degradation products formed during manufacture. The third is the difficulty of isolating the primary degradation products and the complications of the presence of secondary reactions of the primary degradation products. Fourth, there is incomplete knowledge of the interactions of all these factors. Lastly, reactions in the solid state are influenced by other factors such as geometry; crystallinity/morphology; orientation; forming techniques because they affect orientation and formation of voids; and type of nylon which would affect moisture absorption, permeability, and diffusion characteristics. The effects of morphology and crystallinity are much more apparent in degradation reactions in the solid state which is of interest in end-use applications. Unfortunately, many of the studies have been conducted on samples that are poorly characterized. This lack of information makes generalizations difficult.

In theory, nylon degradation can be classified into four types: (a) hydrolytic, (b) thermal, (c) photolytic, and (d) oxidative. For our discussion, solvent and chemical attacks are considered as chemical reactions rather than degradation. However, as stated above, in practice degradation is a combination of these different processes. Molding and extrusion processors are concerned primarily with hydrolytic, oxidative, and thermal degradations in the melt. On the other hand, the end-users may be concerned with all four types of degradation in the solid state depending on the specific environment of the application. Even so, studies of pure degradation processes are necessary for elucidation of the degradation mechanisms.

2.5.1 Hydrolysis [5]

Hydrolysis in nylon has been discussed previously with respect to the equilibrium constant and amide interchange. The emphasis here is on hydrolysis in the solid state as in end-used situations.

Fundamental studies on the rate of hydrolysis were conducted by Myagkov in aqueous sulfuric acid and NaOH at high concentrations. Both

caprolactam and PA-6 showed a reduction in rate with an increase in acid or base concentration. In 21 M (40 wt%) sulfuric acid solution at temperatures of 90 °C to 118 °C, the rate constants were between 0.0025 and 0.011 l/mol-min but in 68 M (92 wt%) sulfuric acid the rate was too slow to measure. A similar inverse relation of reaction rate with concentration was observed by the same investigators in NaOH hydrolysis. Activation energies for both caprolactam and PA-6 in sulfuric acid were 84 kJ/mol and 71 kJ/mol in NaOH. A 100% faster hydrolysis rate of Pa-6 was obtained in KOH at 16% than at 34%. The activation energy in this work was 83 kJ/mol which is significantly higher than that obtained in NaOH. The inverse dependence of hydrolysis rate on the concentration of acid is not unique to caprolactam or nylons. This phenomenon has been well recognized in simple, linear amides. It appears that at fairly high concentrations the water molecule is tied up by the excess acid and is unavailable for reaction. Myagkov also concluded that the equivalence of activation energies in both basic and acidic hydrolyses was an indication that the mechanism of hydrolysis is independent of structure and molecular size. It was shown that in acid solution, the hydrolysis is random and is, therefore, in consort with Flory's theory that all amide groups in the polymer chain have an equal probability of reacting.

One-year stress corrosion studies on injection molded discs in dilute acids at room temperature confirm that the CH_2/CONH ratio, acid concentration, and degree of crystallization affect the loss in molecular mass. The loss is greater with PA-6 or PA-66 ($\text{CH}_2/\text{CONH} = 5:1$) than with PA-610 or PA-8 ($\text{CH}_2/\text{CONH} = 7:1$). The effects of more subtle factors such as percent crystallinity or some parameter indicative of the degree of perfection of the molecular configuration are illustrated in the solubility of PA-6 but not PA-66 in 4 M (14% by wt) hydrochloric acid. Similarly, PA-6 was completely hydrolyzed, PA-66 was less readily hydrolyzed, and PA-610 proved the most difficult to hydrolyze in 8 M (26% by wt) hydrochloric acid. Resistance to hydrolysis increases with increasing hydrocarbon character of the nylon. This can be attributed to the decrease in the amide concentration and lower affinity for water.

There is also evidence that hydrolytic stability at high humidity of stretched fiber of PA-6 decreases with increasing stress. A similar effect in anisotropic moldings or extrusions with frozen-in stresses is to be expected. However, quantifying the degree to which the hydrolytic attack is enhanced is complicated by

the need to know the distribution of orientation and stresses in every part. It appears that the inherent hydrolytic resistance of solid nylons is comparable in both acid and base. Injection molded bars of PA-66 exposed to buffered solutions of pH 4 and pH 10 at 70 °C suffer an equivalent loss in properties after 90 days but only after a year at pH 7. This is consistent with reported acid and base catalysis of hydrolysis in aqueous solutions. There are reports, however, that acid catalysis is observed only if the hydrogen ion concentration exceeds the amount necessary for salt formation with the amine ends of the polymer. A patent claims the use of high amine ends to increase resistance to hydrolysis.

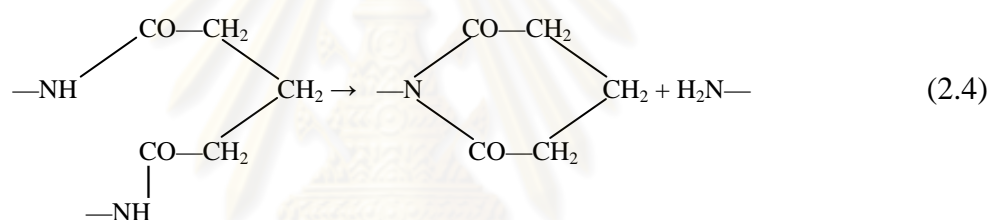
Long-term aging studies at 100% relative humidity (RH) and at 66 °C to 93 °C were reported in both unreinforced and glass-reinforced PA-66 and PA-12. Control tests were conducted at the same time at 0% RH. Unreinforced PA-66 became brittle in 2 months at 66 °C and 100%RH and its tensile strength was reduced by 70%. In contrast, at 0% RH, elongation remained > 50%, and no diminution in tensile strength was observed for over 18 months. At high temperatures, addition of both glass and stabilizers extended the useful life of PA-66 compositions to >18 months. In the same studies, a reinforced PA-12 was found to be more resistant than stabilized, glass-reinforced PA-66. Again, these results appear to show the relatively greater resistance toward hydrolysis of nylons with greater hydrocarbon character. The results above appear to preclude oxidative effects as the permeability of PA-12 at 100% RH is fivefold that of PA-66.

2.5.2 Thermal Degradation [5]

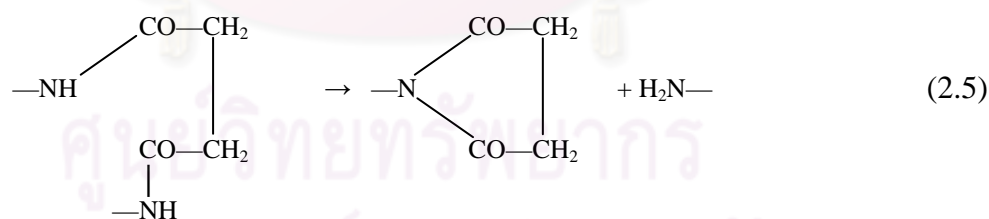
Thermal degradation is degradation induced by elevated temperatures in the absence of oxygen. The rates and specific pathways of thermal degradation are dependent on polymer structure and temperature. Two basic types of reactions should be distinguished: those inherent in the structure of the monomers themselves, and those due to the influence of the amide moiety and involve cleavage of the amide and adjacent bonds. The stability of nylons roughly parallels the thermal stability of their corresponding monomers. Thus, the stability of the polymer is a reflection of the inherent stability of the monomers. Except for the odd-even alternation, the thermal stability of aliphatic dicarboxylic acids increases with increasing size. This increasing stability with increasing chain length has been observed in nylons containing these

diacids. The decomposition temperatures of these diacids, however, are markedly decreased by the presence of other compounds and are much lower under conditions of polymerization.

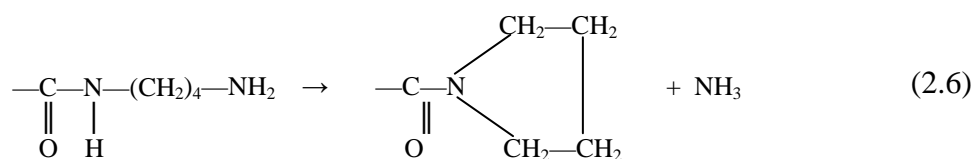
During polymerization, ring formation occurs if the monomers can cyclize to 5- to 7-membered rings. Examples of monomers with a strong tendency to cyclize are succinic acid, glutaric acid, tetramethylenediamine, and 5-aminohexanoic acid. The cyclization tendency for these monomers is so strong that high molecular mass polymers are obtained only when polymerization is conducted below the melting point. Adipic acid and aminohexanoic acid have only a moderate tendency to cyclize and these are capable of producing polymers of high molecular mass in the melt. However, nylons that contain monomers with a tendency to cyclize are more thermally unstable. As an example, nylons containing glutaric acid and succinic acid decompose by cyclizing to the imide (Eq. 2.4):



The succinamide yields the 5-membered imide ring (Eq. 2.5):



The cyclization is also observed with diamine monomers that are capable of forming 5-membered rings (Eq. 2.6). Roerdink et al. [6] report the formation of a pyrrolidine end group as a side reaction in the preparation of PA-46 from tetramethylenediamine and adipic acid.



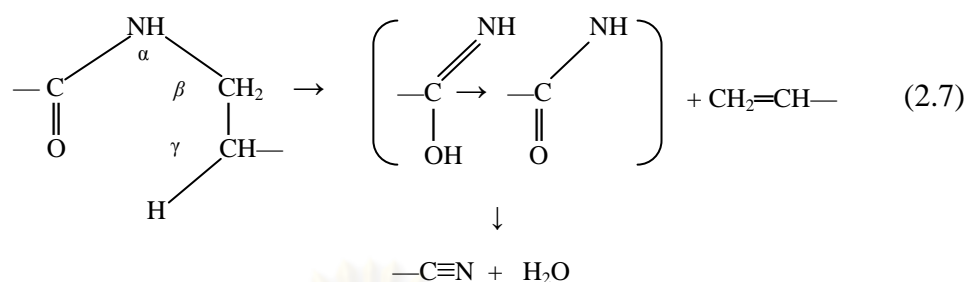
This side reaction precludes the formation of a high molecular mass polymer in the melt. This problem is circumvented by using a two-step process that involves first the formation of a low mass prepolymer from aqueous salt solution at 210 °C to 220 °C followed by solid-state polymerization. The formation of high mass polymer by solid-state polymerization is favorable because the amidation equilibrium constant is higher at lower temperatures and the cyclization reaction has a higher activation energy than the polymerization reaction.

PA-6 is relatively more stable than PA-4 because of the less favorable cyclization to a 7-membered ring. However, cyclization still occurs to a significant extent in the melt. The equilibrium amount of monomer increases with increasing temperature, decreasing molecular mass and increasing water content. The rate of monomer formation is reduced from the crystalline region. Reimschuessel concluded that monomer regeneration occurs by either uncatalyzed or acid-catalyzed ring closure arising from the reaction of the amine end group with the adjacent carbonyl moiety. PA-6 is generally extracted to remove the monomer and oligomers particularly for food contact applications. Even for resin applications, with some exceptions, the extracted material is preferred because of higher tensile strength and stiffness.

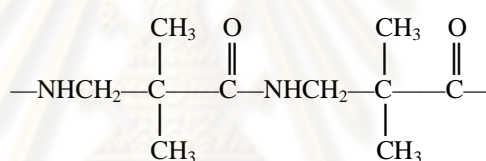
The other thermal decomposition mode in nylons, indicated by early studies on model compounds, involves cleavage of the amide group and adjacent bonds. Cleavage occurs preferentially at the C-N bond adjacent to the amide group. This was rationalized by the relative bond strengths of the C-C and C-N bonds which were reported to be 335 and 285 kJ/mol, respectively. Comparison of C-C and C-N bonds of similar structure shows only a small difference in bond dissociation energies between C-C and C-N. However, although bond strengths are sometimes used to predict reaction pathways, many studies have shown that mechanistic factors such as the energy of the transition state and the thermodynamic energy balance are more important than bond strength in determining reaction pathway.

The presence of nitrile groups in degraded PA-66 and PA-6 is consistent both with a C-N bond cleavage and the cyclic mechanism proposed by

Bailey and Bird in amide decomposition. The degradation produces an amide as the primary product followed by dehydration to the nitrile (Eq. 2.7):

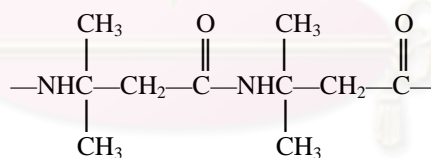


Support for the above degradation pathway has been provided by the study demonstrating that polypivalolactam as shown in Eq. 2.8, which has no γ -hydrogen, is much more stable than poly(β -aminoisovaleric acid) as shown in Eq. 2.8, which cannot be processed in the melt.



Polypivalolactam

(2.8)



Poly(β -aminoisovaleric acid)

Analysis of degradation products formed by PA-6 in the range of 257 °C to 305 °C showed changes in the ratio of the gaseous products evolved (NH₃, CO₂, H₂O) after 120 h of heating. The change in the ratio of products with temperature suggests that these are formed by more than one reaction with differing activation energies. A similar dependence of activation energy on temperature has been observed in other nylons. Later studies on PA-6 also observed branching; the evolution of volatiles became fast at 325 °C, and complete decomposition to monomer occurred at 350 °C.

Other studies on PA-66 and PA-6 involved extended heating in steam at 290 °C. The acid ends decreased and amine ends increased in PA-66 with no change in solution viscosity. The cyclization to cyclopentanone was cited as the cause of the decrease in carboxyl ends. The PA6 used which had low initial monomer content, showed essentially no change in end groups but exhibited diminished solution viscosity which was most probably the result of a decrease in molecular mass due to generation of monomer.

Indications are that PA-610 is more stable than PA-66 and PA-6. Prolonged exposure of PA-610 to steam at 290 °C showed very little change. Another indication of the greater stability of PA-610 over PA-66 is in the work that showed the onset of catastrophic weight loss to occur at 390 °C for PA-66 and at 410 °C for PA-610. This study also showed that in the temperature range of 289 °C to 327 °C the change in molecular mass distribution was bimodal. PA-7 is more stable than PA-6 because of the lower propensity for lactam formation. However, degradation products have been observed to be similar to those from PA-6.

There are a number of observations that suggest that the thermal stability of nylons is affected by the method of synthesis and processing. For example, as noted before, the thermally induced decrease in the degree of polymerization of anionically made PA-6 is considerably faster than that of hydrolytically made PA-6. Although there is disagreement as to the role of the type of metal cations present, there is evidence that they affect the rate of degradation. The stability of PA-66 has been observed also to vary with the method of synthesis. It has been reported that chromium plating in melt extruders decreases the rate of degradation of PA-66. Similarly, the stability of PA-102 [poly(decamethylene oxzamide)] was different when made by a gas or a melt phase process. The effects of synthesis method and/or processing on the stability of nylon could be the result of catalyst residues, presence of impurities, and catalytic effects of traces of metals from the manufacturing equipment. A number of studies have also demonstrated the effect of stress on the rate of degradation. For example, it was shown that PA-6 degradation is accelerated by stress. This is similar to the reported influence of stress on thermo-oxidation and photooxidation.

2.5.3 Oxidative Degradation [5]

All polymer are subject to degradation by oxygen. Oxidative degradation is best classified into thermally induced (thermooxidation) and light-induced (photooxidation) oxidation. The susceptibility of nylons to oxidative attack both in the dark and under light has been observed for a long time.

2.5.3.1 Thermooxidative Degradation [5]

Numerous studies have shown a decrease in stability of nylons in the presence of air. Thermogravimetric studies on PA-6T showed the onset of rapid weight loss at 300 °C in air and 380 °C in nitrogen. Similarly, differential thermal analysis (DTA) of PA-66 fiber heated at 10°C/min shows an onset of an exotherm at 185 °C which is not present when the fiber is heated in nitrogen. Thermooxidative degradation results in a decrease in molecular mass and is accompanied by decreased physical and mechanical properties. Injection molded bars of PA-66 embrittle in <2 h at 250 °C and 2 years at 70 °C. The molecular mass decreased in the surface of the bar but increased in the core. At temperatures of 200 °C to 250 °C, some volatile fractions were obtained. Milling away the low molecular mass fraction at the surface restored toughness of the bars. Degradation was found to be faster in the presence of moisture. Loss of toughness occurs in 8 weeks at 70 °C when the specimen is wet. Faster oxidation in the presence of moisture was also observed with fibers. This was attributed to an increased rate of diffusion of oxygen into the polymer. Studies of thermooxidative stability of other nylons reported lower stability for PA-6, PA-610, and PA-111 compared to PA-66. Other workers showed the oxygen uptake to be $6 < 610 < 66/610/6$ which is in order of decreasing crystallinity.

There is a wide range in the values of activation energies for the thermooxidation of PA-66 reported in the literature. The differing experimental conditions, geometry, and varied history of the samples may account for this scatter. Activation energies ranging from 92 to 113 kJ/mol have been reported for molded PA-66 in air at temperatures from 70 °C to 250 °C. In another study, the decrease in limiting viscosity number was used to estimate an activation energy of 84 kJ/mol at temperatures below 100°C for PA-66 filaments. Studies at 136 °C to 215 °C in air on PA-66 fibers that were moisture equilibrated at 65% RH showed a loss in molecular

mass and a decrease in amine ends but no change in acid ends. The activation energy was calculated to be 167 kJ/mol. On the other hand, heating under nitrogen or in the presence of antioxidants resulted in increased molecular mass. Based on end group analyses the increase in molecular mass was attributed to crosslink rather than amidation. It is believed that loss in molecular mass in air is due to the dominant effect of free radical chain scission over crosslinking. In another study, the kinetics of wet oxidation of PA-66 at temperatures of 170 °C to 180 °C was determined using a disc technique which allowed the separation of kinetics from mass transfer effects. In this case, the activation energy was calculated to be 176 kJ/mol. Although this value is close to those obtained by Valko and Chiklis, [7] this may be fortuitous, as the environments, geometry, and the measure of degradation used in the two studies were different.

The effect of orientation on thermooxidative stability was demonstrated in stretched PA-6. The oxidation resistance was shown to increase with the degree of stretching, and the induction period was found to increase exponentially with draw ratio. Because the gas diffusion coefficients have been observed also to decrease with stretching, this was attributed to increased orientation.

The thermooxidation of PA-6 and PA-66 film has been followed by Fourier transform infrared (FT-IR) spectroscopy. Both the characteristic amorphous and crystalline IR bands were monitored during exposure to nitrogen and air. In nitrogen, no significant changes in the IR absorption bands were observed even up to 2 h at 200 °C. However, in air there was already significant oxidation after only 30 min at 200 °C. The rate was observed to be much faster in the amorphous region compared to the crystalline portion of the polymer. The absorption bands, based on the spectra, suggested the formation of α,β -unsaturated carbonyl species. The effects of keto groups on the oxidation were studied using PA-611CO made from hexamethylenediamine and 6-oxo-1,11-undecanedioyl chloride by interfacial polymerization. The presence of the keto moiety resulted in much faster oxidation than in the case of PA-6 and PA-66 even when carried out at 140 °C for PA-611CO compared to 200 °C for PA-6 and PA-66.

The thermooxidation of fibers at 160 °C was monitored for up to 2 h using UV/VIS and fluorescent excitation/emission spectroscopy. It was postulated that under these conditions the spectral data support the formation of conjugated oligoenimines $-(C=C)_i-C=N-$. The concentration of the various oligoenimine

species is a function of temperature and exposure time. The degree of conjugation increased with time with the consequent shift to longer wavelength of the absorption band. A decrease in amine end group concentration was also observed, and this was interpreted as supporting evidence for the involvement of enimes in the oxidation reactions.

It is the consensus that oxidative degradation is initiated by hydroperoxide. Allen *et al.* [8, 9] investigated its formation in both thermooxidation and photooxidation of PA-66 aged at 120 °C and 180 °C, it showed that during the initial stages (up to 30 min at 120 °C and 45 min at 180 °C) the hydroperoxide growth was autocatalytic. Beyond this period, a rapid decrease was observed. Hence, the rate of formation of hydroperoxide is much faster than its destruction during the first 30 to 45 min. The studies also demonstrated that polymers finished under nitrogen were more susceptible to degradation than those finished under steam. Furthermore, the stability increased with increasing amine end groups. In parallel with the action of hindered amine stabilizers, this can be attributed to the improved stability to the destruction of the hydroperoxides by the amine ends.

2.5.3.2 Photooxidation [5]

Radiation from the sun that reaches the earth is in the range of 1 nm to 3,000 nm (0.1 nm = 1 angstrom). However, because of atmospheric absorption, only radiation with wavelength above 280 nm reaches the earth's surface. Radiation in the range of 280 nm to 400 nm is primarily responsible for photooxidation. Above 415 nm there is almost no light-induced degradation. Photodegradation of unstabilized nylon in air and sunlight has been documented but not in the absence of air except at wavelengths well below 300 nm due to direct bond scission. Studies on model compounds show that aliphatic amides do not absorb radiation below 300 nm. Several investigators have suggested the intervention of other species either formed or incorporated adventitiously during manufacture. There is evidence that these species are α -ketoimides, α,β -unsaturated carbonyl groups, and enimes similar to those identified in thermooxidative degradations.

Understanding of the photooxidation mechanism of nylons has been based on the studies of model compounds. Early work suggested an initiation step

involving scission of the C-N bond of the amide and subsequent abstraction of hydrogen from the methylene alpha to the nitrogen. The resulting radical produces hydroperoxides by reaction with oxygen. The detailed mechanism proposed by Sharkey and Mochel, [10] based on their studies on model compounds. Support for this mechanism has been based on the similarity of decomposition products isolated from photooxidation of PA-66, PA-610, PA-106, and PA-6 to those obtained from model compounds. The presence of hydroperoxides has been quantitatively demonstrated in the irradiation of PA-66 in the presence of oxygen. More recent studies on PA-6, PA-11, and PA-12, initiated by wavelengths in the range of 254 nm to 365 nm from an artificial source, suggested a dual initiation mechanism [11] (Figure 2.2). Photooxidation initiated by wavelengths below 300 nm resulted in direct scission of the NH-CO bond which is similar to the mechanism first proposed by Sharkey [10] (Figure 2.3). The primary intermediate products are amines and aldehydes. Above 340 nm, photodegradation is initiated by excitation of impurities, defects, or additives in the polymer incorporated either adventitiously or purposely during manufacture. Hydroperoxides and imides were the major intermediate products. Although the reaction mechanism is similar for PA-6, PA-11, and PA-12 the rate of formation of intermediate photooxidation products was dependent on the polymer matrix.

Allen *et al.* [8, 9] also investigated the photooxidation of PA-66 at wavelengths > 300 nm. The concentration of products with absorption bands at 294 nm increased with time. Removal of these species by extraction with 2-propanol afforded an improvement in photostability. Also, as was the case with thermal oxidation, the photostability increased with increasing amine end group concentration. As mentioned previously, chromophores and impurities acquired during manufacture affect photostability. Metallic impurities, such as iron and chromium, and pigments such as titanium dioxide, accelerate photooxidation by sensitizing chemical transfer. Some dyes act as photosensitizers and they accelerate degradation. On the other hand, some absorb UV light and act as UV screens.

As in thermal oxidation, resistance to photooxidation in PA-6 fibers was found to increase with draw ratio presumably due to increased orientation. However, for unknown reasons, at a given draw ratio the resistance decreased with applied stress from 10 MPa to 400 MPa.

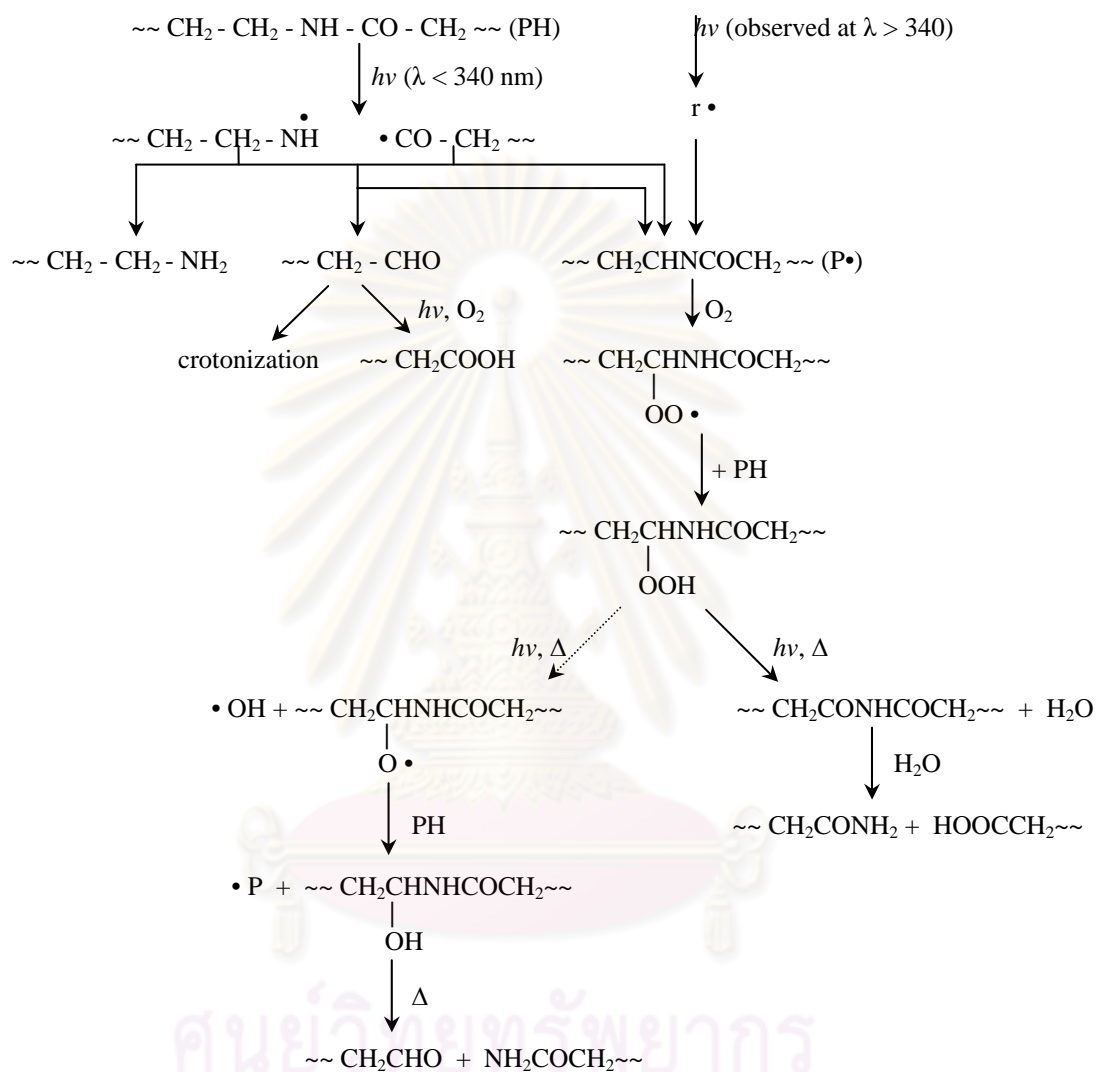


Figure 2.2 Photooxidation pathways for nylons [10].

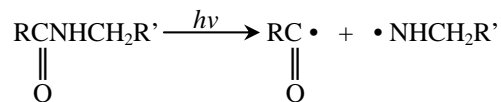
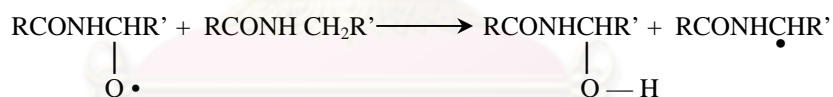
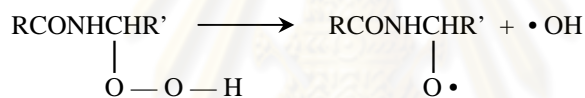
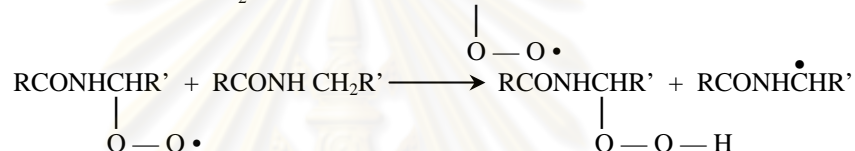
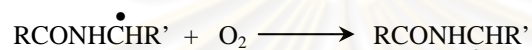
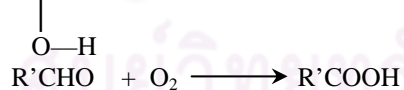
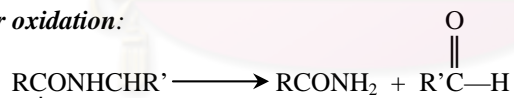
Initiation:**Propagation:****Further oxidation:**

Figure 2.3 Photooxidation of N-alkyl amides [11].

2.6 Literature Reviews

Herrera *et al.* [12] studied of the mechanical properties of short natural-fiber reinforced composites. The degree of fiber-matrix adhesion and its effect on the mechanical reinforcement of short henequen fibers and a polyethylene matrix was studied. The surface treatments were: an alkali treatment, a silane coupling agent and the pre-impregnation process of the HDPE/xylene solution. HDPE-henequen fiber composite materials were prepared with 20% v/v. The comparison of tensile properties of the composites showed that the silane treatment and the matrix-resin pre-impregnation process of the fiber produced a significant increase in tensile strength. It was also shown that the silane treatment produced a significant increase in flexural strength. The shear properties of the composites also increased significantly when the henequen fiber were treated with the silane coupling agent.

Murali *et al.* [13] studied the tensile properties of elephant grass fiber reinforced polyester composites. Elephant grass stalk fibers were extracted using retting and chemical (NaOH) extraction processes. These fibers were treated with KMnO_4 solution to improve adhesion with matrix. The tensile strength and the modulus of chemically extracted elephant grass fiber composites have increased by approximately 1.45 times to those of elephant grass fiber composite extracted by retting. The tensile strength of treated fiber composites has decreased and the tensile modulus has shown a mixed trend for the fibers extracted by both the processes.

Gomes *et al.* [14] studied the effect of alkali treatment on tensile properties of curaura fiber. The development and improvement of mechanical properties of a so-called green composite that was fabricated by reinforcing a cornstarch-based biodegradable resin with high-strength natural fibers extracted from a plant named curaua was investigated. Tensile test results showed that alkali-treated fiber composites increased in fracture strain twice to three times more than untreated fiber composites, without a considerable decrease in strength.

Paulo *et al.* [2] studied the properties polyamide-6/vegetal fiber composite prepared by extrusion and injection molding. Fiber contents of 20, 30 or 40 wt% in polyamide-6/vegetal fiber composites were studied. Fibers were treated with N_2 plasma or washed with NaOH solution, to improve their adhesion to PA-6. These samples were submitted to mechanical and thermal tests. Tensile and flexural properties of this composite are better than unfilled, but lower than glass fiber

reinforced polyamide-6. However, its impact resistance and heat deflection temperature were similar to the glass fiber reinforced polyamide-6

Sui *et al.* [15] investigated the properties of plant fiber reinforced polymer composite prepared by a twin-screw extruder. Polypropylene (PP) composites reinforced using a novel plant fiber, sunflower hull sanding dust (SHSD), were prepared using a twin-screw extruder. Thermal and mechanical properties of the SHSD/PP composites were characterized and compared to an organically modified clay (organo-clay)/PP composite. Differential scanning calorimetry (DSC) analysis showed that the crystallization temperature and the degree of crystallinity of PP exhibited changes with addition of SHSD and organo-clay. Compared to the neat PP and organo-clay/PP, the SHSD/PP composites exhibited a relatively decreasing rate of thermal degradation with increase in temperature. Mechanical properties of the PP were enhanced with the addition of SHSDs.

Araujo *et al.* [16] studied the thermal properties of high density polyethylene composites with natural fibres: Coupling agent effect. High density polyethylene composites with curaua fibers were prepared using an intermeshing co-rotating extruder and two different coupling agents: maleic anhydride and poly(ethylene-co-vinyl acetate). The thermal stability was studied by thermogravimetric and differential scanning analysis. HDPE do not present significant differences in melting point, showing antagonistic interactions for the fibres in presence of HDPE. The composite without coupling agent and that with EVA as a coupling agent have part of their processes of fibre weight loss occurring at higher temperatures, together with the HDPE processes of weight loss. The results for oxidation induction time (OIT) show no significant influence of the curaua fibre/HDPE composites in comparison with HDPE.

Patricia *et al.* [17] studied the mechanical properties of natural fibers/polyamides composites as natural fiber composites for substituting glass fibers. The different natural fibers such as flax, jute, pure cellulose, and wood pulps have been compounded with different polyamides to analyze the effect of fiber content on mechanical properties. Thermal behavior of the different fibers was determined by thermogravimetry to know the boundary for processing at high temperatures, since the melting points of the polyamides are much higher than those of polyolefins and this could lead to a higher degradation of the natural fibers. The mechanical properties were increased when comparison with the unreinforced matrix.

La Mantia *et al.* [18] studied the accelerated weathering of polypropylene/wood flour composites. Wood-plastic composites (WPCs) have received increasing attention during the last decades, because of many advantages related to their use. Some of their main applications are represented by outdoor furnishing and decking; therefore, it is important to assess their behavior under UV exposure. The polypropylene/wood flour composites were prepared by extrusion and compression molding, and were subjected to mechanical tests, FT-IR analysis and molecular weight measurements. The results showed that the composites retained a higher fraction of the original mechanical properties after accelerated weathering; the wood flour did not significantly degrade throughout the irradiation time slot of the investigation and the composites kept a higher percentage of the original molecular weight.

Azuma *et al.* [19] studied the outdoor and accelerated weathering tests for polypropylene and polypropylene/talc composites: A comparative study of their weathering behavior. The comparisons of degradation behavior of polypropylene (PP) and PP/talc composites were carried out with one outdoor weathering test and three accelerated weathering (xenon, metal halide and carbon arc lamps) tests. The outdoor exposure vigorously advanced these degradations with the lowest amount of UV exposure energy. In the case of the existence of talc compound, the degradation was synergistically accelerated by the exposures of the sunshine, the xenon and the metal halide lamps having higher visible light intensities. In addition, the degradations of the PP and the PP/talc composites were found to be synergistically accelerated by sunlight exposure and the acid rain.

CHAPTER III

EXPERIMENTAL

3.1 Materials

Table 3.1 Chemicals used in this study

Chemicals	Function	Commercial Name	Supplier
Polyamide-6	Base polymer	UBE Nylon Resin grade: 1015B	UBE Chemicals (Asia) PCL.
Vetiveria zizanioides	Natural fiber	Vetiver grass	Phitsanulok Province
Sodium hydroxide pellets	Mercerization Treatment	Sodium hydroxide pellets GR for analysis	Merck Co., Ltd.
Deminerized water	Mercerization solvent / Cleaning solvent	Deminerized water	UBE Technical Center (Asia) Limited
Vinyltriethoxysilane	Silane coupilng agent Treatment	Silane coupilng agent	Momentive Specialty Chemicals Inc.
Dicumyl peroxide	Silane coupilng agent Treatment	Peroxide curing agent	Gelest, Inc.
Methanol	Silane coupilng agent solvent	Methanol LabGrade ACS	Merck Co., Ltd.
Talcum/polyamide-6 composite	Reference	UBE Nylon Resin grade: 1015RXN	UBE Chemicals (Asia) PCL.
Glass fiber reinforced polyamide-6 composite	Reference	UBE Nylon Resin grade: 1015GC3	UBE Chemicals (Asia) PCL.
		UBE Nylon Resin grade: 1015GC6	UBE Chemicals (Asia) PCL.

3.2 Instruments

Table 3.2 Instruments used in this study

Instruments	Manufacturer
Cell oven	Espec Corp.
TGA/DSC 1	Mettler-Toledo International Inc.
Twin screw extruder	Labtech Engineering Company Ltd.
Injection molding machine	Nissei Plastic Industrial Co., Ltd.
ISO Type A and ISO Type B mold	Axxicon Moulds Eindhoven BV
Vacuum oven	Yamato Scientific Co., Ltd.
Xenon weather meter	Suga Test Instrument Co., Ltd
Sunshine weather meter	Suga Test Instrument Co., Ltd
Universal testing machine	Instron (Thailand) Co., Ltd.
Chapry impact strength	Yasuda Seki Seisakusho Ltd.
Analytical balance, accurate 0.1 mg	Mettler-Toledo International Inc.
Thermometer, graduated at 0.1 °C	Mettler-Toledo International Inc.
Liquid bath	Mettler-Toledo International Inc.
Scanning electron microscope (SEM)	Jeol Ltd.
Auto fine coater	Jeol Ltd.

3.3 Fiber Preparation

Leaves of Vetiver grass, with 75 cm long, used in this work was obtained from Phitsanulok Province, Thailand. The Vetiver grass fiber was chopped by paper cutter and milled in a five knives rotary mill.

Method I (Mercerization): the fibers were immersed in 5 wt% NaOH solution for 24 h, washed with demineralized water and dried in an oven at 40°C for 24 h.

Method II (by Silane coupling agent): the fibers were pretreated in 5 wt% NaOH solution for 1 h, then washed with demineralized water and dried in an oven at 40°C for 24 h. Then, the fibers were immersed in silane coupling agent solution for 2 h and dried in an oven at 40°C for 24 h. The silane coupling agent solution was prepared by dissolving vinyltriethoxysilane at 1.0% w/w and dicumyl peroxide at 0.5% w/w in a mixture of methanol-water (50/50 v/v) with continuous stirring for 10 min. Figure 3.1 shows the untreated, mercerization treated and silane coupling agent treated Vetiver grass fiber.



Figure 3.1 Vetiver grass fiber (a) Untreated (b) Mercerization treated and (c) Silane coupling agent treated.

3.4 Fiber Characterization

The thermal properties of the Vetiver grass fiber investigated by using thermogravimetric analyzer (Mettler-Toledo, TGA/DSC 1, LF). The sample was placed in aluminium oxide crucible. The temperature was raised under air atmosphere from room temperature to 800 °C at continuous heating rate of 10 °C min⁻¹. The air flow rate was 50 ml min⁻¹. The initial composition and the temperature at maximum loss were evaluated.

3.5 Composites Preparation

Polyamide sample with viscosity number = 143 (UBE Nylon Resin) was used as the base polymer. The polyamide composites were prepared according to the formulation in Table 3.3. All components were mixed by using Thumble blender for 10 min and kept in an aluminum foil bag before feeding into the extruder hopper for

compounding. The samples were compounded using a twin screw extruder ($D = 26$ mm, $L/D = 40$), with vacuum degassing and temperature profile from hopper to die; 205, 205, 210, 210, 210, 215, 215, 215, 220 and 220 °C, screw rotating speed; 180 rpm and throughput rate; 15 kg/h. After extrusion from die, the strands were cooled in water and pelletized.

Table 3.3 Composition of polyamide-6 composites (wt%)

Sample	PA-6	Vetiver Grass Fiber	Glass Fiber	Talcum	Vetiver Grass Fiber Treatment
PA	100	0	0	0	No
PA/V15-N	85	15	0	0	NaOH 24 h
PA/V15-S	85	15	0	0	Silane 2 h
PA/V30-N	70	30	0	0	NaOH 24 h
PA/V30-S	70	30	0	0	Silane 2 h
PA/T30	75	0	0	25	No
PA/V15-S/GF15	70	15	15	0	Silane 2 h
PA/GF15	85	0	15	0	No
PA/GF30	70	0	30	0	No

For test specimen preparation, the composites were dried in a vacuum oven at 90°C for 1 week. The test specimens were injection molded at temperature profile from hopper to nozzle; 210, 230, 230 and 230°C, mold temperature; 80 °C. After molding, the specimens were kept in aluminum foil bag and conditioned at 23 ± 2 °C and 50 ± 5 %RH for 24 h according to ISO 294-1.

3.6 Accelerated Weathering Test

3.6.1 Xenon Weathering

To simulate the direct natural exposure, one set of test specimen was placed in Xenon weathering (SUGA, X75H) with Xenon arc lamp source for 1000 h. The radiant energy was filtered to provide a spectral power distribution closely to the terrestrial daylight. The conditions were as follows, temperature = 65 ± 3 °C, RH = 50

$\pm 5\%$, UV wavelength = 300 - 400 nm at 60 w m^{-2} , spraying time = 18 min and dry interval between spraying time = 102 min, according to ISO 4892-2.

3.6.2 Sunshine Weathering

To simulate the extended-UV exposure, another set of test specimen was placed in sunshine weathering (SUGA, S80 BH) with open flame carbon arc light source for 1000 h. The radiation reaching the test specimens were passed through extended-UV glass filters (type 3). The conditions were as follows, temperature = $63 \pm 3 \text{ }^\circ\text{C}$ and RH = $50 \pm 5\%$, UV wavelength = 320 - 400 nm, spraying time = 18 min and dry interval between spraying time = 102 min, according to ISO 4892-4.

3.7 Mechanical Properties Study

3.7.1 Tensile Properties

The tensile properties of test specimen were measured according to ISO standard 527-1. Tensile properties was measured using universal testing machine (INSTRON, 5567) with cross head speed of 5 mm min^{-1} at the test condition of $23 \pm 2 \text{ }^\circ\text{C}$ and $50 \pm 5\%$ RH. The width and thickness of test specimen were measured by using digital micrometer with the resolution 0.001 mm. An average of five specimens was reported as a representative value. The results of tensile properties were determined as an average. The dumbbell specimen are show in Figure 3.2.

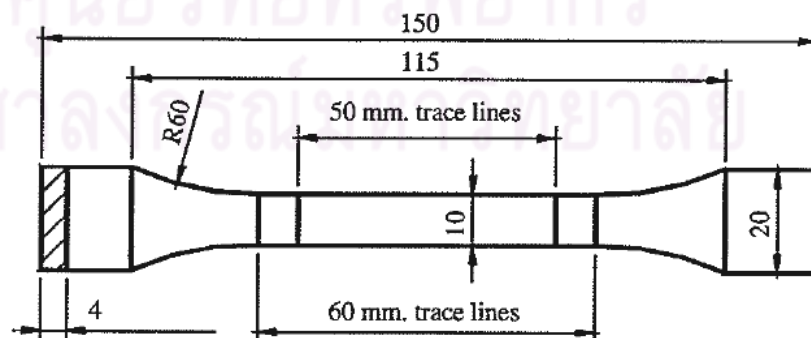


Figure 3.2 Tensile test specimen [20].

3.7.2 Flexural Properties

The flexural properties of test specimen were measured according to ISO standard 178. Flexural properties was measured using universal testing machine (INSTRON, 5567) with cross head speed of 2 mm min^{-1} at the test condition of $23 \pm 2 \text{ }^\circ\text{C}$ and $50 \pm 5 \text{ \%RH}$. An average of five specimens was reported as a representative value. The bar specimen are show in Figure 3.3.

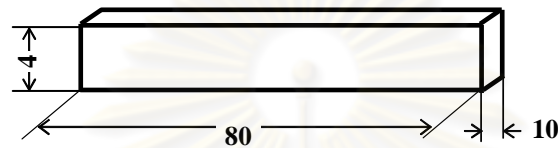


Figure 3.3 Flexural test specimen.

3.7.3 Charpy Impact Strength

The Charpy impact strength of test specimen was measured according to ISO standard 178. Charpy impact strength was measured by Charpy impact machine (Yasuda, 258-PC) at the test condition of $23 \pm 2 \text{ }^\circ\text{C}$ and $50 \pm 5 \text{ \%RH}$. An average of five specimens was reported as a representative value. The bar specimen with notched are show in Figure 3.3.

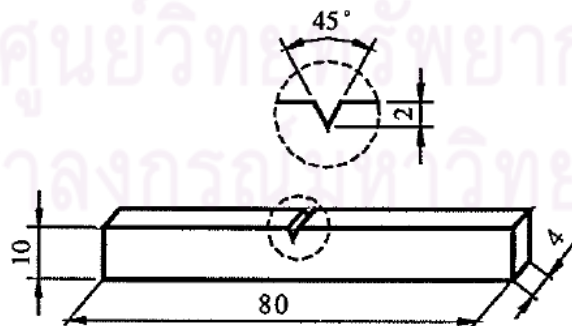


Figure 3.4 Charpy impact strength test specimen [20].

3.8 Density

The density of test specimens after conditioning at 23 ± 2 and 50 ± 5 %RH for 24 h was measured according to ISO standard 1183-1 method A. Density was measured by using an analytical balance and at the room condition of 23 ± 2 °C and the temperature of immersion liquid (Deminerized water) of 23 ± 2 °C. The dimension of test specimen was same as flexural test specimen.

3.9 Morphological Study

The interfacial adhesion fiber/matrix of all composites was analyzed by scanning electron microscopy (SEM), (JEOL, JSM-6340LV) with 5 kV acceleration and X500 magnification. The fracture test specimen after tensile test was coated with a thin gold layer.

CHAPTER IV

RESULTS AND DISCUSSIONS

4.1 Characterization of Vetiver Grass Fiber

Figure 4.1 shows the TGA and DTG curves of Vetiver grass fiber with four decomposition regions as follows:

- First region, moisture in Vetiver grass was decomposed at 57 °C.
- Second region, hemicellulose was decomposed in the range of 263 to 301 °C with maximum decomposition rate at 295 °C.
- Third region, cellulose was decomposed in the range of 380 to 410°C with maximum decomposition rate at of 394 °C.
- Forth region, lignin was decomposed at 445 °C.

The thermodegradation of polysaccharides, like hemicelluloses and cellulose, can occur by cleavage of glycosidic, C-H, C-O and C-C bonds. The dehydration, decarboxylation and decarbonylation reactions, also occur with formation of C-C, C=C, C-O bonds as well as carbonyl and carboxyl groups [21]. The weight loss of lignin occurs at higher temperatures and its degradation is related to dehydration, yielding derivatives with lateral unsaturated chains and the release of water, CO₂, CO and methane. According to Yang *et al.* [22], the gas products obtained by pyrolysis of hemicelluloses, cellulose and lignin; hemicelluloses exhibited higher CO and CO₂ yield, while lignin displayed higher CH₄ production. Organic compounds (C=O, C-O-C), etc.) were mainly released at low temperatures, in the ranges from 200 to 400 °C and from 300 to 450 °C for hemicelluloses and cellulose, respectively. For lignin, no complex organic compounds were reported.

Thus, the first decomposition of Vetiver grass fiber occurred at 263 °C. Therefore, the processing temperature for compounding the Vetiver grass fiber with polyamide-6 by twin screw extruder must be lower than 263 °C.

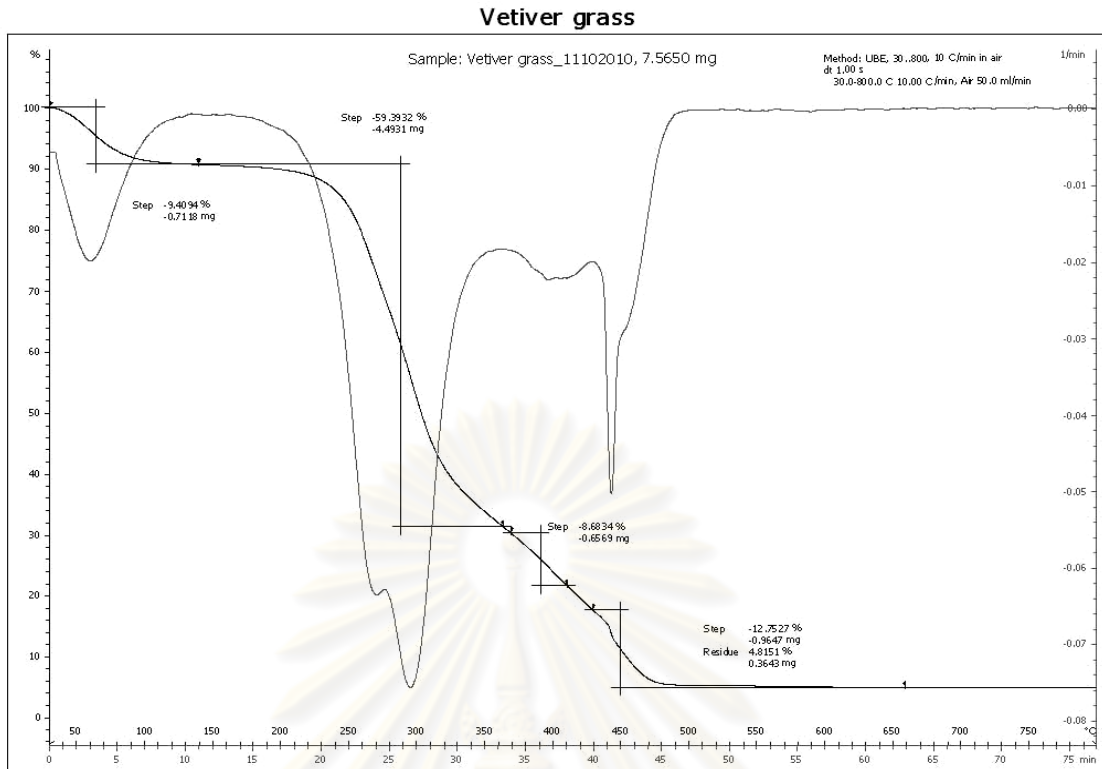


Figure 4.1 TGA and DTG curves of Vetiver grass fiber.

4.2 Vetiver Grass Fiber/Polyamide-6 Composites

4.2.1 Mechanical Properties

From Table 4.1 and Figure 4.2, tensile strength of polyamide-6 composites reinforced with treated grass fiber were lower than that of glass fiber reinforced composites and about the same as unfilled and talc filled composites. Elongation at break (EB) and Charpy impact strength of polyamide-6 composites reinforced with treated grass fiber were lower than that of unfilled and glass fiber reinforced composites, but higher than that of talc filled composites. Tensile and flexural modulus of polyamide-6 composites reinforced with treated grass fiber were higher than unfilled, but lower than that of talc filled and glass fiber reinforced composites. Density of polyamide-6 composites reinforced with treated grass fiber were slightly higher than that of unfilled, but lower than that of talc filled and glass fiber reinforced composites.

From Figure 4.2, for polyamide-6 composites reinforced with treated grass fiber content of 15% and glass fiber content of 15% (PA/V15-S/GF15), tensile

and flexural strength were lower than that of glass fiber reinforced composites but higher than that of unfilled, Vetiver grass fiber reinforced composites and talc filled composites. Elongation at break of polyamide-6 composites reinforced with treated grass fiber content of 15% and glass fiber content of 15% was lower than that of unfilled and glass fiber reinforced composites at content 30% (PA/GF30), but higher than that of Vetiver grass fiber reinforced composites, talc filled composites and glass fiber reinforced composites at content 15% (PA/GF15). Tensile and flexural modulus of polyamide-6 composites reinforced with treated grass fiber content of 15% and glass fiber content of 15% was lower higher than unfilled and Vetiver grass fiber reinforced polyamide-6 composites, but lower than that of glass fiber reinforced composites. From Figure 4.2 (e) and 4.2 (f), Charpy impact strength of polyamide-6 composites reinforced with treated grass fiber content of 15% and glass fiber content of 15% was slightly higher than that of Vetiver grass fiber reinforced composites and talc filled composites, but lower than unfilled and glass fiber reinforced composites. Density of polyamide-6 composites reinforced with treated grass fiber content of 15% and glass fiber content of 15% was slightly higher than that of unfilled and glass fiber reinforced composites at content 15%, but lower than talc filled and glass fiber reinforced composites at content 30% (see Table 4.1).

From the mechanical properties results, it can be noted that the mechanical properties of polyamide-6 composites reinforced with treated grass fiber with silane coupling agent were improved compared with treated grass fiber by mercerization for both fiber contents (15 and 30%).

For polyamide-6 composites reinforced with treated grass fiber content of 15% and glass fiber content of 15%, it can be noted that the mechanical properties of Vetiver treated grass fiber composites and Vetiver treated grass fiber content of 15% and glass fiber content of 15% were lower than that of glass fiber reinforced composites and about the same as talc filled composites.

Table 4.1 Mechanical properties and density of composites after conditioning at 23 °C and 50 %RH for 24 h

Sample	Tensile Strength (MPa)	Elongation at break (%)	Tensile Modulus (GPa)	Flexural Strength (MPa)	Flexural Modulus (GPa)	Charpy Impact Strength (kJ m ⁻²)	Density (g cm ⁻³)
PA	77.8 (2.70)	86.4 (38.05)	2.7 (0.25)	103.0 (2.68)	2.4 (0.13)	5.6 (0.78)	1.12
PA/V15-N	66.7 (4.08)	2.7 (0.78)	3.6 (0.10)	106.9 (1.44)	3.1 (0.10)	2.7 (0.39)	1.17
PA/V15-S	69.4 (1.05)	2.9 (0.21)	3.7 (0.06)	105.9 (1.34)	3.1 (0.08)	2.8 (0.12)	1.17
PA/V30-N	72.9 (2.73)	2.4 (0.51)	4.7 (0.26)	114.0 (2.30)	4.0 (0.15)	2.9 (0.12)	1.21
PA/V30-S	76.9 (0.75)	2.7 (0.33)	4.7 (0.28)	118.6 (3.90)	4.0 (0.09)	3.0 (0.09)	1.21
PA/T30	78.1 (1.71)	1.9 (0.33)	8.5 (0.03)	123.3 (1.59)	7.7 (0.13)	2.0 (0.27)	1.44
PA/V15-S/GF15	82.1 (0.88)	2.9 (0.54)	5.4 (0.17)	132.0 (8.00)	4.7 (0.09)	3.3 (0.13)	1.27
PA/GF15	125.7 (5.22)	2.8 (0.27)	6.2 (0.04)	200.9 (8.68)	5.3 (0.33)	7.5 (1.20)	1.24
PA/GF30	180.1 (2.34)	3.6 (0.66)	9.7 (0.54)	274.6 (3.56)	8.3 (0.16)	14.9 (1.98)	1.36

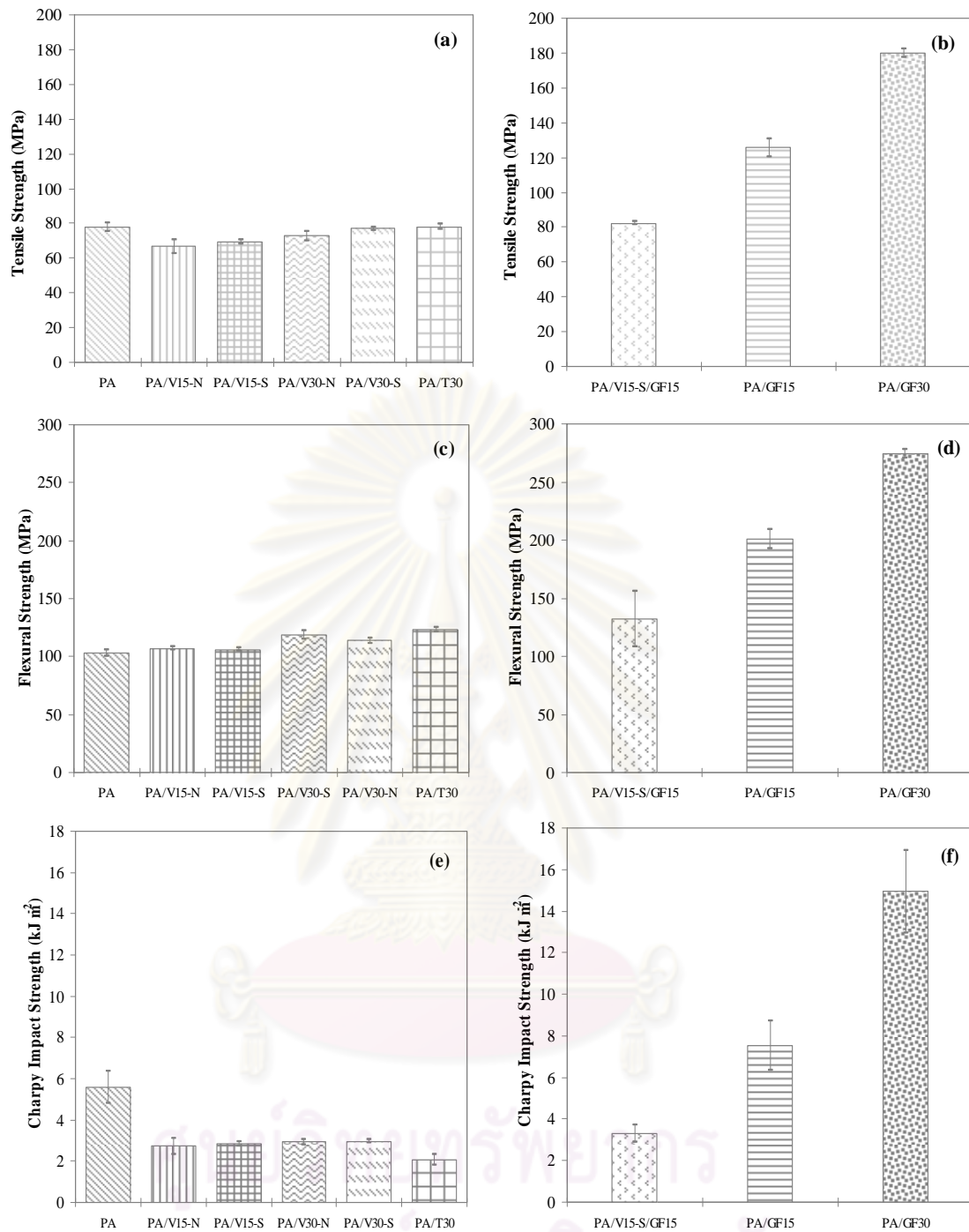


Figure 4.2 Mechanical properties composites after conditioning at 23 °C and 50 %RH for 24 h (a) tensile strength of PA, PA/V15-N, PA/V15-S, PA/V30-N, PA/V30-S and PA/T30 (b) tensile strength of PA/V15-S/GF15, PA/GF15 and PA/GF30 (c) flexural strength of PA, PA/V15-N, PA/V15-S, PA/V30-N, PA/V30-S and PA/T30 (d) flexural strength of PA/V15-S/GF15, PA/GF15 and PA/GF30 (e) Charpy impact strength of PA, PA/V15-N, PA/V15-S, PA/V30-N, PA/V30-S and PA/T30 (f) Charpy impact strength of PA/V15-S/GF15, PA/GF15 and PA/GF30.

4.2.2 Morphology

There have been numerous studies of surface morphology of composites. Scanning electron microscopy (SEM) is the major technique used. Morphological studies concentrate either on the exposed surface or on the interface between the fiber and polymer matrix. [23]

The scanning microscope electron (SEM) was used to examine the tensile fracture surface of Vetiver grass fiber/polyamide-6 composite based on treated Vetiver grass fiber content of 15 %: Figure 4.3 (a) and Figure 4.3 (b), treated Vetiver grass fiber content of 30 %: Figure 4.3 (c) and Figure 4.3 (d) and treated Vetiver grass fiber content of 15% and glass fiber reinforced content of 15%: Figure 4.3 (e).

Figure 4.3 shows that there is no gap between treated grass fiber and polymer matrix (highlighted with a circle). This can be explained that the chemical treatment had improved the surface of Vetiver grass fiber. Therefore, the interfacial adhesion between treated grass fiber and polymer matrix was increased.

It can be noted that improvement of the interfacial adhesion between matrix and treated grass fiber, thus increasing the mechanical properties of the Vetiver grass fiber/polyamide-6 composites than unfilled polyamide-6.

A possible explanation for the results with improvement of the interfacial adhesion between matrix and treated grass fiber is that moisture can cause partial hydrolysis of polyamide-6 at high temperatures, following the reaction (Eq. 4.1) generating carboxylic acid end groups. These are more compatible with the -OH groups of cellulose from the grass fiber, or may react with these groups forming ester bonds. [2]



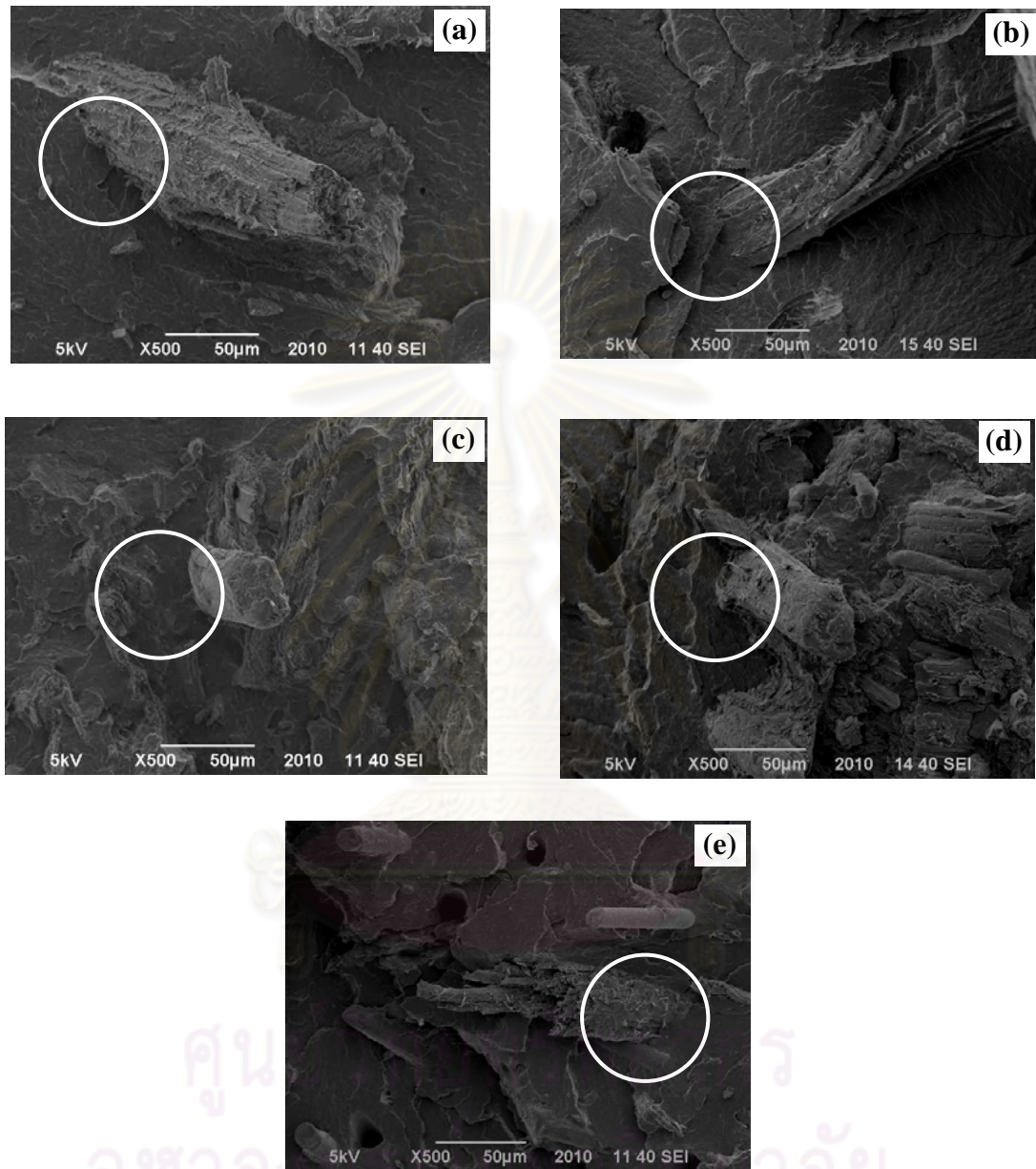


Figure 4.3 SEM micrographs of composites after conditioning at 23 °C and 50 %RH for 24 h: (a) PA/V15-N, (b) PA/V15-S, (c) PA/V30-N (d) PA/V30-S and (e) PA/V15-S/GF15 (X500 magnification, scale bar = 50 µm).

4.3 Accelerated Weathering: Xenon Weathering

Light source: Xenon arc was adapted for accelerated weathering in 1954 in Germany. Initially, there were several problems with the source stability over time and with the choice of proper filters, but, after these were overcome, the Xenon arc lamp emerged as the source most closely resembling UV radiation in the daylight spectrum. Water has an advantage as a cooling medium because it also eliminates part of infrared radiation above 1200 nm. There is no doubt that xenon arc is the artificial radiation source closest to natural daylight. [23]

4.3.1 Mechanical Properties

In this work, the effect of accelerated weathering via Xenon weathering on the mechanical properties of reinforced polyamide-6 were studied and the result of Xenon weathering of composites at 100, 250, 500, and 1000 h are presented in the Table 4.2 - 4.3 and Figure 4.4 - 4.7

From Figure 4.4 (a), tensile strength of silane coupling agent treated grass fibers reinforced composites after accelerated weathering was higher than that of unfilled, mercerization treated grass fiber reinforced composites and talc filled (25%) composites respectively. From Figure 4.4 (b), tensile strength of silane coupling agent treated grass fiber (15%) and glass fiber (15%) reinforced composites (PA/V15-S/GF15) after accelerated weathering was lower than that of glass fiber reinforced composites at both contents (15 and 30%).

From Figure 4.5 (a), tensile modulus of silane coupling agent treated grass fiber (15%) and glass fiber (15%) reinforced composites (PA/V15-S/GF15) after accelerated weathering was lower than that of talc (25%) filled composites and glass fiber reinforced composites at both contents (15 and 30%), but higher than that of treated grass fibers (30%) reinforced composites. From Figure 4.5 (b), flexural modulus of silane coupling agent treated grass fiber (15%) and glass fiber (15%) reinforced composites (PA/V15-S/GF15) after accelerating weathering was lower than that of talc filled (25%) composites and glass fiber reinforced composites at both contents (15 and 30%), but higher than that of treated grass fibers reinforced (30%) composites and unfilled composites.

From Figure 4.6 (a), flexural strength of silane coupling agent treated grass fiber reinforced (30%) composites after accelerated weathering was higher than that of mercerization treated fiber (30%) reinforced composites and talc filled (25%) composites. From Figure 4.6 (b), flexural strength of silane coupling agent treated grass fiber (15%) and glass fiber (15%) reinforced composites (PA/V15-S/GF15) after accelerated weathering was lower than that of glass fiber reinforced composites at both contents (15 and 30%).

From Figure 4.7 (a), Charpy impact strength of silane coupling agent treated grass fiber reinforced composites after accelerated weathering was higher than that of and talc filled (25%) composites and the same as that of mercerization treated fiber reinforced composites when compared at the same content (15% and 30%). From Figure 4.7 (b), Charpy impact strength of silane coupling agent treated grass fiber (15%) and glass fiber (15%) reinforced composites (PA/V15-S/GF15) after accelerated weathering was lower than that of glass fiber reinforced composites at both contents (15 and 30%).

Table 4.2 Tensile properties and retention of composites after accelerated weathering in Xenon weathering meter for 1000 h

Sample	Time (hour)	Tensile Strength (MPa)		Elongation at break (%)		Tensile Modulus (GPa)	
		Weathering	Retention (%)	Weathering	Retention (%)	Weathering	Retention (%)
PA	100	59.0 (1.83)	75.8 (2.34)	5.0 (1.84)	5.8 (2.13)	2.2 (0.19)	82.4 (7.22)
	250	58.3 (1.31)	74.8 (1.68)	4.9 (0.63)	5.7 (0.73)	2.2 (0.21)	84.6 (7.47)
	500	55.2 (2.76)	70.9 (3.55)	4.8 (1.45)	5.6 (1.68)	2.1 (0.34)	79.9 (13.00)
	1000	34.9 (6.54)	44.9 (8.40)	4.1 (4.17)	4.8 (4.82)	1.7 (0.20)	62.9 (7.50)
PA/V15-N	100	59.9 (1.56)	89.8 (2.26)	3.4 (1.20)	126.3 (44.15)	3.6 (0.24)	99.2 (6.39)
	250	59.8 (2.04)	89.6 (3.07)	3.1 (1.06)	115.4 (39.01)	3.4 (0.15)	92.8 (4.19)
	500	58.8 (6.62)	88.1 (9.93)	3.9 (2.28)	145.2 (84.22)	3.3 (0.37)	91.3 (10.16)
	1000	48.2 (2.44)	72.2 (3.66)	2.8 (1.35)	103.6 (49.62)	2.8 (0.18)	76.4 (4.87)
PA/V15-S	100	60.6 (2.37)	87.3 (3.46)	3.6 (1.73)	122.3 (59.66)	3.6 (0.12)	97.1 (3.49)
	250	60.3 (1.50)	86.9 (2.30)	3.4 (1.50)	115.8 (51.65)	3.4 (0.15)	93.7 (4.40)
	500	60.1 (1.21)	86.6 (1.74)	3.4 (0.93)	116.0 (32.02)	3.3 (0.21)	90.5 (5.79)
	1000	49.5 (1.23)	71.3 (1.77)	3.1 (1.33)	107.9 (45.67)	2.8 (0.16)	77.3 (4.49)
PA/V30-N	100	64.5 (2.10)	88.4 (2.90)	2.6 (0.23)	108.3 (9.59)	4.5 (0.39)	97.8 (8.43)
	250	63.9 (3.06)	87.6 (4.18)	2.6 (0.60)	111.1 (25.41)	4.5 (0.42)	96.3 (9.10)
	500	63.3 (3.44)	86.8 (4.72)	2.3 (0.59)	99.2 (24.83)	4.5 (0.55)	95.8 (11.93)
	1000	53.9 (1.24)	73.9 (1.71)	2.3 (0.48)	99.3 (20.31)	3.5 (1.40)	75.4 (30.16)
PA/V30-S	100	70.3 (2.13)	91.4 (2.81)	2.9 (0.48)	109.8 (18.17)	4.7 (0.27)	99.0 (5.87)
	250	70.3 (2.10)	91.5 (2.74)	2.9 (0.86)	109.9 (32.15)	4.4 (0.24)	93.5 (5.04)
	500	70.2 (8.53)	91.3 (11.10)	2.5 (0.39)	92.5 (14.78)	4.3 (0.67)	91.8 (14.27)
	1000	59.2 (1.52)	77.0 (1.98)	2.4 (0.61)	89.5 (22.84)	3.9 (0.45)	82.3 (9.55)
PA/T30	100	67.5 (1.47)	86.5 (1.85)	2.9 (0.33)	152.6 (17.37)	8.0 (0.06)	93.4 (0.67)
	250	66.1 (1.74)	84.6 (2.26)	2.7 (0.21)	144.3 (10.92)	8.0 (0.09)	94.2 (1.08)
	500	65.2 (2.61)	83.5 (3.34)	2.7 (0.52)	143.0 (27.39)	7.6 (0.37)	89.3 (4.33)
	1000	45.0 (1.54)	57.6 (1.98)	2.2 (0.11)	117.2 (5.65)	5.2 (0.17)	60.6 (1.96)
PA/V15-S/GF15	100	74.2 (1.06)	90.4 (1.29)	2.9 (0.42)	99.7 (14.26)	5.2 (0.21)	97.0 (3.91)
	250	73.6 (2.36)	89.6 (2.87)	3.0 (0.40)	102.2 (13.83)	5.2 (0.21)	96.5 (3.98)
	500	73.2 (4.03)	89.2 (4.91)	2.9 (1.40)	98.3 (47.90)	5.2 (0.23)	95.8 (4.34)
	1000	61.1 (6.77)	74.5 (8.24)	2.5 (0.50)	83.9 (16.69)	4.2 (0.44)	78.2 (8.23)
PA/GF15	100	110.9 (1.32)	88.3 (1.10)	4.3 (2.36)	157.1 (85.53)	5.6 (0.12)	90.8 (2.17)
	250	107.9 (3.24)	85.9 (2.62)	4.2 (0.96)	150.4 (34.64)	5.5 (0.39)	89.6 (6.31)
	500	105.5 (4.09)	84.0 (3.25)	2.7 (0.99)	99.1 (36.00)	5.2 (0.85)	84.8 (13.83)
	1000	78.5 (9.09)	62.4 (7.32)	2.8 (0.82)	102.0 (29.69)	4.4 (0.37)	71.0 (5.95)
PA/GF30	100	157.7 (7.17)	87.6 (4.00)	4.0 (0.62)	113.1 (17.37)	9.4 (0.60)	96.6 (6.26)
	250	155.7 (2.58)	87.6 (1.42)	3.9 (0.13)	108.3 (3.77)	9.3 (0.81)	95.4 (5.35)
	500	152.7 (4.41)	84.8 (2.45)	3.1 (0.90)	86.9 (25.07)	9.3 (0.28)	95.6 (2.84)
	1000	134.7 (5.77)	74.8 (3.20)	2.9 (0.85)	81.3 (23.68)	9.0 (2.40)	92.5 (24.67)

Table 4.3 Flexural properties, Charpy impact strength and retention of composites after accelerated weathering in Xenon weathering meter for 1000 h

Sample	Time (hour)	Flexural Strength (MPa)		Flexural Modulus (GPa)		Charpy Impact Strength (kJ m ⁻²)	
		Weathering	Retention (%)	Weathering	Retention (%)	Weathering	Retention (%)
PA	100	78.3 (6.24)	76.1 (6.04)	2.2 (0.04)	90.8 (1.47)	2.6 (0.33)	46.8 (5.98)
	250	69.1 (15.83)	67.1 (15.38)	2.0 (0.10)	83.4 (4.04)	1.4 (0.16)	24.4 (2.55)
	500	62.4 (7.64)	60.6 (7.42)	1.6 (0.17)	68.0 (7.28)	1.3 (0.12)	22.7 (2.16)
	1000	53.7 (4.98)	52.2 (4.84)	1.1 (0.14)	45.6 (5.87)	1.3 (0.06)	22.8 (1.02)
PA/V15-N	100	92.0 (3.81)	86.1 (3.56)	3.1 (0.15)	123.8 (35.23)	2.2 (0.21)	80.9 (6.55)
	250	85.2 (9.03)	79.7 (8.86)	2.9 (0.12)	114.6 (36.38)	1.9 (0.45)	70.9 (16.45)
	500	82.2 (2.77)	76.9 (2.59)	2.8 (0.07)	111.9 (33.54)	1.8 (0.17)	66.7 (6.19)
	1000	81.0 (3.17)	75.8 (2.96)	2.5 (0.04)	98.7 (29.58)	1.3 (0.17)	48.4 (6.40)
PA/V15-S	100	91.9 (10.26)	86.8 (9.66)	3.0 (0.21)	95.9 (6.41)	2.3 (0.64)	80.5 (22.65)
	250	83.6 (7.52)	79.0 (7.08)	2.8 (0.24)	91.5 (7.87)	2.0 (0.16)	69.8 (5.77)
	500	83.7 (3.50)	79.0 (3.31)	2.7 (0.09)	87.4 (3.05)	2.0 (0.38)	70.2 (13.40)
	1000	83.5 (3.08)	78.8 (2.91)	2.4 (0.07)	78.7 (2.22)	1.3 (0.09)	45.4 (3.11)
PA/V30-N	100	97.8 (11.37)	85.8 (9.93)	4.0 (0.18)	99.2 (4.21)	2.9 (0.35)	98.2 (12.04)
	250	88.4 (7.87)	77.6 (6.83)	3.8 (0.27)	93.6 (6.75)	2.8 (0.10)	97.0 (3.27)
	500	88.2 (3.61)	77.4 (3.16)	3.7 (0.16)	92.1 (3.95)	2.7 (0.24)	92.3 (8.23)
	1000	88.0 (6.97)	77.2 (6.12)	3.2 (0.32)	80.5 (8.00)	2.4 (0.16)	82.3 (5.49)
PA/V30-S	100	103.2 (7.17)	87 (6.05)	4.0 (0.09)	99.9 (2.03)	2.9 (0.59)	97.6 (19.85)
	250	93.0 (6.34)	78.4 (5.34)	3.7 (0.24)	93.3 (6.28)	2.8 (0.36)	92.7 (10.64)
	500	97.1 (2.90)	90.3 (2.44)	3.6 (0.13)	89.0 (3.35)	2.7 (0.21)	92.3 (7.14)
	1000	93.8 (3.71)	79.1 (3.13)	3.2 (0.08)	81.1 (1.99)	2.3 (0.29)	77.2 (9.77)
PA/T30	100	86.7 (3.75)	71.7 (2.00)	6.9 (0.96)	90.3 (12.64)	1.8 (0.21)	88.6 (10.43)
	250	85.4 (16.33)	69.3 (13.22)	6.8 (0.06)	89.1 (8.33)	1.7 (0.16)	84.9 (7.79)
	500	80.3 (2.50)	65.1 (2.02)	6.7 (0.17)	86.7 (2.27)	1.5 (0.08)	73.7 (4.12)
	1000	79.5 (17.04)	64.5 (13.82)	6.1 (0.54)	79.7 (6.98)	10.4 (0.33)	68.9 (16.20)
PA/V15-S/GF15	100	114.4 (9.30)	86.7 (7.05)	4.5 (0.20)	96.1 (4.15)	3.4 (0.70)	102.4 (21.12)
	250	111.5 (5.96)	84.4 (4.52)	4.2 (0.08)	90.0 (1.75)	3.4 (0.50)	103.7 (15.07)
	500	111.3 (2.56)	84.3 (1.94)	4.2 (0.08)	88.6 (1.63)	3.0 (0.20)	90.1 (6.05)
	1000	91.8 (9.09)	69.5 (6.89)	3.5 (0.29)	75.3 (6.08)	3.0 (0.22)	90.5 (6.63)
PA/GF15	100	164.5 (20.58)	83.0 (8.23)	4.8 (0.48)	90.0 (9.35)	7.8 (1.03)	103.8 (13.62)
	250	156.1 (18.87)	77.7 (9.38)	4.7 (0.27)	89.4 (5.12)	7.3 (0.80)	97.3 (10.61)
	500	155.3 (5.05)	77.3 (2.51)	4.4 (0.06)	83.1 (1.13)	7.1 (0.91)	94.6 (12.09)
	1000	129.0 (12.90)	64.2 (6.42)	4.0 (0.39)	75.3 (7.43)	6.9 (0.22)	92.0 (2.95)
PA/GF30	100	228.1 (25.53)	80.9 (3.07)	7.7 (0.51)	92.6 (6.28)	16.3 (1.03)	109.4 (6.92)
	250	223.8 (12.66)	81.5 (4.61)	7.6 (0.27)	90.9 (3.26)	15.7 (0.85)	105.2 (5.67)
	500	220.7 (14.28)	80.4 (5.20)	7.2 (0.35)	86.0 (4.23)	15.9 (1.30)	106.3 (8.70)
	1000	187.4 (10.37)	68.2 (3.78)	6.5 (0.54)	78.3 (6.55)	14.1 (0.77)	94.6 (5.19)

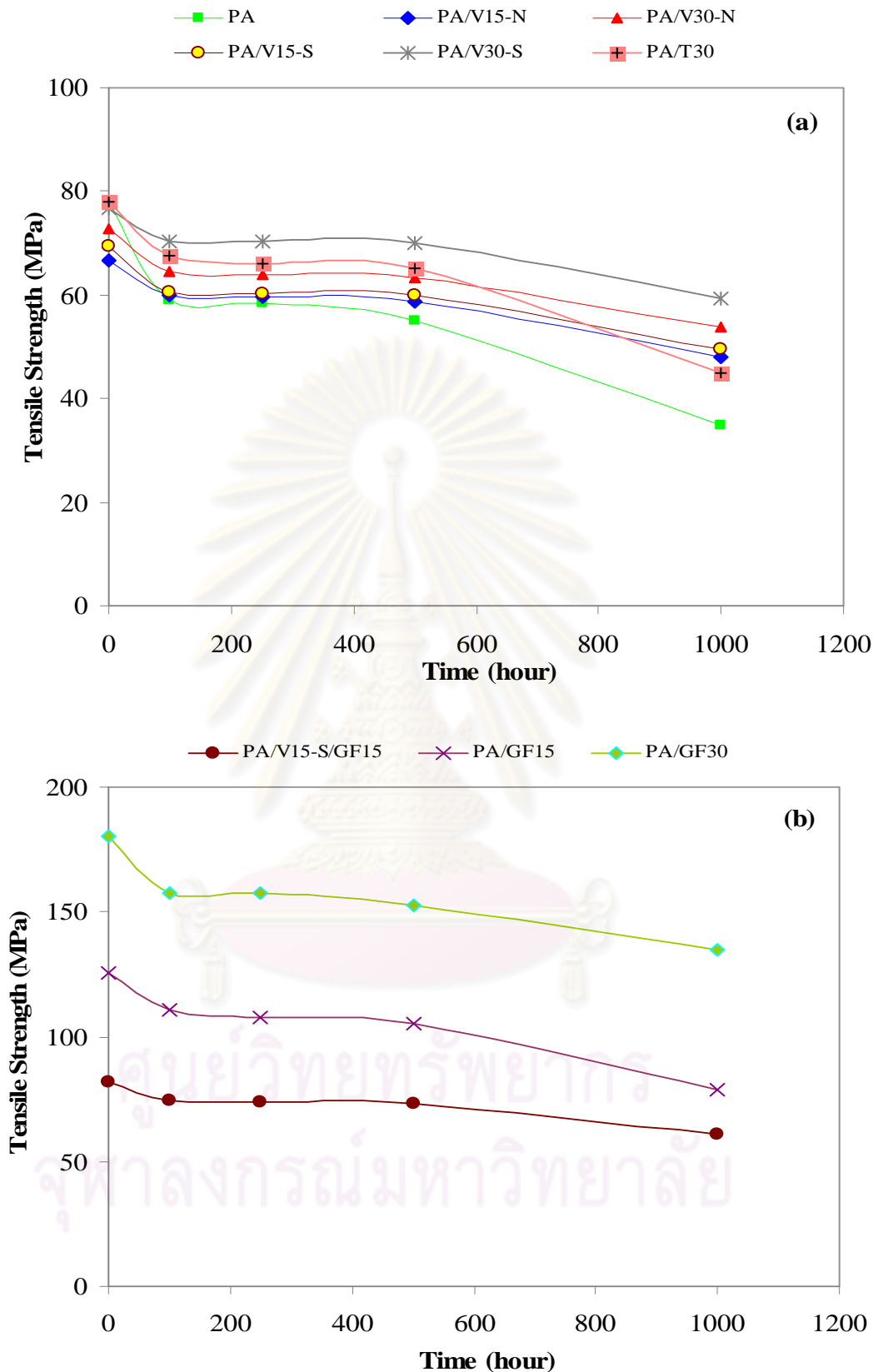


Figure 4.4 Tensile strength of composites after accelerated weathering in Xenon weathering meter 1000 h (a) PA, PA/V15-N, PA/V15-S, PA/V30-N, PA/V30-S and PA/T30 (b) PA/V15-S/GF15, PA/GF15 and PA/GF30.

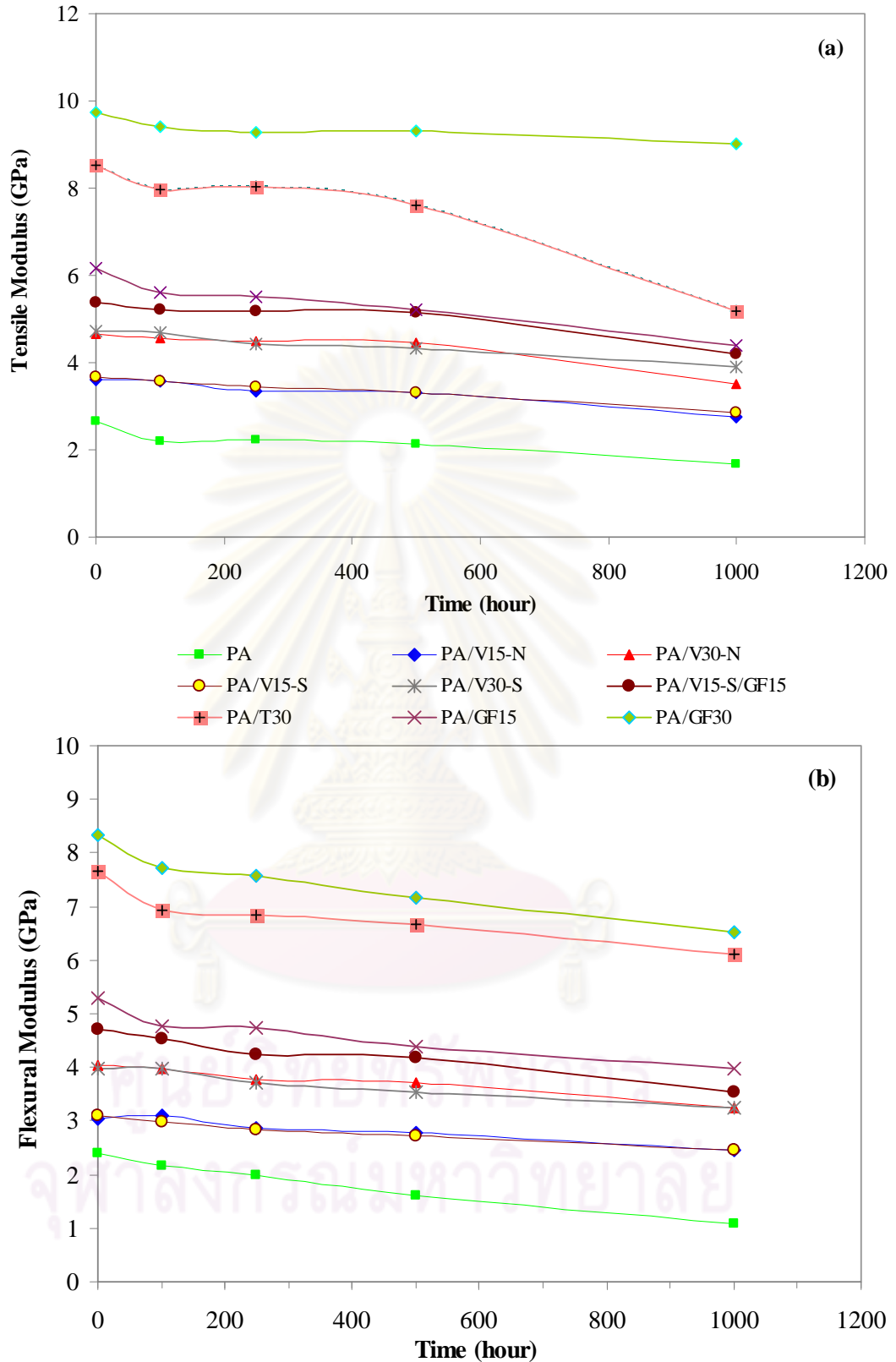


Figure 4.5 Modulus of composites after accelerated weathering in Xenon weathering meter for 1000 h (a) tensile modulus (b) flexural modulus.

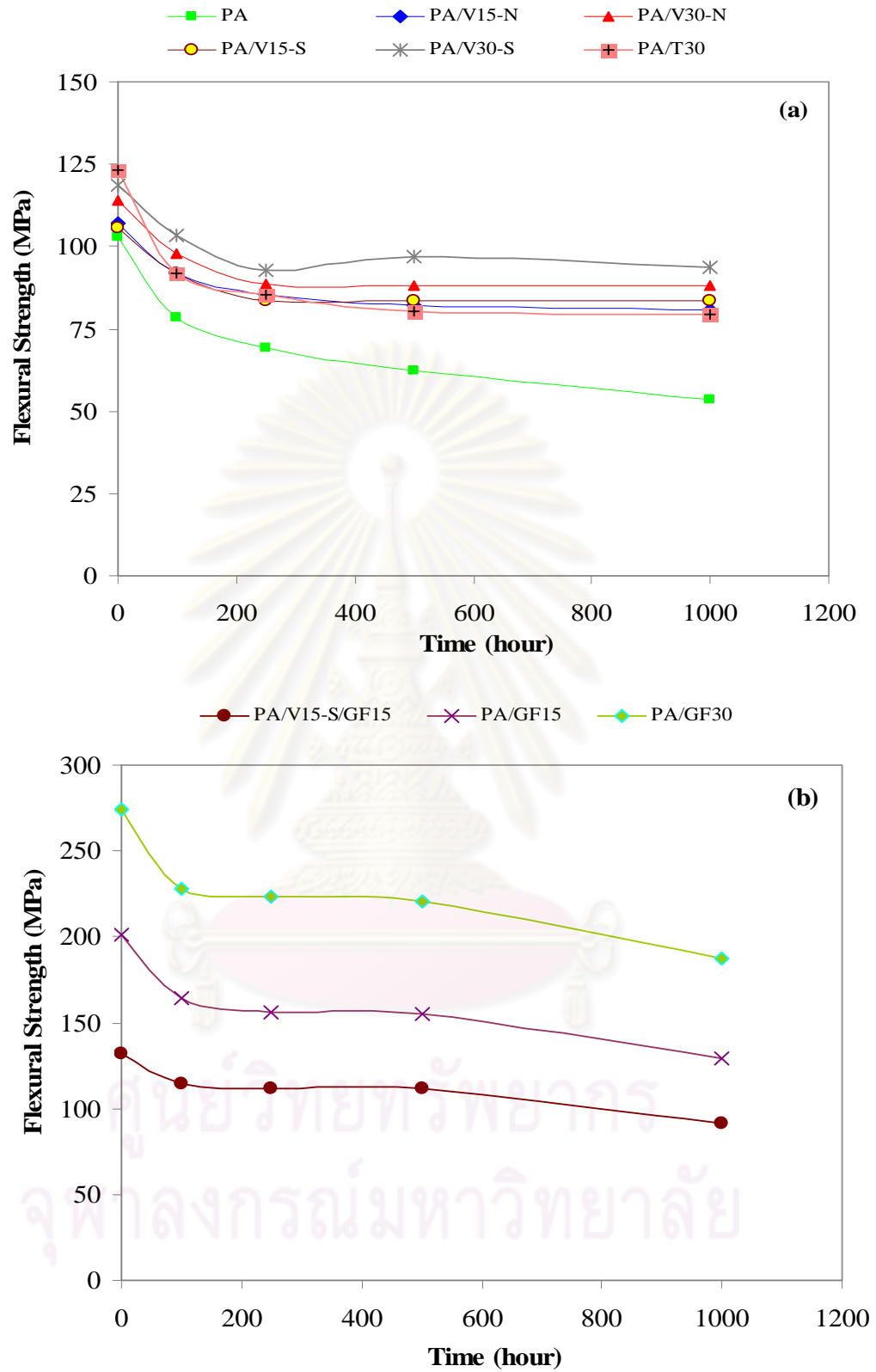


Figure 4.6 Flexural strength of composites after accelerated weathering in Xenon weathering meter for 1000 h (a) PA, PA/V15-N, PA/V15-S, PA/V30-N, PA/V30-S and PA/T30 (b) PA/V15-S/GF15, PA/GF15 and PA/GF30.

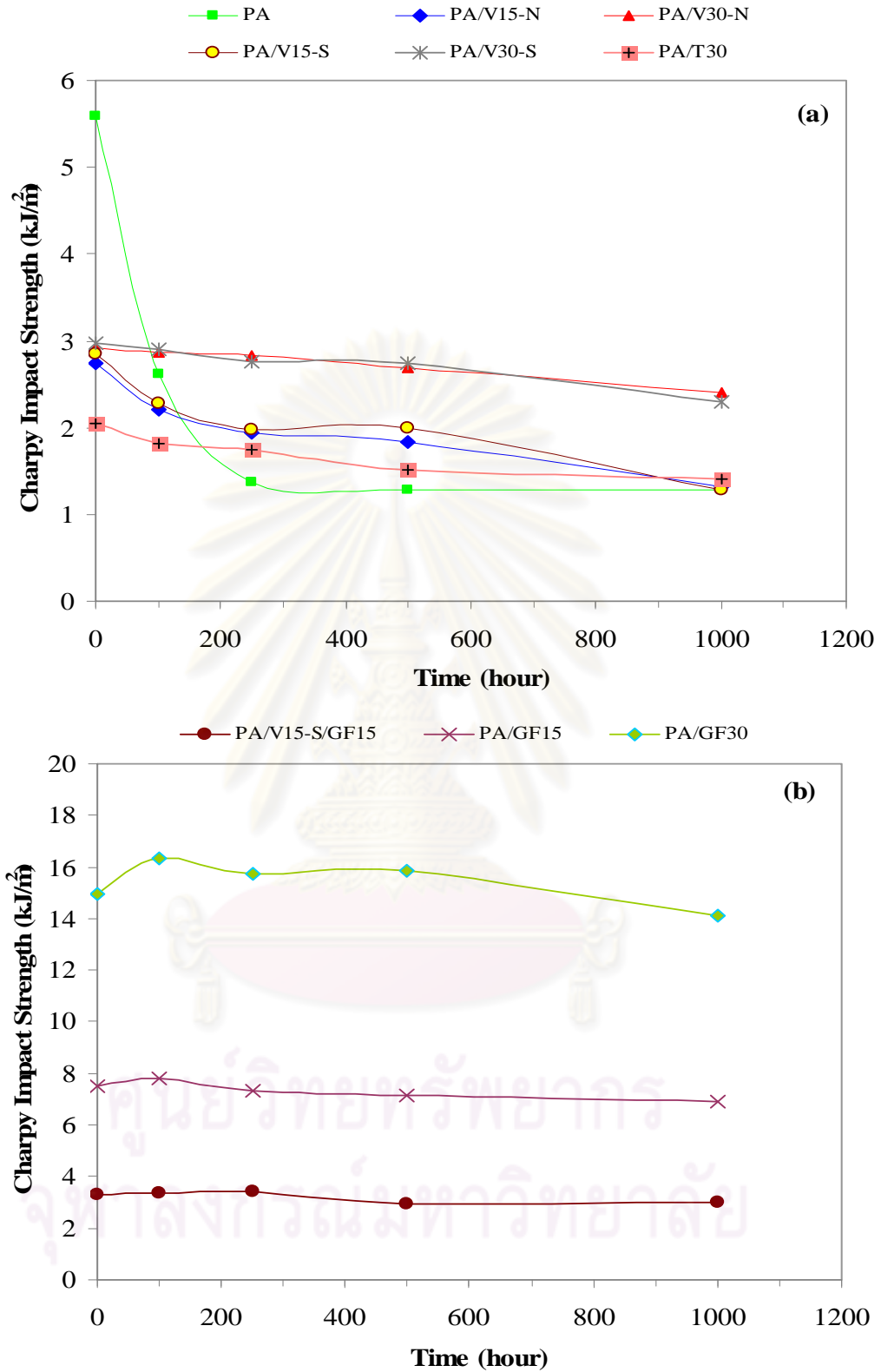


Figure 4.7 Charpy impact strength of composites after accelerated weathering in Xenon weathering meter for 1000 h (a) PA, PA/V15-N, PA/V15-S, PA/V30-N, PA/V30-S and PA/T30 (b) PA/V15-S/GF15, PA/GF15 and PA/GF30.

4.3.2 Retention

For accelerated weathering, the retention rate is defined as follows;

$$\text{Retention rate (\%)} = \frac{\text{Properties after weathering}}{\text{Properties before weathering}} \times 100 \quad (4.2)$$

From Figure 4.8 (a), retention rate of tensile strength of silane coupling agent treated fiber reinforced composites after accelerated weathering for 1000 hour was higher than that of unfilled and talc (25%) filled composite and the same as that of mercerization treated grass fiber reinforced composites when compared at the same fiber content (15% and 30%). From Figure 4.8 (b), retention rate of tensile strength of silane coupling agent treated grass fiber (15%) and glass fiber (15%) reinforced composites (PA/V15-S/GF15) after accelerated weathering for 1000 hour was higher than that of 15% glass fiber reinforced composites (PA/GF15) and the same as that of 30% glass fiber reinforced composites (PA/GF30).

From Figure 4.9 (a), retention rate of elongation at break (EB) of silane coupling agent treated fiber reinforced composites after accelerated weathering for 1000 hour was lower than that of talc (25%) filled composite, but higher than that of unfilled and the same as that of mercerization treated grass fiber reinforced composites when compared at the same fiber content (15% and 30%). From Figure 4.9 (b), retention rate of elongation at break of silane coupling agent treated grass fiber (15%) and glass fiber (15%) reinforced composites (PA/V15-S/GF15) accelerated weathering for 1000 hour was lower than that of 15% glass fiber reinforced composites and the same as that of 30% glass fiber reinforced composites.

From Figure 4.10 (a), retention rate of flexural strength of silane coupling agent treated fiber reinforced composites accelerated weathering for 1000 hour was higher than that of unfilled and talc filled composites and the same as that of mercerization treated grass fiber reinforced composites when compared at the same fiber content (15% and 30%). From Figure 4.10 (b), retention rate of flexural strength of silane coupling agent treated grass fiber (15%) and glass fiber (15%) reinforced composites (PA/V15-S/GF15) accelerated weathering for 1000 hour was lower than that of 15% glass fiber reinforced composites and the same as that of 30% glass fiber reinforced composites.

From Figure 4.11 (a), retention rate of Charpy impact strength of silane coupling agent treated grass fiber (30%) reinforced composites after accelerated weathering for 1000 hour was higher than that of unfilled and talc (25%) filled composites and the same as that of mercerization treated grass fiber reinforced composites when compared at the same fiber content (15% and 30%). From Figure 4.11 (b), retention rate of Charpy impact strength of silane coupling agent treated grass fiber (15%) and glass fiber (15%) reinforced composites (PA/V15-S/GF15) accelerated weathering for 1000 hour was lower than that of 30% glass fiber reinforced composites and the same as that of 15% glass fiber reinforced composites.

The long term stability was decreased in the order following: polyamide composites filled with: glass fiber ~ treated Vetiver grass fiber > talc > unfilled. It is convinced that the Vetiver grass fiber reinforced composites had long term stability against degradation by irradiation of direct natural exposure. These retention results after accelerated weathering with Vetiver grass fiber/polyamide-6 composites enable them to replace talc filled composites and the glass fiber reinforced composites where the mechanical strength is not as the critical specification in automotive applications.

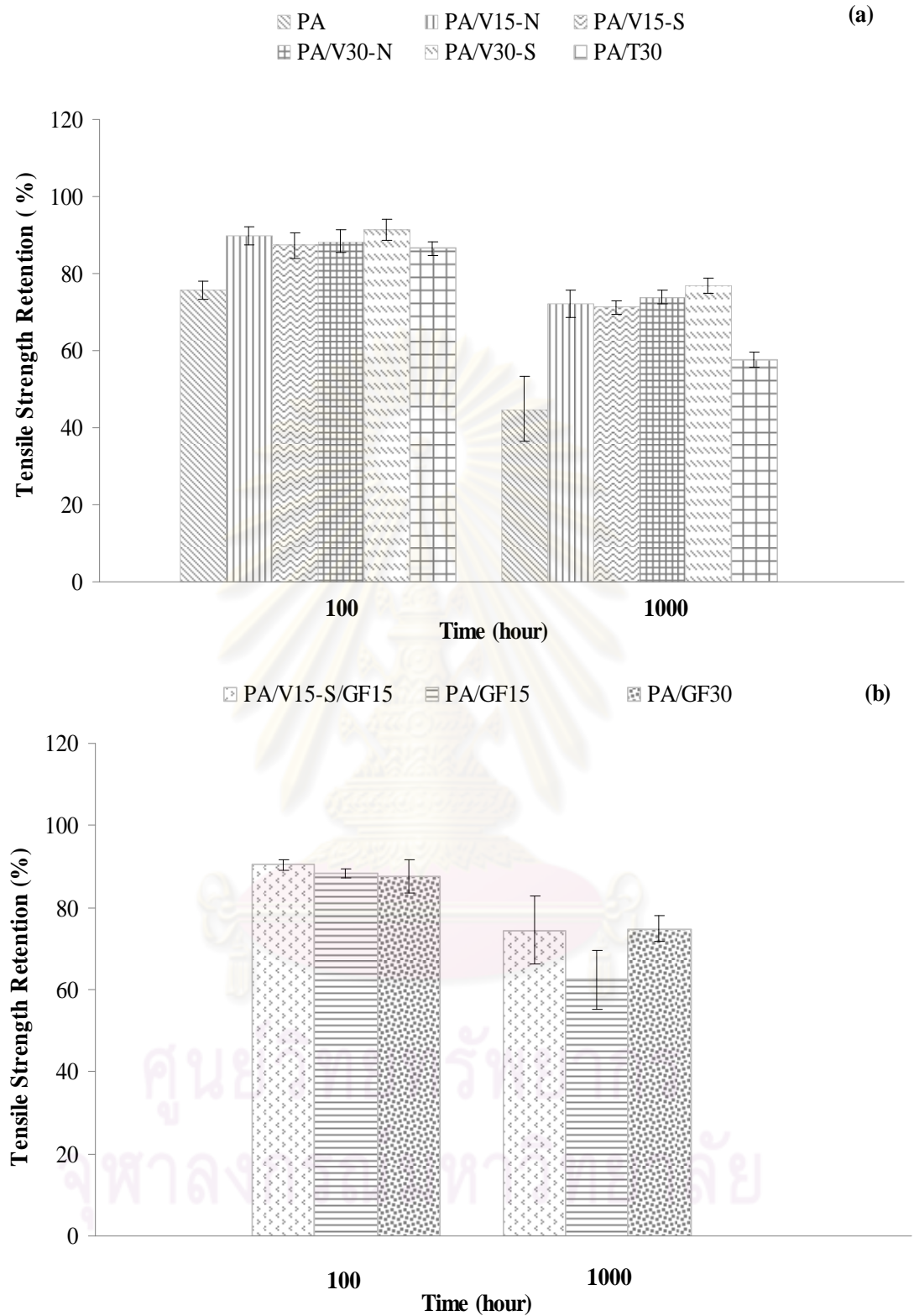


Figure 4.8 Tensile strength retention of composites after accelerated weathering in Xenon weathering meter for 1000 h (a) PA, PA/V15-N, PA/V15-S, PA/V30-N, PA/V30-S and PA/T30 (b) PA/V15-S/GF15, PA/GF15 and PA/GF30.

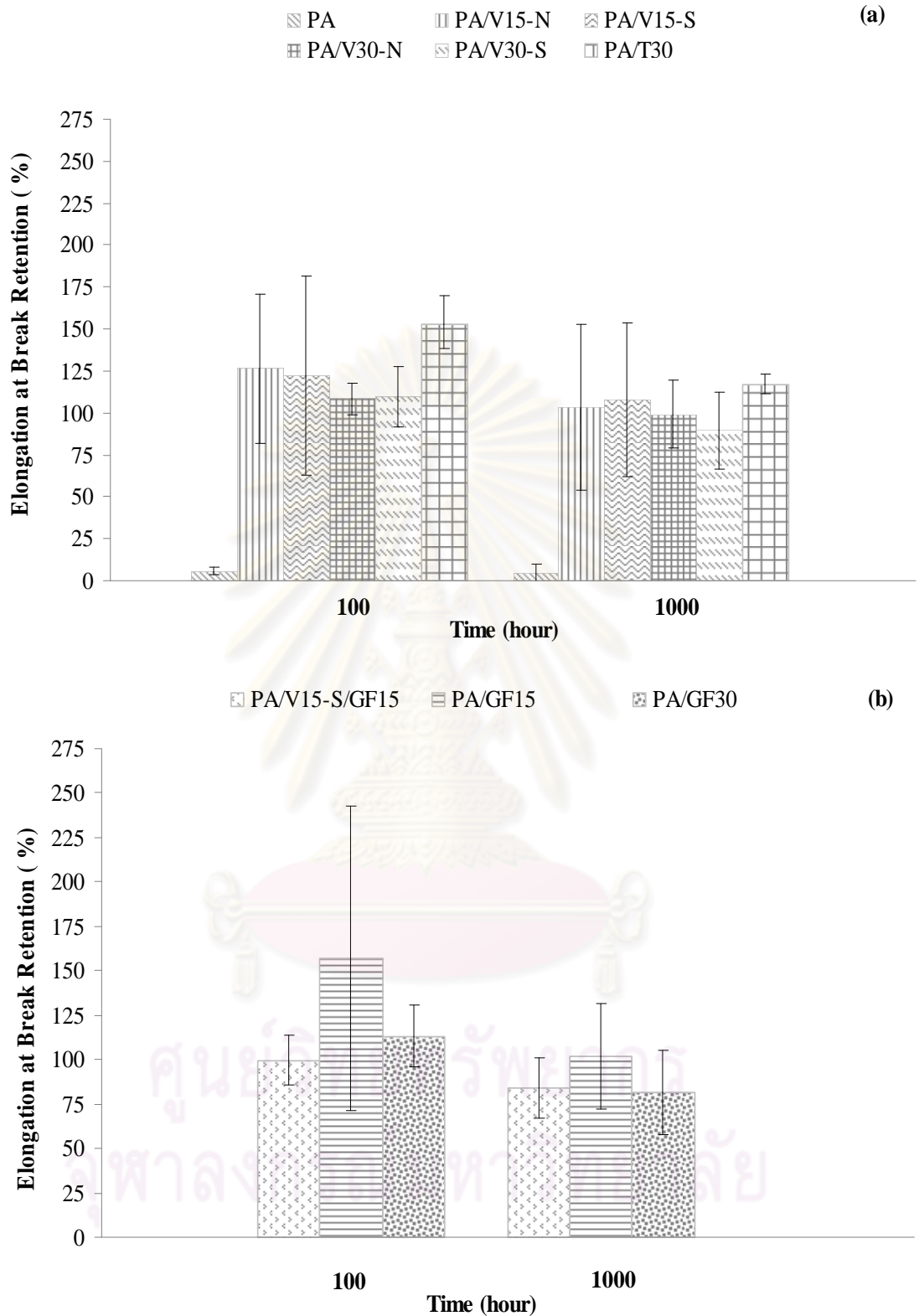


Figure 4.9 Elongation at break retention of composites after accelerated weathering in Xenon weathering meter for 1000 h (a) PA, PA/V15-N, PA/V15-S, PA/V30-N, PA/V30-S and PA/T30 (b) PA/V15-S/GF15, PA/GF15 and PA/GF30.

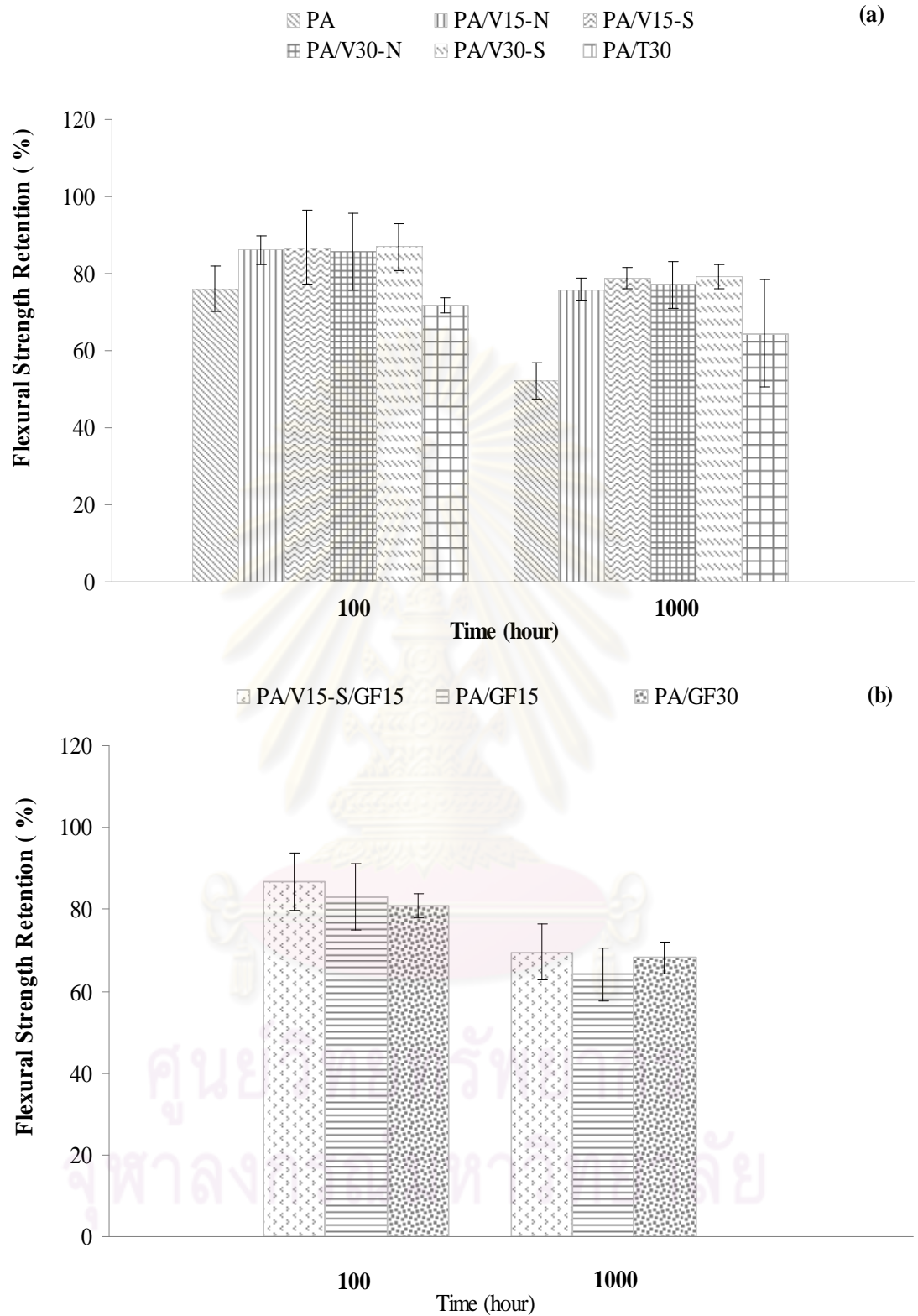


Figure 4.10 Flexural strength retention of composites after accelerated weathering in Xenon weathering meter for 1000 h (a) PA, PA/V15-N, PA/V15-S, PA/V30-N, PA/V30-S and PA/T30 (b) PA/V15-S/GF15, PA/GF15 and PA/GF30.

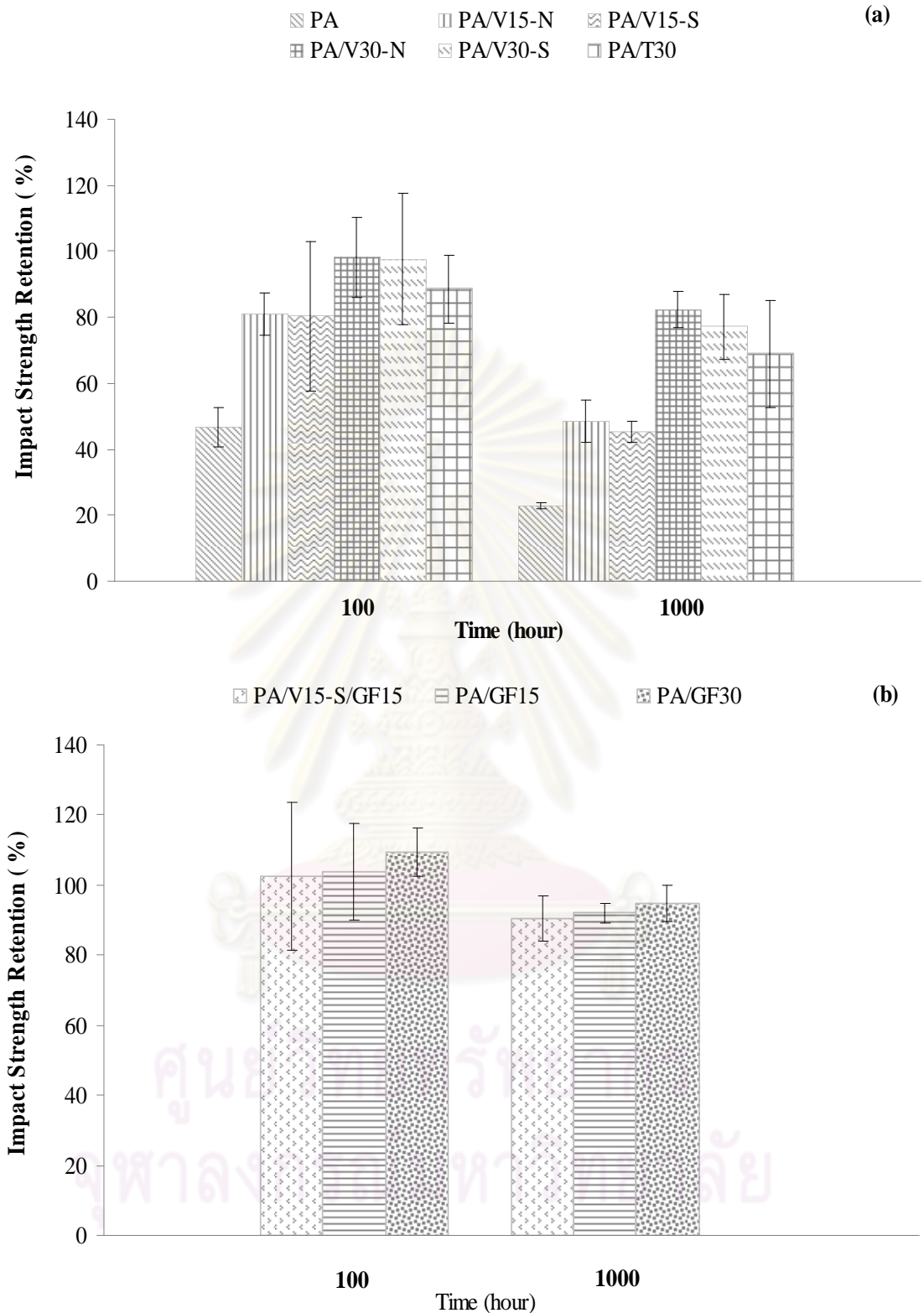


Figure 4.11 Impact strength retention of composites after accelerated weathering in Xenon weathering meter for 1000 h (a) PA, PA/V15-N, PA/V15-S, PA/V30-N, PA/V30-S and PA/T30 (b) PA/V15-S/GF15, PA/GF15 and PA/GF30.

4.3.3 Morphology

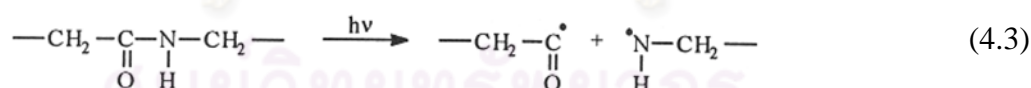
The morphology of fracture surface of treated Vetiver grass fiber composites and treated Vetiver grass fiber (15%) and glass fiber (15%) reinforced composites was investigated.

The scanning microscope electron (SEM) was used to examine the tensile fracture surface of Vetiver grass fiber/poyamide-6 composite after accelerated weathering at 1000 hr based on 15 % of Vetiver grass fiber: Figure 4.12 (a) and Figure 4.12 (b), 30 % of Vetiver grass fiber: Figure 4.12 (c) and Figure 4.12 (d) and treated Vetiver grass fiber (15%) and glass fiber (15%) reinforced composites: Figure 4.12 (e).

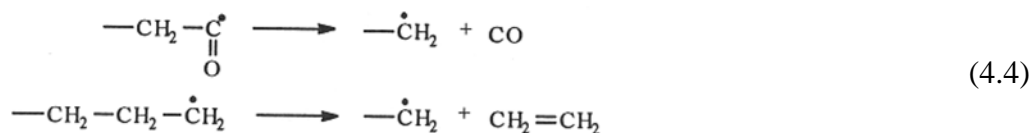
Figure 4.12 shows the slight increase in gap between treated Vetiver grass fiber and polymer matrix. This can be explained that the irradiation had decreased the interfacial adhesion between fiber and polymer matrix. Therefore, the properties of polyamide-6 composites reinforced with treated Vetiver grass fiber after accelerated weathering at 1000 h was decreased compared with the normal composites without weathering.

The accelerated weathering causes the interfacial adhesion between fiber and polymer matrix as follows [23]:

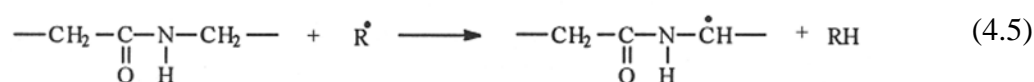
Scission of the amide linkage dominates photolytic reactions as shown in Eq. 4.3:



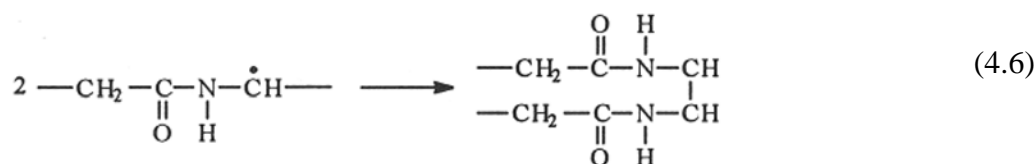
The above reaction is typical for both aliphatic and aromatic polyamides and it is a starting-point of further conversions. The carbonyl radical, after regrouping, forms volatile products, carbon monoxide and ethylene as shown in Eq. 4.4:



Both radicals are capable of abstracting hydrogen from other molecules as shown in Eq. 4.5:

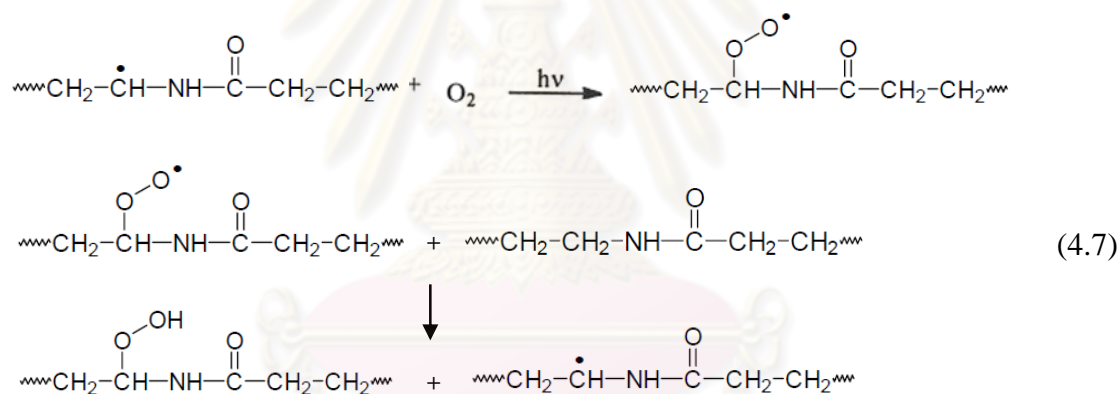


and producing crosslinks as shown in Eq. 4.6.:

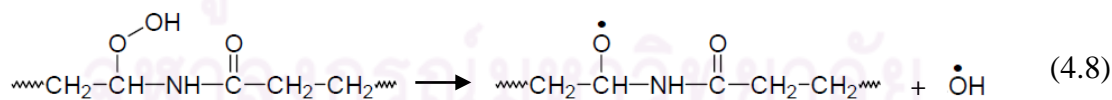


The above radical is very stable and persists to cause crosslinking, crystalline structure of polymer affects probability of crosslinking. In amorphous areas, the number of hydrogen bonds is less which allows radicals to migrate freely and cause crosslinking reactions.

The presence of oxygen during photolysis changes the mechanism of degradation, favors individual reactions, and causes an overall increase in the rate of degradation. The initial steps of photooxidation are similar to photolysis. Both carbonyl and amino radicals are formed. The next stage of photooxidation involves the formation of hydroperoxides from existing radicals as shown in Eq. 4.7:

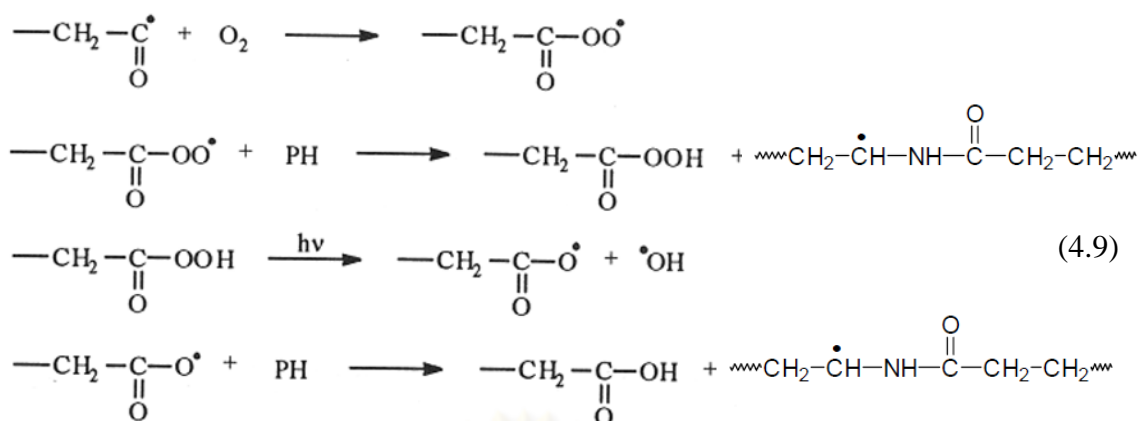


One radical may theoretically produce one molecule of hydroperoxide and a new radical. Hydroperoxyl radical can dissociate further as shown in Eq. 4.8:

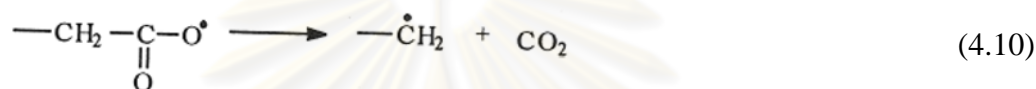


With the production of two new free radicals which autoaccelerate the process. The degree of autoacceleration depends on the energy supplied, and the material composition. Recombination of radicals will decrease the efficiency of photodegradation.

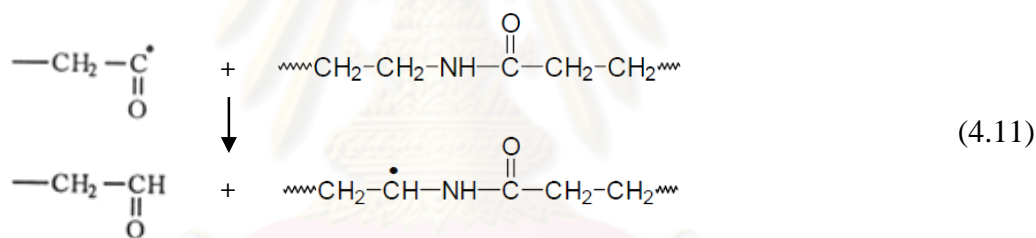
Several typical products are formed during photooxidation. Carboxylic acids are produced as a consequence of carbonyl radical oxidation as shown in Eq. 4.9:



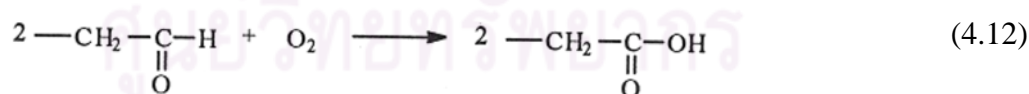
Carboxyl radical may also decompose to form carbon dioxide as shown in Eq. 4.10:



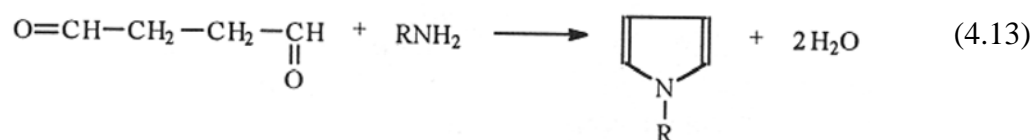
Like carboxylic acids, aldehydes are produced from the carbonyl radical as shown in Eq. 4.11:



and two molecules of aldehydes may be further converted to carboxylic acids as shown in Eq. 4.12:



The yellowing of polyamides is explained by the formation of pyrrole-type compounds which are the condensation products of dicarbonyl compounds with primary amines as shown in Eq. 4.13:



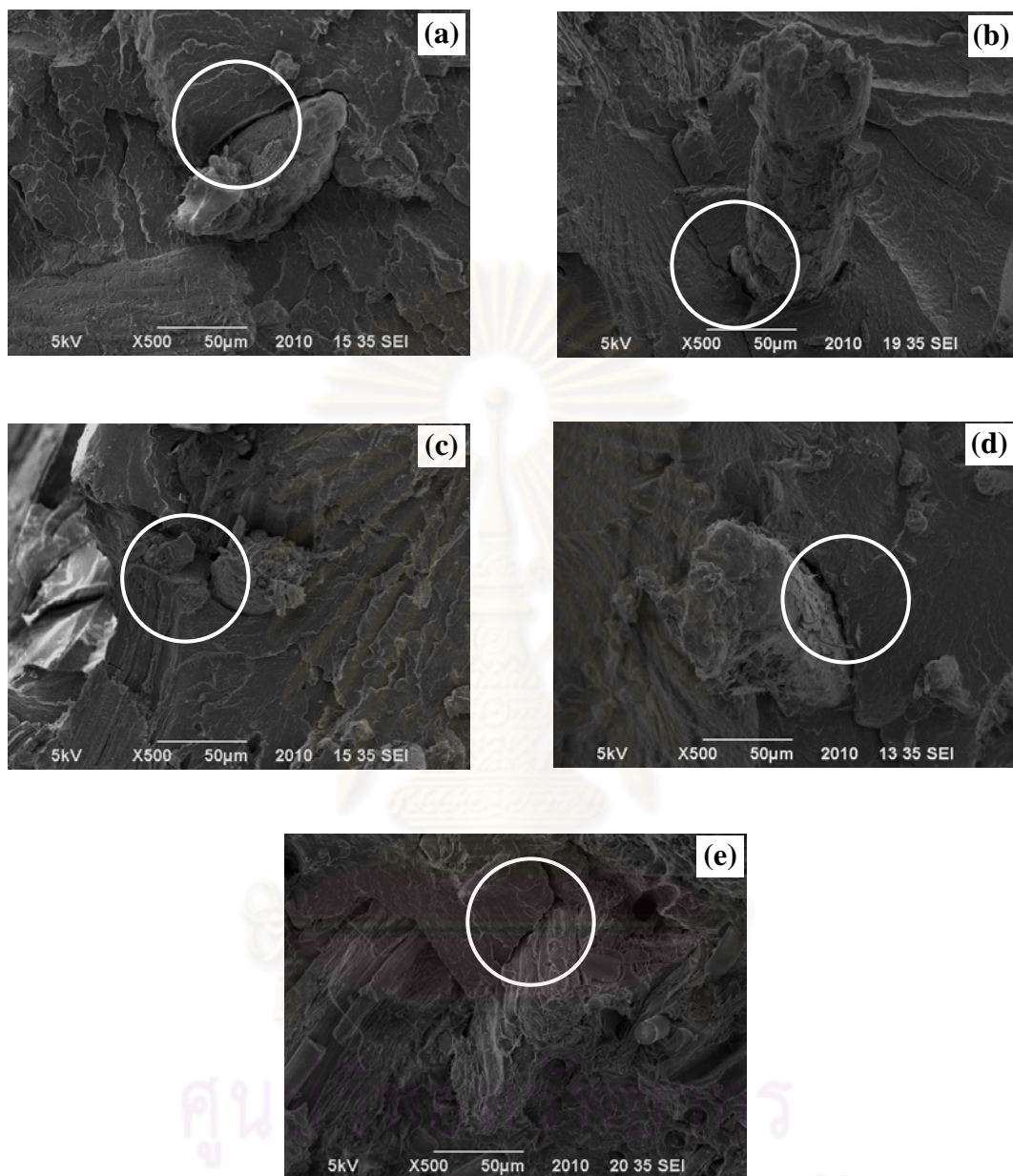


Figure 4.12 SEM micrographs of composites accelerated weathering in Xenon weathering meter for 1000 h: (a) PA/V15-N, (b) PA/V15-S, (c) PA/V30-N, (d) PA/V30-S and (e) PA/V15-S/GF15 (X500 magnification, scale bar = 50 μm).

4.4 Accelerated Weathering: Sunshine Weathering

Light source: Sunshine carbon arc are not found in daylight radiation at the Earth's surface. The radiation spectra of these carbon arcs are very different from daylight spectra. Open flame carbon arc has two strong peaks at 320 and 400 nm which are respectively 4 and 20 times stronger than daylight at the same wavelengths. In other ranges of UV, radiation is substantially lower than in daylight. Sunshine carbon arc offers a substantial improvement over open flame carbon arc but it has a stronger radiation below 320 nm than daylight. This radiation can cause an unrealistic degradation of materials. [23]

4.4.1 Mechanical Properties

In this work, the effect of accelerated weathering via sunshine weathering on the mechanical properties of reinforced polyamide-6 were studied and the result of sunshine weathering of composites at 100, 250, 500, and 1000 h are presented in the Table 4.4 - 4.5 and Figure 4.13 - 4.16.

From Figure 4.13 (a), tensile strength of silane coupling agent treated grass fiber reinforced composites after accelerated weathering for 1000 hour was higher than that of unfilled, mercerization treated grass fiber reinforced composites and talc (25%) filled composite. From Figure 4.13 (b), tensile strength of silane coupling agent treated grass fiber (15%) and glass fiber (15%) reinforced composites (PA/V15-S/GF15) after accelerated weathering for 1000 hour was lower than that of glass fiber reinforced composites at both contents (15 and 30%).

From Figure 4.14 (a), tensile modulus of silane coupling treated grass fiber (15%) and glass fiber (15%) reinforced composites (PA/V15-S/GF15) after accelerated weathering for 1000 hour was lower than that of talc (25%) filled composites and glass fiber reinforced composites, but higher than that of treated grass fiber reinforced composites and unfilled composite. From Figure 4.14 (b), flexural modulus of silane coupling treated grass fiber (15%) and glass fiber (15%) reinforced composites (PA/V15-S/GF15) after accelerated weathering for 1000 hour was lower than that of talc (25%) filled composites and glass fiber reinforced composites at both contents (15 and 30%)., but higher than that of treated grass fiber reinforced composites and unfilled composite.

From Figure 4.15 (a), flexural strength of silane coupling agent treated grass fiber reinforced composites after accelerated weathering for 1000 hour was higher than that of mercerization treated grass fiber reinforced composites when compared at the same content (15 and 30%), but lower than that of talc (25%) filled composites. From Figure 4.15 (b), flexural strength of silane coupling agent treated grass fiber (15%) and glass fiber (15%) reinforced composites (PA/V15-S/GF15) after accelerated weathering was lower than that of glass fiber reinforced composites at both contents (15 and 30%).

From Figure 4.16 (a), Charpy impact strength of silane coupling agent treated grass fibers reinforced composites accelerated weathering for 1000 hour was higher than that of and talc (25%) filled composite and the same as that of mercerization treated grass fiber reinforced composites when compared at the same fiber content (15 and 30%). From Figure 4.16 (b), Charpy impact strength of silane coupling agent treated grass fiber (15%) and glass fiber (15%) reinforced composites (PA/V15-S/GF15) after accelerated weathering was lower than that of glass fiber reinforced composites at both contents (15 and 30%).

Table 4.4 Tensile properties and retention of composites after accelerated weathering in sunshine weathering meter for 1000 h

Sample	Time (hour)	Tensile Strength (MPa)		Elongation at break (%)		Tensile Modulus (GPa)	
		Weathering	Retention (%)	Weathering	Retention (%)	Weathering	Retention (%)
PA	100	63.8 (4.74)	81.9 (6.09)	4.3 (0.66)	4.9 (0.76)	2.7 (0.26)	101.6 (9.69)
	250	65.5 (2.20)	84.1 (2.82)	3.6 (3.31)	4.1 (3.83)	2.8 (0.80)	104.9 (30.32)
	500	54.4 (9.74)	69.9 (12.51)	3.1 (2.66)	3.6 (3.08)	2.8 (0.26)	105.6 (9.94)
	1000	34.6 (8.48)	44.4 (10.89)	1.3 (0.33)	1.5 (0.38)	2.5 (0.28)	92.6 (10.39)
PA/V15-N	100	69.7 (2.53)	104.4 (3.79)	2.7 (0.23)	98.7 (8.40)	3.8 (0.18)	104.2 (4.93)
	250	67.8 (3.60)	101.6 (5.39)	2.7 (0.41)	99.3 (15.30)	3.7 (0.25)	101.1 (6.92)
	500	60.3 (6.60)	90.3 (9.88)	2.4 (0.95)	87.5 (35.02)	3.7 (0.58)	103.6 (16.14)
	1000	45.1 (5.43)	67.6 (8.14)	1.2 (0.58)	45.9 (21.29)	3.3 (1.35)	91.6 (37.46)
PA/V15-S	100	70.2 (1.56)	101.2 (2.26)	3.3 (0.54)	115.2 (18.46)	3.7 (0.52)	99.8 (9.42)
	250	66.3 (9.85)	95.6 (14.19)	2.8 (1.90)	97.9 (65.36)	3.6 (0.35)	96.8 (9.42)
	500	61.9 (4.47)	89.2 (6.44)	2.5 (0.41)	85.0 (14.12)	3.5 (0.21)	94.0 (5.85)
	1000	42.4 (8.71)	61.2 (12.55)	1.2 (0.23)	41.4 (7.98)	3.6 (0.34)	99.3 (9.17)
PA/V30-N	100	74.6 (3.71)	102.4 (5.10)	2.4 (0.48)	100.6 (20.47)	4.8 (0.40)	102.2 (8.67)
	250	72.1 (5.18)	98.9 (7.11)	2.3 (0.72)	95.5 (30.40)	4.7 (0.91)	102.1 (19.55)
	500	70.8 (4.03)	97.1 (5.53)	2.5 (0.60)	105.4 (25.56)	4.8 (0.76)	103.8 (16.26)
	1000	70.0 (3.13)	96.0 (4.29)	2.1 (0.42)	88.8 (17.99)	4.4 (0.46)	95.5 (9.80)
PA/V30-S	100	78.6 (4.00)	102.2 (5.20)	2.8 (0.59)	104 (22.19)	4.9 (0.18)	102.7 (3.91)
	250	78.5 (1.25)	102.1 (1.63)	2.8 (1.13)	103.7 (42.53)	4.7 (0.79)	98.8 (16.77)
	500	73.5 (2.80)	95.7 (3.65)	2.5 (0.79)	93.6 (29.66)	4.4 (0.56)	93.9 (11.86)
	1000	66.0 (9.06)	85.8 (11.79)	1.6 (0.66)	59.0 (24.71)	4.3 (1.13)	90.2 (23.80)
PA/T30	100	76.9 (6.77)	98.5 (8.67)	2.1 (1.06)	110.2 (55.67)	8.9 (0.69)	103.7 (8.07)
	250	75.6 (6.19)	96.7 (7.92)	2.2 (1.23)	114.9 (64.95)	8.8 (1.71)	103.3 (20.01)
	500	74.8 (3.32)	95.7 (4.25)	2.6 (0.66)	138.9 (34.77)	8.6 (0.46)	100.7 (5.42)
	1000	73.5 (2.64)	94.1 (3.37)	2.5 (0.28)	133.2 (14.76)	8.5 (0.49)	99.1 (5.71)
PA/V15-S/GF15	100	83.6 (1.28)	101.8 (1.56)	2.8 (0.32)	94.5 (10.96)	5.4 (0.26)	100.5 (4.92)
	250	83.9 (2.98)	102.2 (3.63)	2.8 (0.38)	95.9 (12.87)	5.3 (0.31)	99.4 (5.68)
	500	79.8 (7.70)	97.2 (9.38)	2.6 (1.28)	87.4 (43.66)	5.2 (0.24)	97.2 (4.40)
	1000	78.6 (8.15)	95.7 (9.93)	2.0 (0.77)	67.0 (26.41)	5.2 (0.71)	96.9 (13.15)
PA/GF15	100	125.5 (1.39)	99.9 (1.11)	2.8 (0.33)	101.6 (12.06)	6.0 (0.17)	98.0 (2.82)
	250	123.4 (7.61)	98.2 (6.06)	2.8 (0.52)	99.9 (18.93)	6.0 (0.12)	97.5 (1.97)
	500	115.8 (3.90)	92.1 (3.10)	2.7 (0.64)	97.3 (23.08)	5.8 (0.25)	94.5 (3.98)
	1000	111.6 (10.28)	88.8 (8.18)	2.4 (0.80)	85.2 (28.88)	5.8 (1.50)	94.2 (24.32)
PA/GF30	100	178.1 (2.54)	98.9 (1.41)	3.6 (0.72)	100.3 (20.01)	9.8 (0.29)	100.4 (2.97)
	250	176.9 (1.87)	98.2 (1.04)	3.6 (0.36)	99.4 (10.12)	9.7 (0.47)	99.5 (4.79)
	500	174.1 (1.58)	96.7 (0.88)	3.4 (0.37)	94.3 (10.30)	9.8 (0.48)	100.3 (4.91)
	1000	171.7 (2.58)	95.3 (1.43)	2.8 (0.50)	77.6 (13.90)	9.0 (2.18)	92.5 (22.42)

Table 4.5 Flexural properties, Charpy impact strength and retention of composites after accelerated weathering in sunshine weathering meter for 1000 h

Sample	Time (hour)	Flexural Strength (MPa)		Flexural Modulus (GPa)		Charpy Impact Strength (kJ m ⁻²)	
		Weathering	Retention (%)	Weathering	Retention (%)	Weathering	Retention (%)
PA	100	99.9 (3.02)	97.0 (2.94)	2.4 (0.02)	102.0 (0.71)	1.3 (0.08)	23.6 (1.42)
	250	43.8 (2.30)	42.6 (2.23)	2.4 (0.18)	102.3 (7.57)	1.4 (0.36)	25.4 (6.42)
	500	40.5 (8.79)	39.3 (8.54)	2.5 (0.07)	105.3 (2.77)	1.3 (0.26)	23.6 (4.65)
	1000	35.2 (9.20)	34.2 (8.93)	1.9 (0.09)	80.6 (3.58)	1.3 (0.07)	24.1 (1.26)
PA/V15-N	100	107.0 (4.07)	100.1 (3.81)	3.3 (0.10)	133.5(39.20)	1.6 (0.25)	60.1 (9.01)
	250	106.1 (3.83)	99.3 (3.58)	3.2 (0.13)	127.0 (41.95)	1.4 (0.53)	52.5 (19.20)
	500	101.9 (17.99)	95.3 (16.84)	3.2 (0.10)	128.4 (40.76)	1.3 (0.10)	47.7 (3.57)
	1000	80.1 (11.62)	75.0 (10.88)	3.0 (0.05)	120.7 (37.54)	1.4 (0.25)	50.0 (9.30)
PA/V15-S	100	104.2 (32.27)	98.4 (30.47)	3.6 (1.82)	118.4 (60.71)	1.3 (0.14)	47.3 (5.01)
	250	104.1 (3.62)	98.3 (3.42)	3.2 (0.09)	105.1 (2.92)	1.3 (0.30)	45.7 (10.35)
	500	105.6 (2.02)	99.7 (1.90)	3.2 (0.06)	107.4 (1.90)	1.3 (0.05)	46.9 (1.75)
	1000	112.2 (1.21)	106.0 (1.14)	3.1 (0.18)	101.8 (6.13)	1.3 (0.23)	44.3 (8.14)
PA/V30-N	100	114.0 (7.35)	100.0 (6.45)	4.2 (0.09)	104.4 (2.25)	2.6 (0.62)	87.7 (21.15)
	250	113.2 (5.19)	99.3 (4.55)	4.1 (0.08)	102.1 (1.90)	2.5 (0.50)	85.9 (17.14)
	500	112.4 (5.39)	98.6 (4.73)	4.1 (0.15)	102.3 (3.71)	2.5 (0.33)	87.1 (11.35)
	1000	107.9 (3.93)	94.6 (3.44)	3.8 (0.11)	95.4 (2.67)	2.4 (0.42)	82.6 (14.40)
PA/V30-S	100	118.5 (3.40)	100.0 (2.87)	4.1 (0.22)	102.6 (5.42)	2.3 (0.14)	78.1 (4.71)
	250	116.6 (4.30)	98.4 (3.63)	4.1 (0.14)	102.8 (3.62)	2.4 (0.81)	81 (27.16)
	500	118.0 (3.68)	99.5 (3.10)	4.1 (0.13)	103.1 (3.32)	2.4 (0.19)	81.3 (6.37)
	1000	114.7 (11.02)	96.7 (9.30)	3.8 (0.08)	95.5 (1.96)	2.4 (0.36)	81.7 (12.14)
PA/T30	100	121.7 (2.16)	98.7 (1.75)	7.7 (0.20)	99.9 (2.61)	2.0 (0.40)	98.9 (19.56)
	250	120.8 (4.30)	97.9 (3.48)	7.7 (0.26)	100.6 (3.43)	1.9 (0.56)	93.7 (27.40)
	500	119.3 (3.56)	96.7 (2.89)	7.8 (0.17)	102.3 (2.17)	1.6 (0.15)	79.8 (7.08)
	1000	117.9 (6.07)	95.6 (4.92)	7.7 (0.21)	100.8 (2.71)	1.6 (0.09)	76.2 (4.50)
PA/V15-S/GF15	100	131.3 (2.05)	99.5 (1.79)	4.6 (0.13)	98 (2.68)	3.2 (0.18)	96.0 (5.37)
	250	127.5 (5.59)	96.6 (4.23)	4.6 (0.11)	98.3 (2.32)	3.1 (0.47)	93.9 (14.31)
	500	127.3 (11.03)	96.4 (8.36)	4.7 (0.19)	98.8 (3.97)	3.1 (0.09)	94.7 (2.74)
	1000	127.2 (6.19)	96.3 (4.69)	4.4 (0.20)	94.3 (4.28)	3.1 (0.16)	94.2 (4.94)
PA/GF15	100	200.9 (3.01)	100 (1.50)	5.4 (0.13)	101.9 (2.44)	7.5 (0.58)	100.1 (7.68)
	250	174.8 (11.30)	87.0 (5.63)	5.3 (0.07)	101.2 (1.28)	7.3 (0.58)	97.5 (7.68)
	500	151.2 (15.50)	75.2 (7.71)	5.3 (0.17)	100.1 (3.25)	7.3 (1.07)	97.0 (14.19)
	1000	150.8 (13.08)	75.0 (6.51)	4.9 (0.23)	92.5 (4.31)	7.1 (0.34)	93.6 (4.55)
PA/GF30	100	273.1 (3.77)	99.5 (1.37)	8.3 (0.30)	99.3 (3.62)	14.6 (2.13)	97.7 (14.23)
	250	264.7 (7.14)	96.4 (2.60)	8.4 (0.52)	101.5 (6.22)	14.5 (1.61)	97.0 (00.81)
	500	264.3 (9.71)	96.3 (3.54)	8.3 (0.17)	99.6 (2.10)	14.3 (0.64)	96.0 (4.30)
	1000	247.8 (6.44)	90.2 (2.35)	8.1 (0.26)	96.8 (3.14)	14.3 (2.11)	95.8 (14.14)

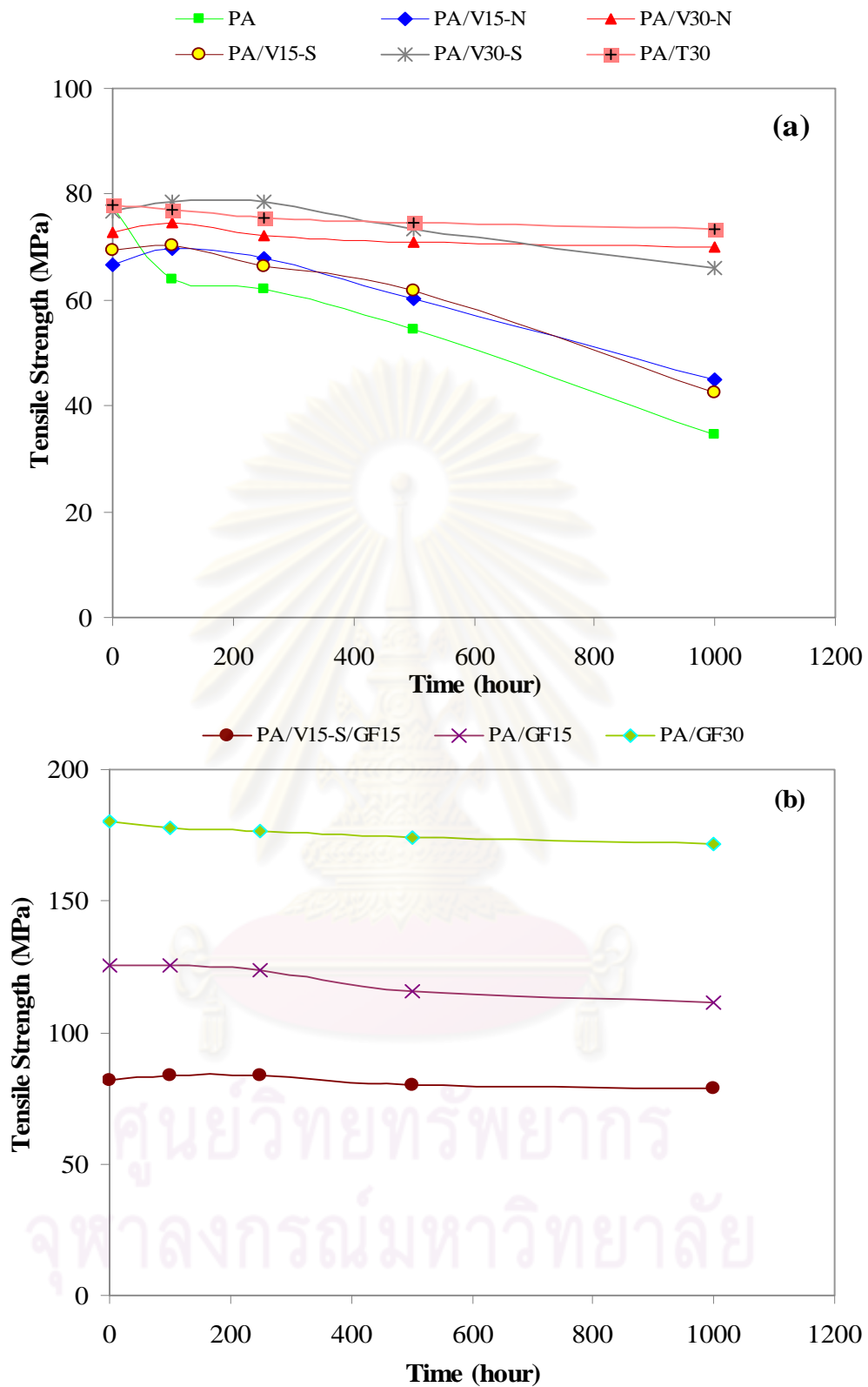


Figure 4.13 Tensile strength of composites after accelerated weathering in sunshine weathering meter 1000 h (a) PA, PA/V15-N, PA/V15-S, PA/V30-N, PA/V30-S and PA/T30 (b) PA/V15-S/GF15, PA/GF15 and PA/GF30

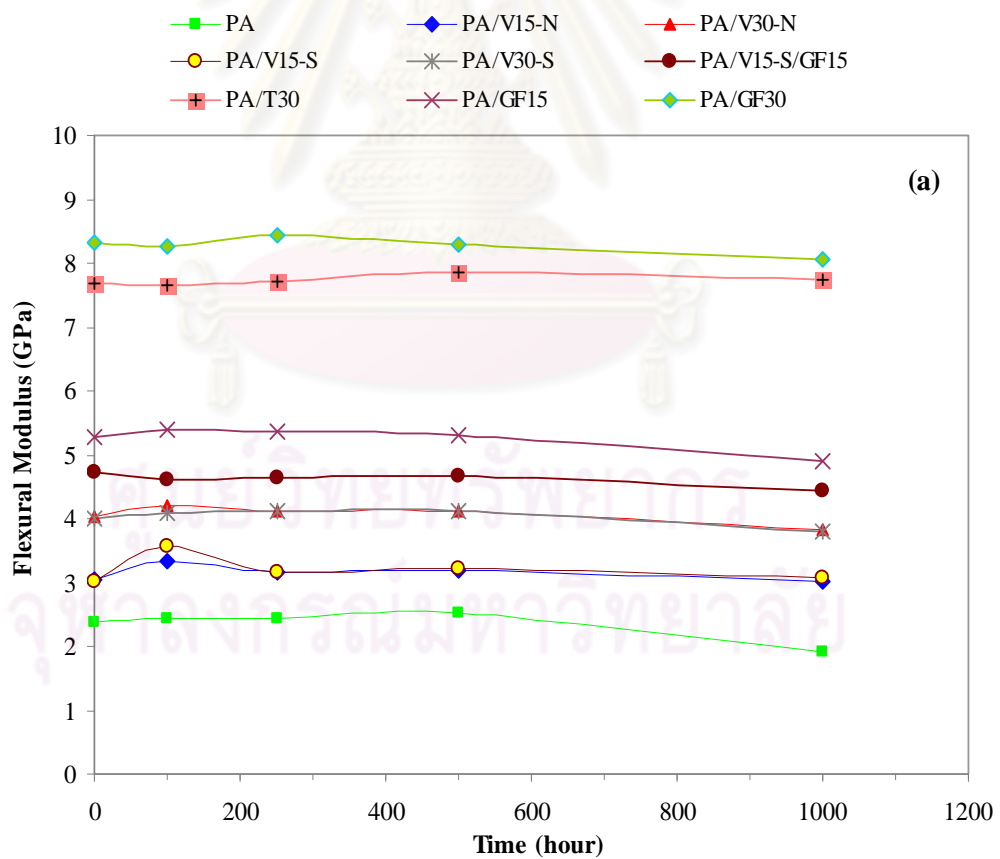
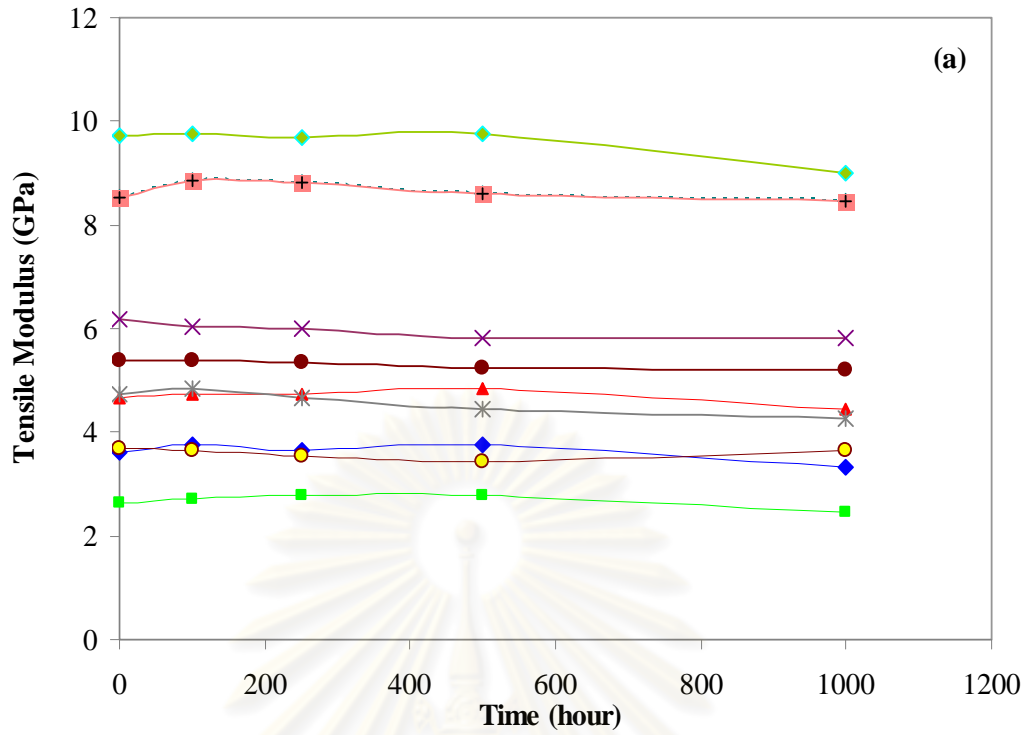


Figure 4.14 Modulus of composites after accelerated weathering in sunshine weathering meter 1000 h (a) tensile modulus (b) flexural modulus.

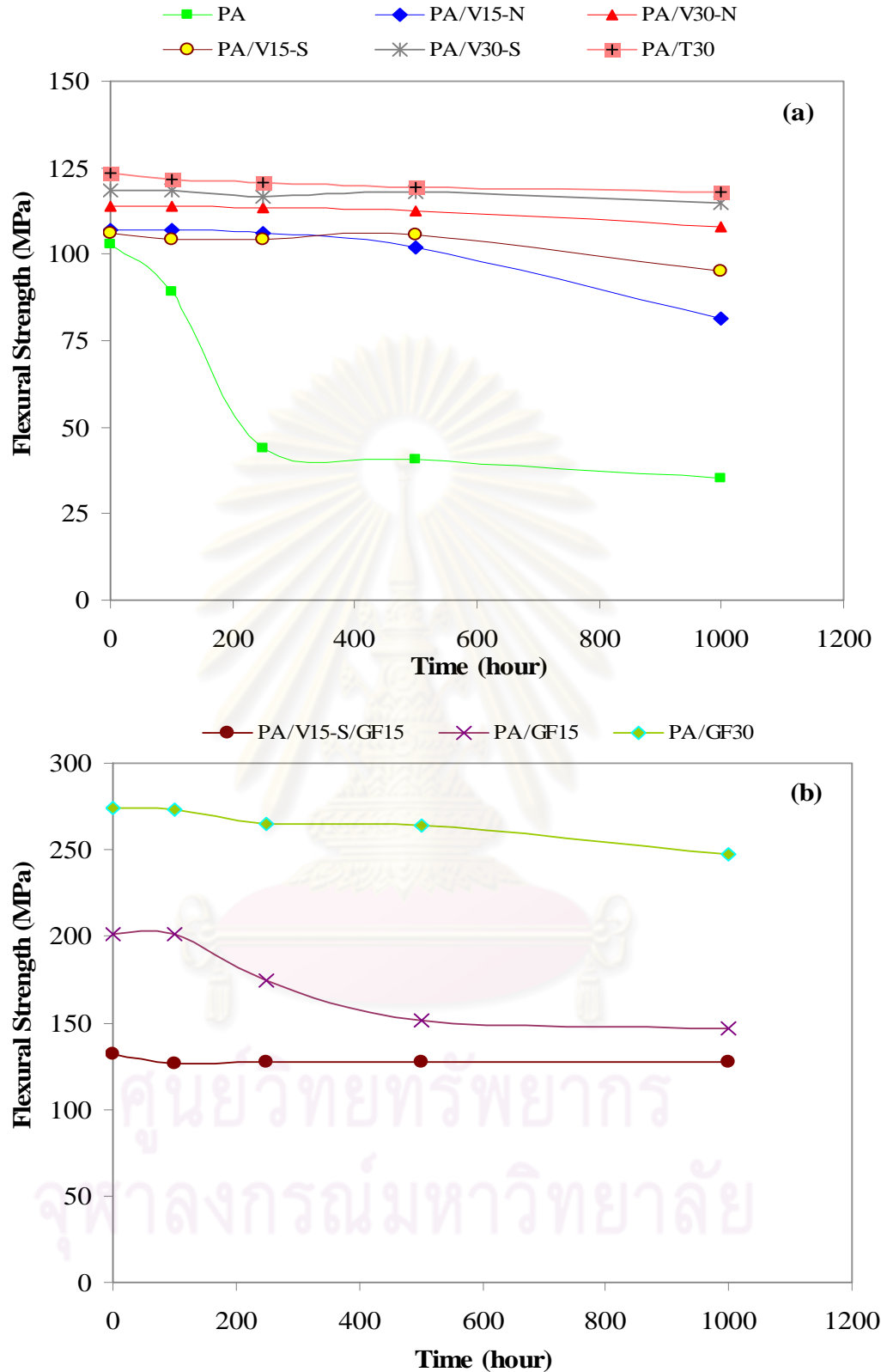


Figure 4.15 Flexural strength of composites after accelerated weathering in sunshine weathering meter 1000 h (a) PA, PA/V15-N, PA/V15-S, PA/V30-N, PA/V30-S and PA/T30 (b) PA/V15-S/GF15, PA/GF15 and PA/GF30.

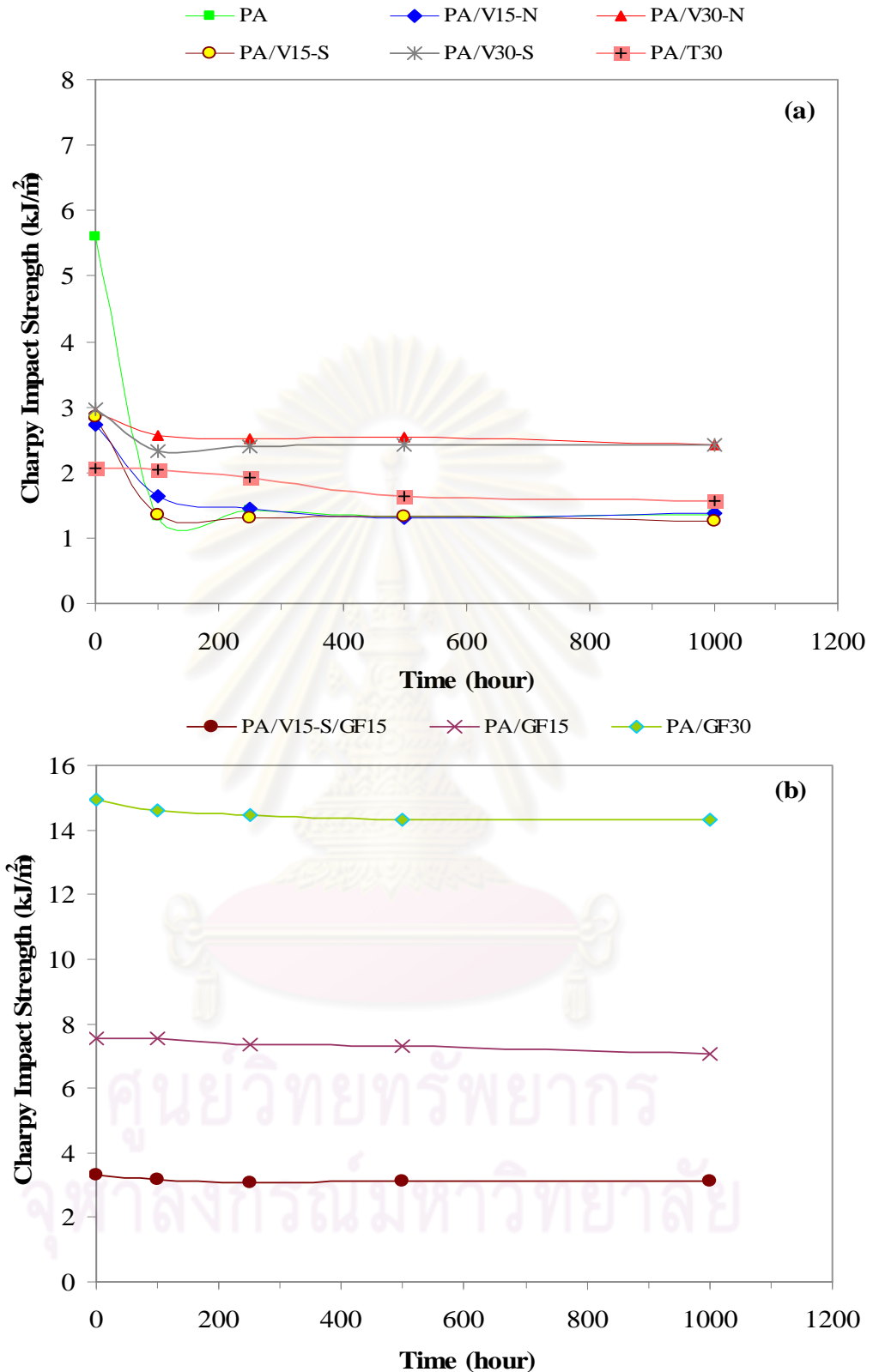


Figure 4.16 Charpy impact strength of composites after accelerated weathering in sunshine weathering meter 1000 h (a) PA, PA/V15-N, PA/V15-S, PA/V30-N, PA/V30-S and PA/T30 (b) PA/V15-S/GF15, PA/GF15 and PA/GF30.

4.4.2 Retention

From Figure 4.17 (a), retention rate of tensile strength of silane coupling agent treated grass fiber (15%) reinforced composites after accelerated weathering for 1000 hour was higher than that of unfilled composite and the same as that of mercerization treated grass fiber reinforced at the same fiber content. Retention rate of silane coupling agent treated grass fiber (30%) after accelerated weathering for 1000 hour was higher than that of unfilled, but lower than that of mercerization treated grass fiber reinforced composites as the same fiber content and the same as that of talc filled composite. From Figure 4.17 (b), retention rate of tensile strength of silane coupling agent treated grass fiber (15%) and glass fiber (15%) reinforced composites (PA/V15-S/GF15) after accelerated weathering for 1000 hour was higher than that of 15% glass fiber reinforced composites and the same as that of 30% glass fiber reinforced composites.

From Figure 4.18 (a), retention rate of elongation at break (EB) of silane coupling agent treated grass fiber reinforced composites after accelerated weathering for 1000 hour was lower than that of talc filled composite, but higher than that of unfilled composite and the same as that of mercerization treated grass fiber reinforced composites when compared at the same fiber content (15 and 30%). From Figure 4.18 (b), retention rate of elongation at break of silane coupling agent treated grass fiber (15%) and glass fiber (15%) reinforced composites (PA/V15-S/GF15) after accelerated weathering for 1000 hour was lower than that of glass fiber reinforced composites at both contents (15 and 30%).

From Figure 4.19 (a), retention rate of flexural strength of silane coupling agent treated grass fiber (15%) reinforced composites after accelerated weathering for 1000 hour was higher than that of unfilled and mercerization treated fiber reinforced composites at the same content (15%). Retention rate of flexural strength of silane coupling agent treated grass fiber (30%) reinforced composites after accelerated weathering for 1000 hour was higher than that of unfilled and the same as that of mercerization treated fiber reinforced composites when compared at the same fiber content (30%). From Figure 4.19 (b), retention rate of flexural strength of silane coupling agent treated grass fiber (15%) and glass fiber (15%) reinforced composites (PA/V15-S/GF15) after accelerated weathering for 100 hour was higher than that of glass fiber reinforced composites at both contents (15 and 30%).

From Figure 4.20 (a), retention rate of Charpy impact strength of silane coupling agent treated grass fiber reinforced composites after accelerated weathering for 1000 hour was higher than that of unfilled composite, but slightly lower than that of talc filled composite and the same as that of mercerization treated grass fiber reinforced composites. From Figure 4.20 (b), retention rate of Charpy impact strength of silane coupling agent treated grass fiber (15%) and glass fiber (15%) reinforced composites (PA/V15-S/GF15) after accelerated weathering for 1000 hour was same as that of glass fiber reinforced composites at both contents (15 and 30%).

The long term stability was decreased in the following order: polyamide composites filled with: glass fiber ~ treated grass fiber > talc > unfilled. It convinced that the fiber reinforced composites had long term stability against degradation by irradiation of extended-UV exposure. These retention results after accelerated weathering with Vetiver grass fiber/polyamide-6 composites enable them to replace talc filled composite and the glass fiber reinforced composites where the mechanical strength is not as the critical specification in automotive applications same as Vetiver grass fiber/polyamide-6 composites after accelerated weathering.

4.4.3 Comparison of Accelerated Weathering: Xenon Weathering Meter and Sunshine Weathering Meter

The accelerated weathering by Xenon weathering meter is the source most closely resembling UV radiation in the daylight spectrum. There is the artificial radiation source closest to natural daylight. But the accelerated weathering by sunshine weathering meter is not found in daylight radiation at the Earth's surface. The radiation spectra are very different from daylight spectra. Sunshine weathering meter has two strong peaks at 320 and 400 nm which are respectively 4 and 20 times stronger than daylight at the same wavelengths. This radiation can cause an unrealistic and high accelerated degradation of materials. [23]

From both accelerated weathering results, the silane coupling treated grass fiber reinforced composites had the high potential to replace the talc filled composites in automotive applications such as engine cover. The silane treated grass fiber (15%) and glass fiber (15%) reinforced composites had the good mechanical properties and long term stability. This composite had the high potential to replace the glass fiber

reinforced composites in non-critical automotive applications, depending on strength and the environment conditions where the part is being applied.

The mechanical properties of silane treated grass fiber reinforced composites (67-77 MPa) and silane treated grass fiber (15%) and glass fiber (15%) reinforced composites (82 MPa) were lower than that of the mercerization treated curaua fiber (20%)/polyamide-6 composites (82-92 MPa) [2] and the natural fibers (30%) /polyamide-6 composites (114-122 MPa) [17]. Considering the production for the treated Vetiver grass fibers/polyamide-6 composites, the cost of preparation and treatment of Vetiber grass fiber are higher than that of glass fiber. Therefore, the treatments of Vetiver grass fiber increase the cost of production.



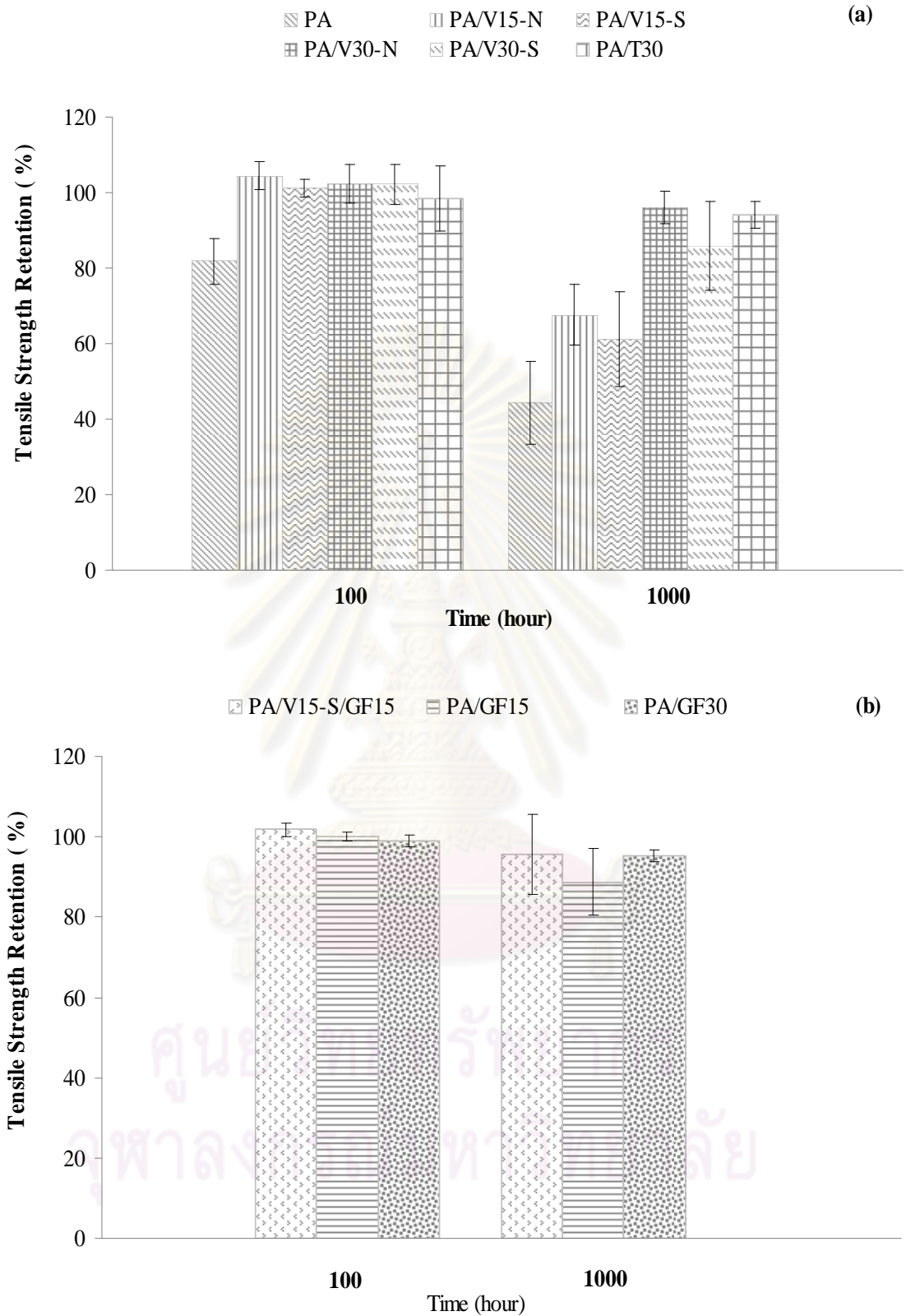


Figure 4.17 Tensile strength retention of composites after accelerated weathering in sunshine weathering meter for 1000 h (a) PA, PA/V15-N, PA/V15-S, PA/V30-N, PA/V30-S and PA/T30 (b) PA/V15-S/GF15, PA/GF15 and PA/GF30.

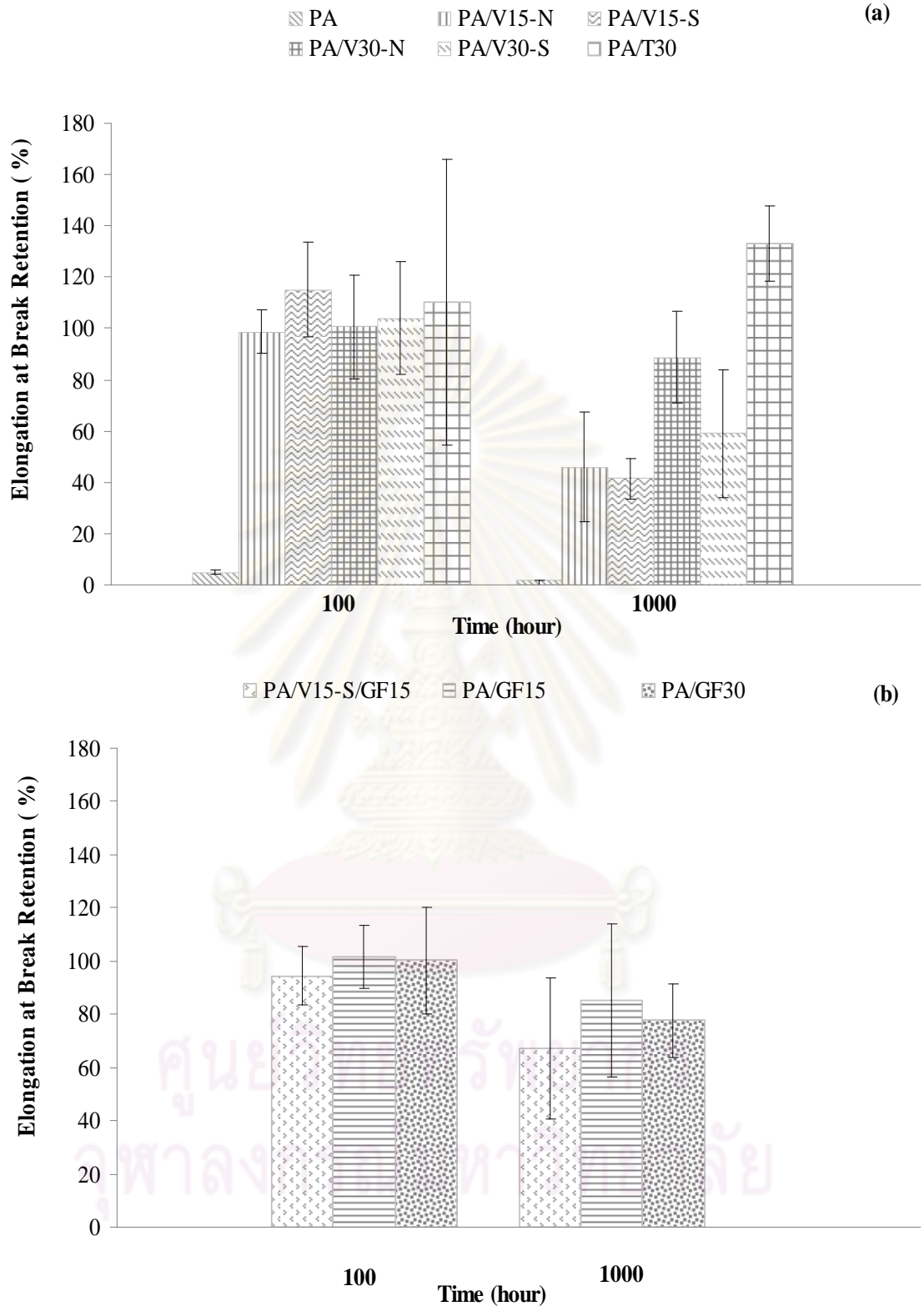


Figure 4.18 Elongation at break retention of composites after accelerated weathering in sunshine weathering meter for 1000 h (a) PA, PA/V15-N, PA/V15-S, PA/V30-N, PA/V30-S and PA/T30 (b) PA/V15-S/GF15, PA/GF15 and PA/GF30.

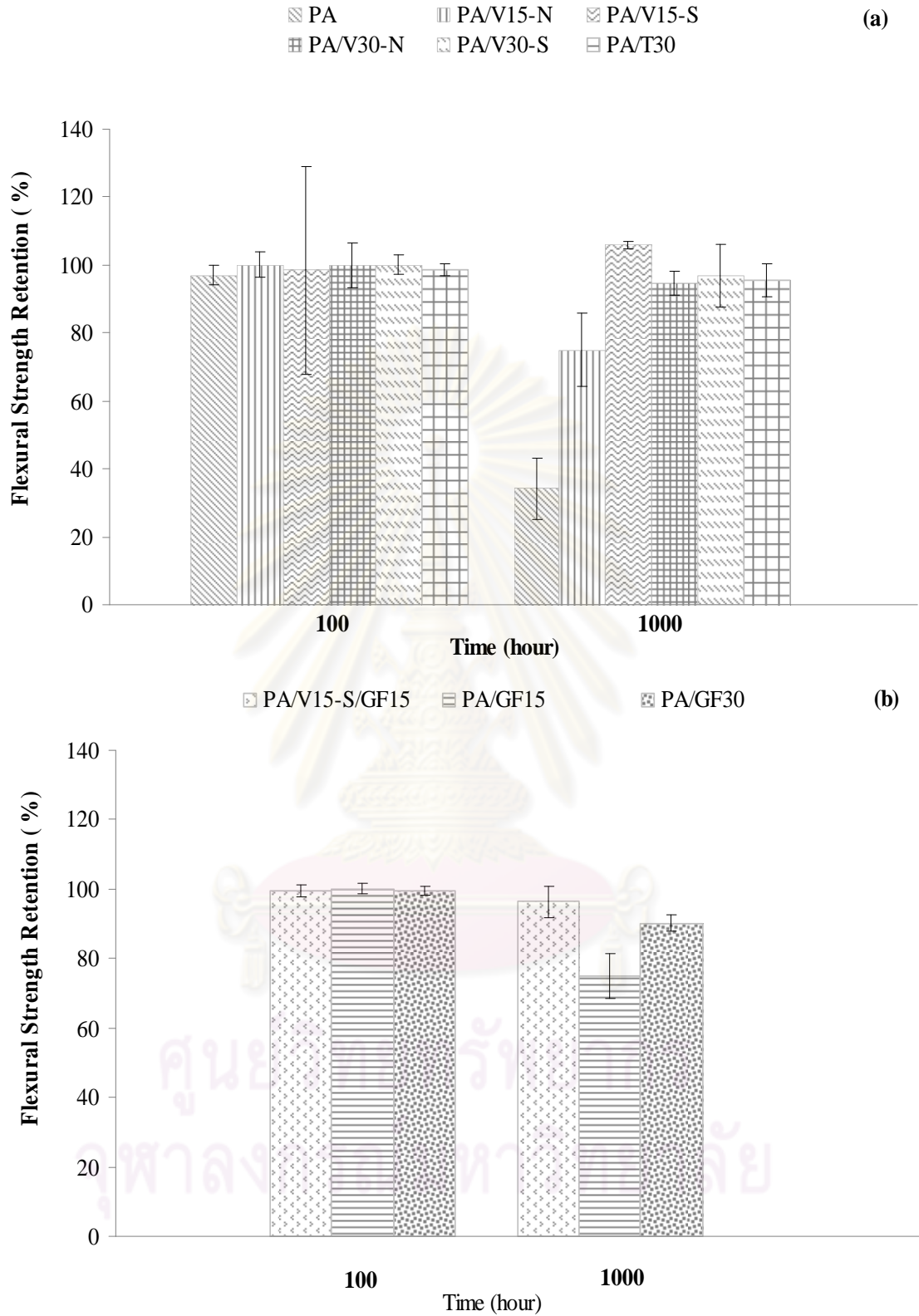


Figure 4.19 Flexural strength retention of composites after accelerated weathering in sunshine weathering meter for 1000 h (a) PA, PA/V15-N, PA/V15-S, PA/V30-N, PA/V30-S and PA/T30 (b) PA/V15-S/GF15, PA/GF15 and PA/GF30.

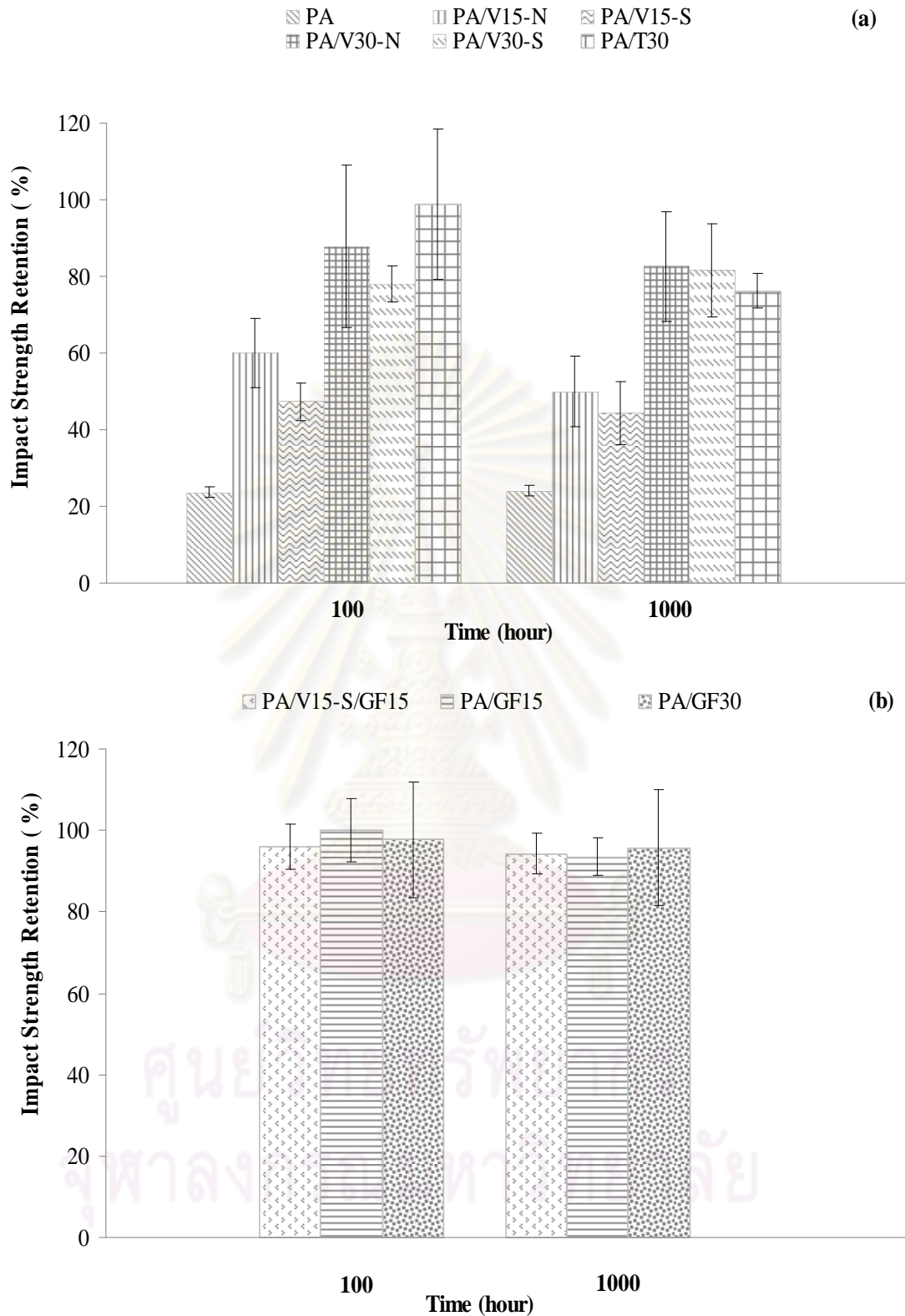


Figure 4.20 Impact strength retention of composites after accelerated weathering in sunshine weathering meter for 1000 h (a) PA, PA/V15-N, PA/V15-S, PA/V30-N, PA/V30-S and PA/T30 (b) PA/V15-S/GF15, PA/GF15 and PA/GF30.

4.4.4 Morphology

The morphology of fracture surface of treated Vetiver grass fiber composites and treated Vetiver grass fiber (15%) and glass fiber (15%) reinforced composites was investigated.

The scanning microscope electron (SEM) was used to examine the tensile fracture surface of Vetiver grass fiber/poyamide-6 composite after accelerated weathering at 1000 hour based on 15 % of Vetiver grass fiber: Figure 4.21 (a) and Figure 4.21 (b), 30 % of Vetiver grass fiber: Figure 4.21 (c) and Figure 4.21 (d) and treated Vetiver grass fiber (15%) and glass fiber (15%) reinforced composites: Figure 4.21 (e).

Figure 4.21 shows the slight increase in gap between treated Vetiver grass fiber and polymer matrix. This can be explained that the irradiation had decreased the interfacial adhesion between fiber and polymer matrix. Therefore, the properties of polyamide-6 composites reinforced with treated Vetiver grass fiber after accelerated weathering at 1000 h was decreased compared with the normal composites without weathering.

The accelerated weathering causes the interfacial adhesion between fiber and polymer matrix same as the accelerated in Xenon weathering (Eg. 4.3 - 4.13)

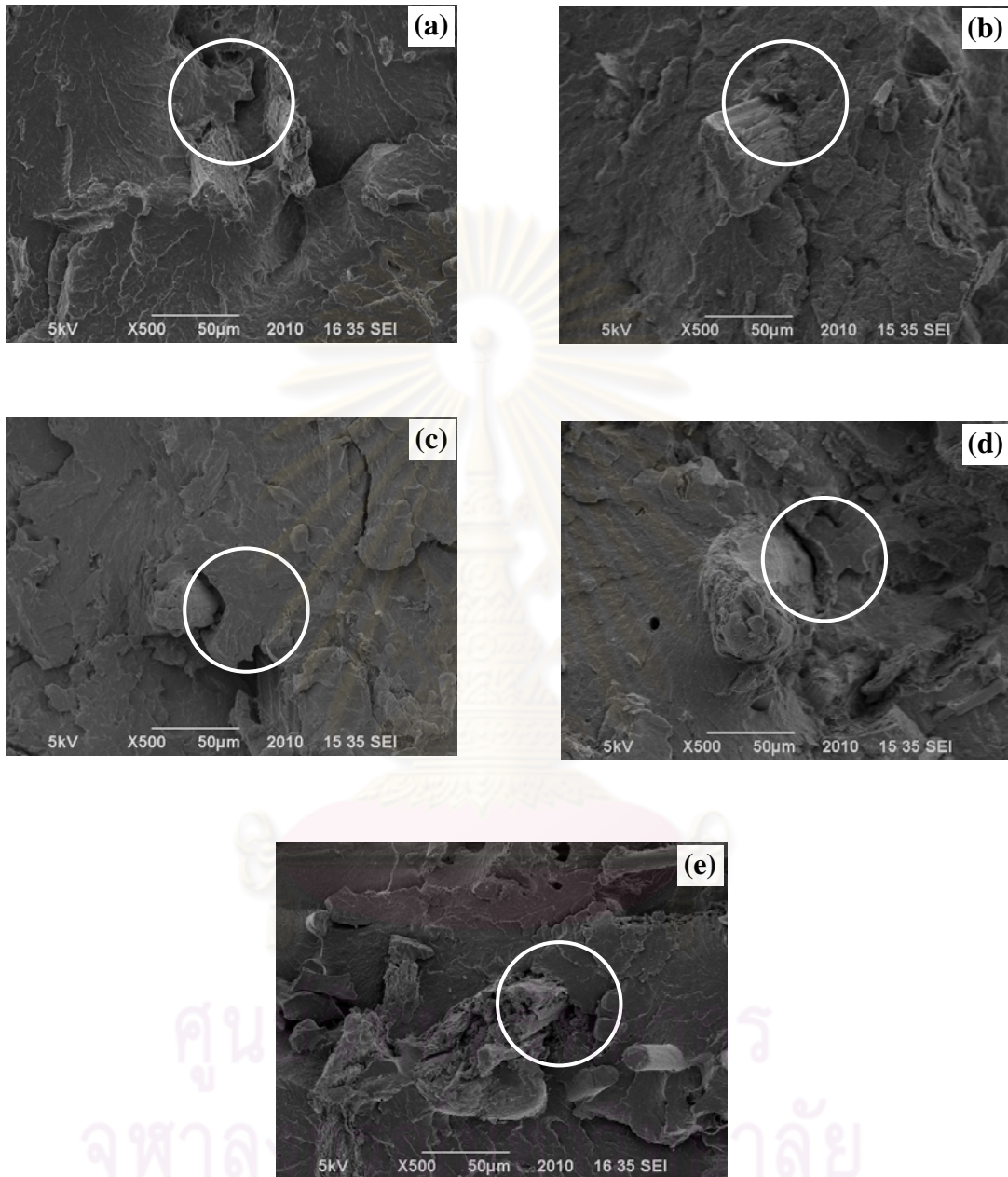


Figure 4.21 SEM micrographs of composites accelerated weathering in sunshine weathering meter for 1000 h: (a) PA/V15-N, (b) PA/V15-S, (c) PA/V30-N, (d) PA/V30-S and (e) PA/V15-S/GF15 (X500 magnification, scale bar = 50 μm).

CHAPTER V

CONCLUSIONS

5.1 Conclusions

The application of natural fiber as reinforcement in composite materials requires a strong adhesion between fiber and the synthetic matrix. In this work, the surface treatments were mercerization and applying the silane coupling agent. The Vetiver grass fiber reinforced polyamide-6 composites at various contents of Vetiver grass fiber (15 and 30%) were prepared by using twin screw extruders. The present study could be concluded as follows;

1. Vetiver grass fiber treated with silane coupling agent/polyamide-6 exhibited higher mechanical properties in terms of tensile strength and flexural strength when compared with mercerization treated grass fiber/polyamide-6 composites. The increasing of Vetiver grass content in polyamide-6 composites resulted in the increase of mechanical properties. Polyamide-6 composites reinforced with fibers treated with silane coupling agent had lower mechanical properties than glass fiber reinforced composites, but higher than unfilled composite and about the same as talc filled composite. Polyamide-6 composites reinforced with treated grass fibers content (15%) and glass fiber content (15%) had higher mechanical properties than unfilled and Vetiver grass/polyamide-6 composites, but lower than glass fiber reinforced composites and about the same as talc filled composite.

2. From the retention after accelerated weathering, it convinced that the Vetiver grass fiber reinforced composites had long term stability against degradation by irradiation of direct natural exposure and extended-UV exposure. Therefore, the treated Vetiver grass fiber could enhance the resistance to photooxidation that accelerated the degradation reaction.

3. The Vetiver grass fiber/polyamide-6 composites had the high potential to replace the talc filled composites and glass fiber reinforced composites in non-critical automotive applications, depending on strength and the environment conditions where the part is being applied.

5.2 Suggestion for Future Work

In the area of natural fiber reinforced composite, Vetiver grass fiber treated with chemical treatment could be used to reinforce the polyamide-6 at various fiber content of 15 and 30%, further study should be done as the following aspects:

1. The surface treatment of Vetiver grass fiber by various silane coupling agent should be investigated. The end group as carboxyl group of polyamide-6 forms the good adhesion with aminosilane coupling agent.
2. The effect of the processing condition for compounding Vetiver grass fiber/polyamide-6 composites by using twin screw extruder should be studied.



REFERENCES

- [1] Mohanty, A.K., and Misra, M. Studies on Jute Composites-A Literature Review. Polymer-Plastics Technology and Engineering. 34 (1995): 729.
- [2] Paulo, S.A., Marcia, S.A.S., Karen, F.K.G., and Marco, D.P.A. Polyamide-6/vegetal fiber composite prepared by extrusion and injection molding. Composites: Part A 38 (2007): 2404-2411.
- [3] Kalia, S., Kaith, B.S, and Kaur, I. Pretreatments of natural fibers and their application as reinforcing material in polymer composites-A Review. Polymer Engineering and Science (2009): 1-20.
- [4] Chaipattana network. What is Vetiver Grass? http://www.chaipat.or.th/intranet/article/vetiver/body_vetiver_e.html (1996).
- [5] Kohan, M. I. Nylon plastics handbook. Munich Vienna New York. Hanser Publishers (1995).
- [6] Roerdink, E., and Warnier, J.M.M. Solid-state polyamidation of nylon salts. Polymer 26 (1985): 1582-8.
- [7] Vachon, R.N., Rebenfeld L., and Taylor, H.S. Oxidative degradation of Nylon 66 filaments. Text. Res. J. 38 (1968): 716.
- [8] Allen, N.S. Thermal and photo-chemical oxidation of nylon 6,6: Some aspects of the importance of α,β -unsaturated carbonyl groups and hydroperoxides. Polymer Degradation and Stability. 8(1984): 55-62.
- [9] Allen, N.S., and Harrison, M.J. Polymer Degradation and Stability. 19 (1987): 77-95.
- [10] Sharkey, W.H., and Mochel, W.E. Mechanism of the Photooxidation of Amides. J. Am. Chem. Soc. 81 (1959): 3000-9.
- [11] Lemair, J., Gardette, J., Rivaton, A., and Roger, A. Dual photo-chemistries in aliphatic polyamides, bisphenol A polycarbonate and aromatic polyurethanes—A short review. Polymer Degradation and Stability. 15 (1986): 1-13.
- [12] Herrera-Franco, P.J., and Valadez-Gonzalez A. A study of the mechanical properties of short natural-fiber reinforced composites. Composites: Part B 36 (2005): 597-608.

- [13] Murali, M.R.K., RatnaPrasad, A.V., RangaBabu, M.N.V, Mohan, R.K., and Gupta, V.S.S.K.S. Tensile properties of elephant grass fiber reinforced polyester composites. J Mater Sci 42 (2007): 3266-3272.
- [14] Gomes, A., Matsuo, T., Goda, K., and Ohgi, J. Development and effect of alkali treatment on tensile properties of curaua fiber green composites. Composites: Part A 38 (2007):1811-1820.
- [15] Sui, G., Fuqua, M.A., Ulven, C.A., and Zhong, W.H. A plant fiber reinforced polymer composite prepared by a twin-screw extruder. Bioresource Technology 100 (2009):1246-1251.
- [16] Araujo, J.R., Waldman, W.R., and De Paoli, M.A. Thermal properties of high density polyethylene composites with natural fibres: Coupling agent effect. Polymer Degradation and Stability 93 (2008): 1770-1775.
- [17] Patricia, A.A., Alon, R.A.A., Jose, M.K., and Inaki, M. Mechanical properties of natural fibers/polyamides composites. Polymer Composite (2009) 258-264.
- [18] La Mantia, F.P., and Morreale, M. Accelerated weathering of polypropylene/ wood flour composites. Polymer Degradation and Stability 93 (2008): 1252-1258.
- [19] Azuma, Y., Takeda, H., Watanabe, S., and Nakatani, H. Outdoor and accelerated weathering tests for polypropylene and polypropylene/talc composites: A comparative study of their weathering behavior. Polymer Degradation and Stability 94 (2009): 2267-2274.
- [20] Abdulkadir, G., Ahmet, O., and Emin, O. Experimental investigation of the effect of glass fibres on the mechanical properties of polypropylene (PP) and polyamide 6 (PA6) plastics. Materials and Design 27 (2006): 316-323.
- [21] Garcia-Perez, M., Chaala, A., Yang, J., and Roy C. Co-pyrolysis of sugarcane bagasse with petroleum residue. Part I: Thermogravimetric analysis. Fuel 80 (2001): 1245-1258.
- [22] Yang. H., Yan. R., Chen, H., Lee, D. F., and Zheng, C. Characteristics of hemicelluloses, cellulose and lignin pyrolysis. Fuel 86 (2007): 1781-1788.
- [23] George, W. Handbook of Material Weathering. Canada. ChemTec Publishing. 1995.



APPENDICES

ศูนย์วิทยทรัพยากร
จุฬาลงกรณ์มหาวิทยาลัย

APPENDIX A

Density of Composites after Conditioning at 23 °C and 50 %RH for 24 h

Table A-1 Density of composites

Sample	Temperature (°C)	Density of water (g/cm ³)	Apparent mass of the specimen in air (g)	Apparent mass of the specimen in liquid (g)	Density (g/cm ³)
PA	24.0	0.9973	1.85	0.21	1.12
PA/V15-N	24.4	0.9972	1.73	0.25	1.17
PA/V15-S	24.2	0.9972	1.90	0.27	1.17
PA/V30-N	24.4	0.9972	1.79	0.31	1.21
PA/V30-S	24.2	0.9972	1.95	0.34	1.21
PA/T30	24.0	0.9973	2.34	0.73	1.44
PA/V15-S/GF15	24.2	0.9972	2.07	0.45	1.27
PA/GF15	24.2	0.9972	2.02	0.39	1.24
PA/GF30	24.0	0.9973	2.17	0.57	1.35

ศูนย์วิทยทรัพยากร
จุฬาลงกรณ์มหาวิทยาลัย

APPENDIX B

Mechanical Properties of Composites after Conditioning at 23 °C and 50 %RH for 24 h and after Accelerated Weathering in Xenon Weathering Meter

Table B-1 Tensile strength and elongation at break of composites

Sample	No.	Tensile strength (MPa) in each exposed time in hour					Sample	No.	Elongation at break (%) in each exposed time in hour				
		0	100	250	500	1000			0	100	250	500	1000
PA	1	78.8	58.7	58.5	55.4	33.2	PA	1	80.2	5.2	5.2	4.2	2.6
	2	77.8	59.7	58.9	56.6	33.6		2	106.5	6.0	4.8	5.2	3.5
	3	77.4	59.5	57.9	55.0	36.5		3	62.1	4.4	4.8	4.4	5.2
	4	76.6	58.9	58.0	54.2	33.4		4	43.2	5.0	5.0	5.2	3.5
	5	78.6	58.2	57.9	54.6	38.0		5	140.2	4.7	4.7	5.2	5.9
	mean	77.8	59.0	58.3	55.2	34.9		mean	86.4	5.0	4.9	4.8	4.1
	SD	0.90	0.61	0.44	0.92	2.18		SD	38.05	0.61	0.21	0.48	1.39
	3SD	2.70	1.82	1.31	2.76	6.54		3SD	114.16	1.84	0.63	1.45	4.17
PA/V15-N	1	64.6	60.7	58.7	60.4	48.0	PA/V15-N	1	2.3	3.6	3.1	4.3	3.3
	2	66.5	59.9	60.2	59.2	48.7		2	2.7	3.0	3.0	4.6	2.9
	3	66.7	59.3	60.3	54.9	48.6		3	2.7	3.0	2.9	4.4	2.1
	4	67.7	60.0	60.2	59.4	48.7		4	3.0	3.5	3.8	3.6	2.7
	5	68.1	59.8	59.5	59.9	46.8		5	2.9	4.0	2.9	2.8	3.0
	mean	66.7	59.9	59.8	58.8	48.2		mean	2.7	3.4	3.1	3.9	2.8
	SD	1.36	0.50	0.68	2.21	0.81		SD	0.26	0.40	0.35	0.76	0.45
	3SD	4.08	1.51	2.05	6.62	2.44		3SD	0.77	1.20	1.06	2.28	1.35
PA/V15-S	1	69.7	61.4	60.5	60.3	48.9	PA/V15-S	1	3.0	3.8	3.2	3.4	3.6
	2	69.7	61.4	60.7	59.7	49.4		2	2.9	4.4	3.9	3.1	3.1
	3	69.1	59.8	59.4	59.6	50.0		3	2.8	3.4	3.9	3.0	3.4
	4	69.0	59.8	60.1	60.5	49.4		4	2.9	3.0	3.1	3.7	2.5
	5	69.4	60.6	60.6	60.3	49.7		5	2.9	3.1	2.7	3.7	3.1
	mean	69.4	60.6	60.3	60.1	49.5		mean	2.9	3.6	3.4	3.4	3.1
	SD	0.33	0.80	0.53	0.40	0.41		SD	0.07	0.58	0.50	0.31	0.44
	3SD	0.98	2.40	1.60	1.21	1.23		3SD	0.20	1.73	1.50	0.93	1.33
PA/V30-N	1	73.9	64.3	64.6	63.5	53.8	PA/V30-N	1	2.5	2.5	2.5	2.6	2.3
	2	73.6	63.8	64.9	62.4	53.6		2	2.5	2.5	2.7	2.3	2.4
	3	72.9	65.2	63.3	64.6	53.6		3	2.3	2.7	2.9	2.4	2.3
	4	71.6	65.2	62.4	64.0	53.8		4	2.1	2.6	2.3	2.4	2.5
	5	72.5	63.8	64.1	61.8	54.6		5	2.3	2.5	2.7	2.0	2.1
	mean	72.9	64.5	63.9	63.3	53.9		mean	2.4	2.6	2.6	2.3	2.3
	SD	0.91	0.71	1.02	1.15	0.41		SD	0.17	0.08	0.20	0.20	0.16
	3SD	2.74	2.12	3.05	3.44	1.24		3SD	0.52	0.23	0.60	0.59	0.48
PA/V30-S	1	77.1	70.7	70.8	71.9	58.7	PA/V30-S	1	2.8	3.0	2.9	2.4	2.4
	2	77.0	71.2	69.1	71.4	58.7		2	2.6	3.1	2.6	2.3	2.4
	3	76.8	70.0	70.7	66.2	59.4		3	2.6	2.9	2.8	2.5	2.4
	4	76.5	70.2	70.6	73.1	59.9		4	2.5	2.7	3.4	2.5	2.6
	5	77.0	69.3	70.5	68.3	59.2		5	2.8	3.0	3.0	2.6	2.1
	mean	76.9	70.3	70.3	70.2	59.2		mean	2.7	2.9	2.9	2.5	2.4
	SD	0.24	0.72	0.70	2.84	0.51		SD	0.10	0.16	0.29	0.13	0.20
	3SD	0.72	2.16	2.11	8.53	1.52		3SD	0.31	0.48	0.86	0.39	0.61
PA/T30	1	78.4	66.8	66.5	63.7	45.2	PA/T30	1	1.9	3.0	2.7	2.8	2.2
	2	79.0	67.4	65.9	65.4	45.4		2	2.1	2.8	2.7	2.5	2.2
	3	77.8	67.7	66.7	65.5	45.1		3	1.8	2.8	2.8	2.6	2.3
	4	77.6	67.7	66.2	65.6	45.2		4	1.8	3.0	2.8	2.9	2.3
	5	77.8	68.1	65.2	65.9	44.1		5	1.9	2.9	2.8	2.7	2.2
	mean	78.1	67.5	66.1	65.2	45.0		mean	1.9	2.9	2.7	2.7	2.2
	SD	0.58	0.48	0.59	0.87	0.51		SD	0.10	0.11	0.07	0.17	0.04
	3SD	1.73	1.45	1.76	2.61	1.54		3SD	0.31	0.33	0.21	0.52	0.11
PA/V15-S/GF15	1	82.2	73.7	72.3	73.5	61.1	PA/V15-S/GF15	1	3.0	2.8	3.0	3.0	2.7
	2	81.9	74.4	73.9	73.6	60.3		2	2.8	3.1	3.2	2.8	2.4
	3	82.6	74.6	73.8	70.9	61.1		3	3.1	2.9	3.0	2.1	2.2
	4	82.0	74.0	73.5	74.3	64.7		4	3.1	2.9	2.8	3.0	2.5
	5	81.9	74.3	74.4	73.9	58.5		5	2.7	2.8	2.9	3.4	2.5
	mean	82.1	74.2	73.6	73.2	61.1		mean	2.9	2.9	3.0	2.9	2.5
	SD	0.29	0.35	0.79	1.34	2.26		SD	0.18	0.14	0.13	0.47	0.17
	3SD	0.88	1.06	2.36	4.03	6.77		3SD	0.54	0.42	0.40	1.40	0.50
PA/GF15	1	124.7	111.2	107.4	106.2	77.4	PA/GF15	1	2.7	3.7	3.9	2.5	3.1
	2	128.1	110.2	109.4	105.9	78.5		2	2.9	3.9	4.5	3.0	2.9
	3	126.3	111.4	106.7	103.8	74.0		3	2.7	3.7	4.0	2.8	2.4
	4	125.8	110.8	107.4	104.5	81.0		4	2.8	5.0	4.5	2.3	2.9
	5	123.5	111.0	108.7	107.2	81.5		5	2.7	5.3	3.9	3.1	2.8
	mean	125.7	110.9	107.9	105.5	78.5		mean	2.8	4.3	4.2	2.7	2.8
	SD	1.73	0.46	1.10	1.36	3.03		SD	0.09	0.79	0.32	0.33	0.27
	3SD	5.19	1.38	3.30	4.09	9.09		3SD	0.27	2.36	0.96	0.99	0.82
PA/GF30	1	180.4	157.7	157.0	151.0	135.2	PA/GF30	1	3.4	3.8	3.9	2.8	3.3
	2	180.3	160.0	156.6	154.5	134.0		2	3.9	4.0	3.9	3.4	2.9
	3	178.9	153.8	158.0	151.6	137.4		3	3.6	3.9	3.9	2.8	3.1
	4	181.0	159.1	158.5	153.8	134.6		4	3.6	4.3	3.8	3.1	2.7
	5	179.9	158.2	158.4	152.4	132.1		5	3.3	4.2	3.8	3.4	2.6
	mean	180.1	157.7	157.7	152.7	134.7		mean	3.6	4.0	3.9	3.1	2.9
	SD	0.78	2.40	0.85	1.47	1.92		SD	0.22	0.21	0.04	0.30	0.28
	3SD	2.33	7.21	2.56	4.41	5.77		3SD	0.65	0.62	0.13	0.90	0.85

Table B-2 Tensile modulus of composites

Sample	No.	Tensile Modulus (GPa) in each exposed time in hour				
		0	100	250	500	1000
PA	1	2.7	2.1	2.2	2.3	1.8
	2	2.7	2.2	2.3	2.1	1.6
	3	2.6	2.2	2.3	2.1	1.6
	4	2.6	2.2	2.2	2.0	1.6
	5	2.6	2.1	2.2	2.1	1.7
	mean	2.7	2.2	2.2	2.1	1.7
	SD	0.08	0.06	0.07	0.11	0.07
PA/V15-N	3SD	0.25	0.19	0.20	0.34	0.20
	1	3.6	3.7	3.4	3.5	2.8
	2	3.6	3.6	3.4	3.3	2.7
	3	3.7	3.5	3.3	3.2	2.7
	4	3.6	3.6	3.3	3.2	2.8
	5	3.6	3.6	3.4	3.3	2.8
	mean	3.6	3.6	3.4	3.3	2.8
PA/V15-S	SD	0.03	0.08	0.05	0.12	0.06
	3SD	0.10	0.23	0.15	0.37	0.18
	1	3.7	3.5	3.5	3.3	2.8
	2	3.7	3.6	3.5	3.4	2.9
	3	3.7	3.5	3.4	3.2	2.8
	4	3.7	3.6	3.4	3.4	2.9
	5	3.7	3.6	3.4	3.4	2.8
PA/V30-N	mean	3.7	3.6	3.4	3.3	2.8
	SD	0.02	0.04	0.05	0.07	0.05
	3SD	0.06	0.13	0.16	0.21	0.16
	1	4.6	4.5	4.7	4.5	3.7
	2	4.5	4.4	4.4	4.3	2.7
	3	4.7	4.7	4.4	4.3	3.7
	4	4.7	4.7	4.5	4.6	3.7
PA/V30-S	5	4.7	4.5	4.4	4.6	3.7
	mean	4.7	4.5	4.5	4.5	3.5
	SD	0.09	0.13	0.14	0.18	0.47
	3SD	0.26	0.39	0.42	0.55	1.40
	1	4.7	4.7	4.5	4.3	3.7
	2	4.7	4.8	4.3	4.2	3.8
	3	4.6	4.6	4.4	4.3	3.8
PA/T30	4	4.9	4.7	4.5	4.7	4.1
	5	4.7	4.6	4.4	4.2	3.9
	mean	4.7	4.7	4.4	4.3	3.9
	SD	0.09	0.09	0.08	0.22	0.15
	3SD	0.28	0.28	0.24	0.67	0.45
	1	8.5	8.0	8.0	7.5	5.2
	2	8.5	8.0	8.0	7.6	5.2
PA/V15-S/GF15	3	8.7	8.0	8.1	7.7	5.2
	4	8.4	8.0	8.1	7.8	5.2
	5	8.5	8.0	8.1	7.5	5.1
	mean	8.5	8.0	8.0	7.6	5.2
	SD	0.11	0.02	0.03	0.12	0.06
	3SD	0.33	0.06	0.09	0.37	0.17
	1	5.5	5.2	5.2	5.2	4.1
PA/GF15	2	5.4	5.1	5.1	5.1	4.0
	3	5.3	5.2	5.1	5.2	4.3
	4	5.3	5.2	5.3	5.1	4.4
	5	5.4	5.3	5.2	5.1	4.3
	mean	5.4	5.2	5.2	5.2	4.2
	SD	0.06	0.07	0.07	0.08	0.15
	3SD	0.17	0.21	0.21	0.23	0.44
PA/GF30	1	6.1	5.6	5.6	5.6	4.2
	2	6.2	5.5	5.7	5.1	4.4
	3	6.4	5.5	5.5	4.9	4.4
	4	6.2	5.6	5.4	5.1	4.3
	5	6.0	5.6	5.5	5.4	4.6
	mean	6.2	5.6	5.5	5.2	4.4
	SD	0.13	0.04	0.13	0.28	0.12
PA/GF30	3SD	0.40	0.13	0.39	0.85	0.37
	1	9.8	9.4	9.5	9.2	8.3
	2	9.5	9.7	9.3	9.3	8.7
	3	9.8	9.1	9.1	9.2	8.4
	4	9.6	9.5	9.3	9.5	9.4
	5	10.0	9.3	9.2	9.3	10.2
	mean	9.7	9.4	9.3	9.3	9.0
PA/GF30	SD	0.18	0.20	0.17	0.09	0.80
	3SD	0.54	0.61	0.52	0.28	2.40

Table B-3 Flexural properties of composites

Sample	No.	Flexural Strength (MPa) in each exposed time in hour					
		0	100	250	500	1000	
PA	1	104.3	78.9	71.3	58.7	51.8	
	2	102.4	81.5	59.8	61.2	53.2	
	3	102.9	76.3	72.2	62.8	54.1	
	4	103.3	76.7	72.1	65.4	56.3	
	5	101.9	78.2	70.2	63.7	53.2	
	mean	103.0	78.3	69.1	62.4	53.7	
	SD	0.92	2.07	5.28	2.55	1.66	
PA/V15-N	3SD	2.75	6.22	15.83	7.64	4.98	
	1	106.3	93.9	90.8	81.0	81.1	
	2	107.3	91.5	83.2	82.9	80.2	
	3	107.4	92.5	84.3	82.4	81.2	
	4	106.5	90.5	84.0	83.1	82.6	
	5	106.8	91.7	83.7	81.4	79.9	
	mean	106.9	92.0	85.2	82.2	81.0	
PA/V15-S	SD	0.48	1.27	3.16	0.92	1.06	
	3SD	1.45	3.81	9.47	2.77	3.17	
	1	106.3	95.9	79.8	82.0	81.9	
	2	105.9	89.2	85.0	83.7	84.6	
	3	105.5	87.7	84.5	83.7	83.6	
	4	106.4	94.2	82.6	83.7	83.2	
	5	105.4	92.4	86.2	85.3	84.1	
PA/V30-N	mean	105.9	91.9	83.6	83.7	83.5	
	SD	0.45	3.41	2.50	1.17	1.03	
	3SD	1.36	10.23	7.50	3.50	3.08	
	1	113.3	91.4	90.2	87.4	91.8	
	2	114.7	99.4	90.8	87.1	86.7	
	3	113.2	101.1	85.7	88.6	88.2	
	4	113.9	99.4	89.9	87.8	87.6	
PA/V30-S	5	114.9	97.8	85.5	90.1	85.7	
	mean	114.0	97.8	88.4	88.2	88.0	
	SD	0.78	3.77	2.60	1.20	2.32	
	3SD	2.34	11.32	7.79	3.61	6.97	
	1	119.6	102.4	91.0	98.1	93.0	
	2	119.6	104.8	91.9	98.1	92.1	
	3	116.5	103.3	95.1	96.6	95.3	
PA/V30-S	4	119.1	99.6	95.4	96.1	94.1	
	5	118.0	105.8	91.4	96.4	94.3	
	mean	118.6	103.2	93.0	97.1	93.8	
	SD	1.32	2.39	2.11	0.97	1.24	
	3SD	3.97	7.17	6.34	2.90	3.71	
	1	122.8	-	88.8	80.8	86.2	
	2	123.7	87.9	93.2	79.6	80.0	
PA/T30	3	123.0	-	82.1	81.4	83.8	
	4	124.0	85.4	80.1	80.2	74.3	
	5	123.1	86.7	82.8	79.4	73.3	
	mean	123.3	86.7	85.4	80.3	79.5	
	SD	0.51	1.25	5.43	0.83	5.68	
	3SD	1.52	3.75	16.30	2.50	17.04	
	1	134.0	118.6	112.1	111.3	95.7	
PA/V15-S/GF15	2	131.5	114.8	114.5	110.2	91.7	
	3	135.2	112.0	109.3	111.2	91.1	
	4	131.0	115.8	111.1	112.6	93.1	
	5	128.4	110.8	110.3	111.2	87.4	
	mean	132.0	114.4	111.5	111.3	91.8	
	SD	2.67	3.10	1.99	0.85	3.03	
	3SD	8.00	9.30	5.96	2.56	9.09	
PA/GF15	1	201.6	172.6	162.6	156.0	125.4	
	2	201.3	-	151.8	153.5	124.3	
	3	199.2	161.2	162.0	156.9	128.7	
	4	205.2	162.9	148.2	156.5	132.1	
	5	197.5	170.1	155.9	153.4	134.4	
	mean	200.9	166.7	156.1	155.3	129.0	
	SD	2.89	5.51	6.28	1.68	4.30	
PA/GF30	3SD	8.68	16.53	18.85	5.05	12.90	
	1	274.2	224.8	227.2	225.7	192.4	
	2	274.2	-	221.0	218.4	186.2	
	3	273.1	222.3	229.5	215.4	186.2	
	4	275.0	219.2	220.6	218.2	183.2	
	5	276.3	-	220.8	225.8	188.9	
	mean	274.6	222.1	223.8	220.7	187.4	
PA/GF30	SD	1.19	2.81	4.22	4.76	3.46	
	3SD	3.56	8.42	12.65	14.28	10.37	
	Sample	No.	Flexural Modulus (GPa) in each exposed time in hour				
			0	100	250	500	1000
	PA	1	2.5	2.2	2.0	1.6	1.1
		2	2.3	2.1	2.0	1.6	1.1
		3	2.4	2.2	2.0	1.6	1.0
4		2.4	2.2	1.9	1.7	1.1	
5		2.4	2.2	2.0	1.6	1.0	
mean		2.4	2.2	2.0	1.6	1.1	
SD		0.04	0.01	0.03	0.06	0.05	
PA/V15-N	3SD	0.13	0.04	0.10	0.17	0.14	
	1	3.0	3.1	2.8	2.8	2.5	
	2	3.1	3.1	2.9	2.8	2.5	
	3	3.1	3.1	2.9	2.8	2.4	
	4	3.0	3.0	2.8	2.8	2.5	
	5	3.0	3.1	2.9	2.8	2.4	
	mean	3.1	3.1	2.9	2.8	2.5	
PA/V15-S	SD	0.03	0.05	0.04	0.02	0.01	
	3SD	0.10	0.16	0.11	0.07	0.04	
	1	3.1	3.1	2.7	2.7	2.4	
	2	3.1	3.0	2.9	2.7	2.4	
	3	3.1	2.9	2.8	2.7	2.4	
	4	3.1	3.0	2.9	2.7	2.5	
	5	3.1	3.0	2.9	2.7	2.4	
PA/V30-N	mean	3.1	3.0	2.8	2.7	2.4	
	SD	0.03	0.07	0.08	0.03	0.02	
	3SD	0.08	0.20	0.24	0.09	0.07	
	1	4.0	3.9	3.8	3.6	3.4	
	2	4.1	4.1	3.8	3.7	3.1	
	3	4.0	4.0	3.6	3.7	3.2	
	4	4.1	4.0	3.8	3.7	3.2	
PA/V30-S	5	4.0	3.9	3.7	3.8	3.2	
	mean	4.0	4.0	3.8	3.7	3.2	
	SD	0.05	0.06	0.09	0.05	0.11	
	3SD	0.15	0.17	0.27	0.16	0.32	
	1	4.0	4.0	3.8	3.6	3.2	
	2	4.0	4.0	3.6	3.5	3.2	
	3	4.0	4.0	3.8	3.6	3.3	
PA/T30	4	4.0	4.0	3.7	3.5	3.2	
	5	4.0	3.9	3.7	3.6	3.2	
	mean	4.0	4.0	3.7	3.6	3.2	
	SD	0.03	0.03	0.08	0.04	0.03	
	3SD	0.09	0.08	0.25	0.13	0.08	
	1	7.7	7.3	6.9	6.6	6.3	
	2	7.6	6.9	7.1	6.6	6.1	
PA/V15-S/GF15	3	7.7	7.2	6.8	6.7	6.2	
	4	7.7	6.7	6.8	6.7	5.9	
	5	7.6	6.6	6.5	6.6	6.1	
	mean	7.7	6.9	6.8	6.7	6.1	
	SD	0.04	0.32	0.21	0.06	0.18	
	3SD	0.13	0.97	0.64	0.17	0.54	
	1	4.7	4.6	4.2	4.2	3.7	
PA/GF15	2	4.7	4.5	4.3	4.2	3.6	
	3	4.7	4.5	4.3	4.2	3.4	
	4	4.7	4.5	4.3	4.2	3.5	
	5	4.7	4.4	4.2	4.2	3.5	
	mean	4.7	4.5	4.2	4.2	3.5	
	SD	0.03	0.07	0.03	0.03	0.10	
	3SD	0.09	0.20	0.08	0.08	0.29	
PA/GF30	1	5.2	5.0	4.9	4.4	3.9	
	2	5.3	4.7	4.7	4.4	4.0	
	3	5.2	4.6	4.8	4.4	3.9	
	4	5.4	4.6	4.7	4.4	4.2	
	5	5.4	4.8	4.7	4.4	4.0	
	mean	5.3	4.8	4.7	4.4	4.0	
	SD	0.11	0.16	0.09	0.02	0.13	
PA/GF30	3SD	0.33	0.49	0.27	0.06	0.39	
	1	8.4	7.6	7.6	7.3	6.7	
	2	8.3	7.9	7.5	7.1	6.7	
	3	8.3	7.6	7.7	7.1	6.4	
	4	8.2	7.6	7.5	7.0	6.3	
	5	8.4	7.9	7.5	7.3	6.5	
	mean	8.3	7.7	7.6	7.2	6.5	
PA/GF30	SD	0.05	0.17	0.09	0.12	0.18	
	3SD	0.16	0.52	0.27	0.35	0.54	

Table B-4 Charpy Impact Strength of composites

Sample	No.	Charpy Impact Strength (kJ m ⁻²) in each exposed time in hour				
		0	100	250	500	1000
PA	1	5.7	2.7	1.4	1.2	1.3
	2	5.3	2.4	1.3	1.3	1.3
	3	5.3	2.7	1.4	1.3	1.3
	4	5.8	2.6	1.4	1.3	1.2
	5	5.8	2.6	1.3	1.3	1.3
	mean	5.6	2.6	1.4	1.3	1.3
	SD	0.26	0.11	0.05	0.04	0.02
	3SD	0.78	0.33	0.14	0.12	0.06
	PA/V15-N	1	2.8	2.3	1.8	1.9
2	2.5	2.1	1.8	1.8	1.3	
3	2.8	2.2	2.2	1.9	1.3	
4	2.7	2.2	2.0	1.8	1.2	
5	2.9	2.2	1.9	1.8	1.3	
mean	2.7	2.2	1.9	1.8	1.3	
SD	0.13	0.06	0.15	0.06	0.06	
3SD	0.39	0.18	0.45	0.17	0.17	
PA/V15-S	1	2.9	2.4	2.1	1.9	1.3
2	2.8	2.2	2.0	1.9	1.2	
3	2.9	2.1	1.9	1.9	1.3	
4	2.9	2.6	1.9	2.1	1.3	
5	2.8	2.1	2.0	2.1	1.3	
mean	2.8	2.3	2.0	2.0	1.3	
SD	0.04	0.21	0.05	0.13	0.03	
3SD	0.12	0.64	0.16	0.38	0.09	
PA/V30-N	1	2.9	2.7	2.8	2.7	2.5
2	3.0	3.0	2.8	2.6	2.3	
3	2.9	2.9	2.8	2.6	2.4	
4	2.9	2.9	2.9	2.8	2.4	
5	3.0	2.8	2.8	2.7	2.5	
mean	2.9	2.9	2.8	2.7	2.4	
SD	0.04	0.12	0.03	0.08	0.05	
3SD	0.13	0.35	0.10	0.24	0.16	
PA/V30-S	1	2.9	2.9	2.9	2.7	2.3
2	3.0	3.2	2.7	2.7	2.4	
3	3.0	2.8	2.6	2.8	2.3	
4	3.0	2.9	2.8	2.8	2.3	
5	3.0	2.7	2.8	2.8	2.1	
mean	3.0	2.9	2.8	2.7	2.3	
SD	0.03	0.20	0.11	0.07	0.10	
3SD	0.08	0.59	0.32	0.21	0.29	
PA/T30	1	2.0	1.8	1.8	1.5	1.3
2	2.1	1.9	1.8	1.5	1.3	
3	2.0	1.8	1.7	1.5	1.6	
4	1.9	1.8	1.7	1.5	1.4	
5	2.1	1.8	1.7	1.5	1.4	
mean	2.0	1.8	1.7	1.5	1.4	
SD	0.09	0.07	0.05	0.03	0.11	
3SD	0.27	0.21	0.16	0.08	0.33	
PA/V15-S/GF15	1	3.2	3.5	3.4	3.1	2.9
2	3.3	3.5	3.7	2.9	3.0	
3	3.3	3.3	3.3	2.9	3.1	
4	3.3	3.6	3.4	3.0	2.9	
5	3.4	3.0	3.3	3.0	3.0	
mean	3.3	3.4	3.4	3.0	3.0	
SD	0.04	0.23	0.17	0.07	0.07	
3SD	0.13	0.70	0.50	0.20	0.22	
PA/GF15	1	7.8	7.4	7.5	7.2	7.0
2	7.8	8.2	7.3	7.6	6.9	
3	7.8	7.6	7.6	7.1	7.0	
4	6.9	8.1	6.9	6.9	6.9	
5	7.5	7.9	7.3	6.9	6.9	
mean	7.5	7.8	7.3	7.1	6.9	
SD	0.40	0.34	0.27	0.30	0.07	
3SD	1.20	1.03	0.80	0.91	0.22	
PA/GF30	1	15.4	16.1	15.8	16.1	14.4
2	14.5	15.8	15.5	16.2	14.3	
3	14.7	16.6	15.5	16.3	13.8	
4	15.8	16.6	16.2	15.4	14.0	
5	14.3	16.6	15.7	15.4	14.1	
mean	14.9	16.3	15.7	15.9	14.1	
SD	0.67	0.34	0.28	0.43	0.26	
3SD	2.00	1.03	0.85	1.30	0.77	

APPENDIX C

Mechanical Properties of Composites after Conditioning at 23 °C and 50 %RH for 24 h and after Accelerated Weathering in Sunshine Weather Meter

Table C-1 Tensile strength and elongation at break of composites

Sample	No.	Tensile strength (MPa) in each exposed time in hour					Sample	No.	Elongation at break (%) in each exposed time in hour				
		0	100	250	500	1000			0	100	250	500	1000
PA	1	78.8	62.1	-	53.8	32.1	PA	1	80.2	4.6	2.0	2.9	1.2
	2	77.8	62.7	64.9	54.4	35.7		2	106.5	4.2	3.5	3.1	1.4
	3	77.4	64.7	65.0	57.3	31.0		3	62.1	4.3	3.5	4.6	1.2
	4	76.6	63.3	65.4	57.3	37.0		4	43.2	4.3	3.8	2.4	1.4
	5	78.6	66.0	66.5	49.4	37.0		5	140.2	4.0	5.1	2.4	1.4
	mean	77.8	63.8	65.5	54.4	34.6		mean	86.4	4.3	3.6	3.1	1.3
	SD	0.90	1.58	0.73	3.25	2.83	SD	38.05	0.22	1.10	0.89	0.11	
	3SD	2.70	4.74	2.20	9.74	8.48	3SD	114.16	0.66	3.31	2.66	0.33	
PA/V15-N	1	64.6	69.8	68.9	60.9	46.7	PA/V15-N	1	2.3	2.7	2.8	2.3	0.9
	2	66.5	70.2	68.0	60.0	45.0		2	2.7	2.7	2.8	2.3	1.4
	3	66.7	68.2	69.0	57.5	42.9		3	2.7	2.8	2.8	2.1	1.3
	4	67.7	70.0	66.9	63.5	47.1		4	3.0	2.7	2.5	2.9	1.4
	5	68.1	70.2	66.3	59.4	43.8		5	2.9	2.6	2.6	2.3	1.3
	mean	66.7	69.7	67.8	60.3	45.1		mean	2.7	2.7	2.7	2.4	1.2
	SD	1.36	0.84	1.20	2.20	1.81	SD	0.26	0.08	0.14	0.32	0.19	
	3SD	4.08	2.53	3.60	6.60	5.43	3SD	0.77	0.23	0.41	0.95	0.58	
PA/V15-S	1	69.7	69.5	68.5	59.3	39.0	PA/V15-S	1	3.0	3.1	2.8	2.2	1.1
	2	69.7	70.7	69.3	62.8	41.1		2	2.9	3.4	3.1	2.6	1.2
	3	69.1	70.7	60.9	62.8	41.2		3	2.8	3.5	2.0	2.6	1.1
	4	69.0	70.1	66.6	62.6	45.9		4	2.9	3.5	2.5	2.5	1.3
	5	69.4	69.9	66.3	61.9	45.0		5	2.9	3.2	3.7	2.5	1.3
	mean	69.4	70.2	66.3	61.9	42.4		mean	2.9	3.3	2.8	2.5	1.2
	SD	0.33	0.52	3.28	1.49	2.90	SD	0.07	0.18	0.63	0.14	0.08	
	3SD	0.98	1.56	9.85	4.47	8.71	3SD	0.20	0.54	1.90	0.41	0.23	
PA/V30-N	1	73.9	73.8	72.1	71.9	70.5	PA/V30-N	1	2.5	2.3	2.4	2.6	2.2
	2	73.6	75.7	72.5	69.0	70.3		2	2.5	2.5	2.0	2.6	1.9
	3	72.9	73.0	73.4	70.9	68.4		3	2.3	2.1	2.4	2.2	2.1
	4	71.6	75.9	73.4	69.9	69.5		4	2.1	2.5	2.4	2.4	2.0
	5	72.5	74.8	69.2	72.2	71.1		5	2.3	2.5	2.0	2.6	2.2
	mean	72.9	74.6	72.1	70.8	70.0		mean	2.4	2.4	2.3	2.5	2.1
	SD	0.91	1.24	1.73	1.34	1.04	SD	0.17	0.16	0.24	0.20	0.14	
	3SD	2.74	3.71	5.18	4.03	3.13	3SD	0.52	0.48	0.72	0.60	0.42	
PA/V30-S	1	77.1	76.6	78.9	73.3	68.5	PA/V30-S	1	2.8	2.6	2.8	2.4	1.3
	2	77.0	79.8	79.0	72.7	67.9		2	2.6	2.9	3.0	2.3	1.7
	3	76.8	78.0	78.1	73.0	62.0		3	2.6	2.6	2.7	2.3	1.4
	4	76.5	78.9	78.3	75.1	68.1		4	2.5	2.8	3.1	2.9	1.7
	5	77.0	79.7	78.2	73.6	63.5		5	2.8	3.0	2.2	2.5	1.7
	mean	76.9	78.6	78.5	73.5	66.0		mean	2.7	2.8	2.8	2.5	1.6
	SD	0.24	1.33	0.42	0.93	3.02	SD	0.10	0.20	0.38	0.26	0.22	
	3SD	0.72	4.00	1.25	2.80	9.06	3SD	0.31	0.59	1.13	0.79	0.66	
PA/T30	1	78.4	72.9	76.3	75.8	73.8	PA/T30	1	1.9	1.5	2.7	2.8	2.6
	2	79.0	77.9	77.0	73.7	74.1		2	2.1	2.2	2.1	2.6	2.5
	3	77.8	78.2	77.1	73.7	74.5		3	1.8	2.3	2.2	2.8	2.4
	4	77.6	78.0	75.3	74.6	72.7		4	1.8	2.4	2.3	2.3	2.7
	5	77.8	77.6	72.1	76.0	72.5		5	1.9	2.2	1.6	2.7	2.5
	mean	78.1	76.9	75.6	74.8	73.5		mean	1.9	2.1	2.2	2.6	2.5
	SD	0.58	2.26	2.06	1.11	0.88	SD	0.10	0.35	0.41	0.22	0.09	
	3SD	1.73	6.77	6.19	3.32	2.64	3SD	0.31	1.06	1.23	0.66	0.28	
PA/V15-S/GF15	1	82.2	83.3	84.4	76.8	74.5	PA/V15-S/GF15	1	3.0	2.8	2.9	2.0	1.8
	2	81.9	83.0	82.2	78.7	80.4		2	2.8	2.8	2.6	3.0	1.9
	3	82.6	83.8	83.9	81.7	80.4		3	3.1	2.9	2.8	2.9	1.7
	4	82.0	84.1	84.3	83.2	77.1		4	3.1	2.7	2.8	2.2	2.4
	5	81.9	83.6	84.7	78.8	80.6		5	2.7	2.6	2.9	2.8	2.0
	mean	82.1	83.6	83.9	79.8	78.6		mean	2.9	2.8	2.8	2.6	2.0
	SD	0.29	0.43	0.99	2.57	2.72	SD	0.18	0.11	0.13	0.43	0.26	
	3SD	0.88	1.28	2.98	7.70	8.15	3SD	0.54	0.32	0.38	1.28	0.77	
PA/GF15	1	124.7	126.0	123.0	117.2	113.7	PA/GF15	1	2.7	2.8	2.7	2.9	2.6
	2	128.1	125.0	125.2	116.7	111.0		2	2.9	2.7	2.9	2.6	2.4
	3	126.3	125.9	126.3	115.9	110.8		3	2.7	2.9	2.9	2.6	2.5
	4	125.8	125.1	119.7	113.9	106.8		4	2.8	2.7	2.5	2.4	2.3
	5	123.5	125.7	122.9	115.2	115.9		5	2.7	2.9	2.7	2.9	1.9
	mean	125.7	125.5	123.4	115.8	111.6		mean	2.8	2.8	2.8	2.7	2.4
	SD	1.73	0.46	2.54	1.30	3.43	SD	0.09	0.11	0.17	0.21	0.27	
	3SD	5.19	1.39	7.61	3.90	10.28	3SD	0.27	0.33	0.52	0.64	0.80	
PA/GF30	1	180.4	178.3	176.8	174.4	173.1	PA/GF30	1	3.4	3.6	3.4	3.4	3.0
	2	180.3	177.3	175.8	173.4	171.0		2	3.9	3.9	3.6	3.5	2.6
	3	178.9	178.1	177.2	173.7	171.8		3	3.6	3.8	3.5	3.3	2.7
	4	181.0	179.4	177.3	174.7	171.7		4	3.6	3.4	3.6	3.3	2.8
	5	179.9	177.4	177.2	174.2	171.0		5	3.3	3.4	3.7	3.5	2.8
	mean	180.1	178.1	176.9	174.1	171.7		mean	3.6	3.6	3.6	3.4	2.8
	SD	0.78	0.85	0.62	0.53	0.86	SD	0.22	0.24	0.12	0.12	0.17	
	3SD	2.33	2.54	1.87	1.58	2.58	3SD	0.65	0.72	0.36	0.37	0.50	

Table C-2 Tensile modulus of composites

Sample	No.	Tensile Modulus (GPa) in each exposed time in hour				
		0	100	250	500	1000
PA	1	2.7	2.8	2.7	2.6	2.4
	2	2.7	2.6	3.2	2.8	2.5
	3	2.6	2.6	2.5	2.8	2.5
	4	2.6	2.7	2.7	2.8	2.6
	5	2.6	2.7	2.8	2.9	2.3
	mean	2.7	2.7	2.8	2.8	2.5
	SD	0.08	0.09	0.27	0.09	0.09
	3SD	0.25	0.26	0.80	0.26	0.28
PA/V15-N	1	3.6	3.8	3.6	4.1	3.7
	2	3.6	3.8	3.8	3.6	2.5
	3	3.7	3.7	3.7	3.7	3.5
	4	3.6	3.8	3.6	3.7	3.3
	5	3.6	3.8	3.6	3.6	3.5
	mean	3.6	3.8	3.7	3.7	3.3
	SD	0.03	0.06	0.08	0.19	0.45
	3SD	0.10	0.18	0.25	0.58	1.35
PA/V15-S	1	3.7	3.5	3.6	3.5	3.7
	2	3.7	3.7	3.5	3.4	3.6
	3	3.7	3.6	3.7	3.3	3.6
	4	3.7	3.9	3.5	3.5	3.6
	5	3.7	3.7	3.5	3.5	3.8
	mean	3.7	3.7	3.6	3.5	3.6
	SD	0.02	0.17	0.12	0.07	0.11
	3SD	0.06	0.52	0.35	0.21	0.34
PA/V30-N	1	4.6	4.8	4.6	5.2	4.2
	2	4.5	4.9	5.3	4.6	4.4
	3	4.7	4.7	4.6	4.9	4.5
	4	4.7	4.8	4.5	4.6	4.4
	5	4.7	4.5	4.7	4.7	4.7
	mean	4.7	4.8	4.7	4.8	4.4
	SD	0.09	0.13	0.30	0.25	0.15
	3SD	0.26	0.40	0.91	0.76	0.46
PA/V30-S	1	4.7	4.8	4.7	4.6	4.6
	2	4.7	4.9	4.5	4.6	3.9
	3	4.6	4.9	4.4	4.5	4.5
	4	4.9	4.9	4.8	4.3	3.8
	5	4.7	4.8	5.1	4.2	4.5
	mean	4.7	4.9	4.7	4.4	4.3
	SD	0.09	0.06	0.26	0.19	0.38
	3SD	0.28	0.18	0.79	0.56	1.13
PA/T30	1	8.5	9.3	8.7	8.6	8.4
	2	8.5	8.7	9.8	8.3	8.4
	3	8.7	8.8	8.6	8.6	8.4
	4	8.4	8.8	8.6	8.7	8.7
	5	8.5	8.8	8.3	8.8	8.4
	mean	8.5	8.9	8.8	8.6	8.5
	SD	0.11	0.23	0.57	0.15	0.16
	3SD	0.33	0.69	1.71	0.46	0.49
PA/V15-S/GF15	1	5.5	5.3	5.4	5.3	5.2
	2	5.4	5.4	5.4	5.3	5.3
	3	5.3	5.3	5.3	5.1	4.9
	4	5.3	5.5	5.2	5.2	5.2
	5	5.4	5.5	5.4	5.2	5.5
	mean	5.4	5.4	5.3	5.2	5.2
	SD	0.06	0.09	0.10	0.08	0.24
	3SD	0.17	0.26	0.31	0.24	0.71
PA/GF15	1	6.1	6.1	6.0	5.7	5.2
	2	6.2	6.1	6.0	5.8	5.7
	3	6.4	6.0	6.1	5.9	5.5
	4	6.2	6.1	6.0	5.9	6.0
	5	6.0	6.0	6.0	5.8	6.5
	mean	6.2	6.0	6.0	5.8	5.8
	SD	0.13	0.06	0.04	0.08	0.50
	3SD	0.40	0.17	0.12	0.25	1.50
PA/GF30	1	9.8	9.7	9.9	9.8	9.9
	2	9.5	9.8	9.7	9.9	8.5
	3	9.8	9.7	9.8	9.9	9.5
	4	9.6	9.9	9.6	9.7	9.0
	5	10.0	9.7	9.5	9.5	8.1
	mean	9.7	9.8	9.7	9.8	9.0
	SD	0.18	0.10	0.16	0.16	0.73
	3SD	0.54	0.29	0.47	0.48	2.18

Table C-3 Flexural properties of composites

Sample	No.	Flexural Strength (MPa) in each exposed time in hour				
		0	100	250	500	1000
PA	1	104.3	99.3	43.8	37.0	39.6
	2	102.4	98.9	42.5	44.4	36.7
	3	102.9	101.2	44.3	39.2	35.1
	4	103.3	100.0	44.3	39.4	32.0
	5	101.9	-	44.2	42.5	32.8
	mean	103.0	99.9	43.8	40.5	35.2
	SD	0.92	1.01	0.77	2.93	3.07
	3SD	2.75	3.02	2.30	8.79	9.20
PA/V15-N	1	106.3	107.4	104.1	104.5	78.6
	2	107.3	106.4	107.6	92.0	77.2
	3	107.4	108.2	106.2	100.5	84.5
	4	106.5	108.0	106.0	106.5	-
	5	106.8	104.9	106.6	105.9	-
	mean	106.9	107.0	106.1	101.9	80.1
	SD	0.48	1.36	1.28	6.00	3.87
	3SD	1.45	4.07	3.83	17.99	11.62
PA/V15-S	1	106.3	100.1	102.8	105.7	-
	2	105.9	100.2	104.2	104.7	-
	3	105.5	123.3	104.6	105.9	112.3
	4	106.4	100.0	103.1	105.3	112.6
	5	105.4	97.3	105.8	106.5	111.8
	mean	105.9	104.2	104.1	105.6	112.2
	SD	0.45	10.76	1.21	0.67	0.40
	3SD	1.36	32.27	3.62	2.02	1.21
PA/V30-N	1	113.3	114.1	114.4	112.4	108.7
	2	114.7	115.0	114.2	110.0	107.3
	3	113.2	116.9	113.6	111.8	106.0
	4	113.9	113.6	113.8	112.6	109.4
	5	114.9	110.2	110.2	115.0	107.9
	mean	114.0	114.0	113.2	112.4	107.9
	SD	0.78	2.45	1.73	1.80	1.31
	3SD	2.34	7.35	5.19	5.39	3.93
PA/V30-S	1	119.6	118.7	118.3	117.6	108.7
	2	119.6	118.5	114.4	118.8	115.6
	3	116.5	119.8	116.5	117.2	115.3
	4	119.1	118.9	117.3	116.7	118.8
	5	118.0	116.7	116.6	119.7	114.9
	mean	118.6	118.5	116.6	118.0	114.7
	SD	1.32	1.13	1.43	1.23	3.67
	3SD	3.97	3.40	4.30	3.68	11.02
PA/T30	1	122.8	120.6	122.6	120.0	119.1
	2	123.7	122.1	120.0	117.7	120.7
	3	123.0	122.2	119.0	120.6	116.7
	4	124.0	122.3	120.5	119.6	117.3
	5	123.1	121.4	121.8	118.4	115.6
	mean	123.3	121.7	120.8	119.3	117.9
	SD	0.51	0.72	1.43	1.19	2.02
	3SD	1.52	2.16	4.30	3.56	6.07
PA/V15-S/GF15	1	134.0	131.4	126.3	130.6	126.8
	2	131.5	132.4	128.1	128.2	128.4
	3	135.2	130.9	125.0	125.4	123.8
	4	131.0	130.6	128.7	130.4	129.1
	5	128.4	-	129.6	121.9	127.7
	mean	132.0	131.3	127.5	127.3	127.2
	SD	2.67	0.68	1.86	3.68	2.06
	3SD	8.00	2.05	5.59	11.03	6.19
PA/GF15	1	201.6	199.5	175.8	156.1	148.5
	2	201.3	200.4	169.9	148.8	146.7
	3	199.2	201.0	172.9	148.3	-
	4	205.2	201.8	180.1	157.3	156.7
	5	197.5	201.9	175.1	145.6	151.2
	mean	201.0	200.9	174.8	151.2	150.8
	SD	2.90	1.00	3.77	5.17	4.36
	3SD	8.69	3.01	11.30	15.50	13.08
PA/GF30	1	274.2	271.7	265.7	264.6	248.7
	2	274.1	274.8	261.9	262.4	244.2
	3	273.1	273.5	262.4	268.4	247.7
	4	275.0	273.4	266.2	266.0	249.9
	5	276.3	272.0	267.2	260.0	248.3
	mean	274.5	273.1	264.7	264.3	247.8
	SD	1.19	1.26	2.38	3.24	2.15
	3SD	3.58	3.77	7.14	9.71	6.44

Sample	No.	Flexural Modulus (GPa) in each exposed time in hour				
		0	100	250	500	1000
PA	1	2.5	2.4	2.4	2.5	1.9
	2	2.3	2.4	2.5	2.5	1.9
	3	2.4	2.4	2.5	2.5	1.9
	4	2.4	2.4	2.4	2.5	2.0
	5	2.4	2.4	2.4	2.5	1.9
	mean	2.4	2.4	2.4	2.5	1.9
	SD	0.04	0.01	0.06	0.02	0.03
	3SD	0.13	0.02	0.18	0.07	0.09
PA/V15-N	1	3.0	3.4	3.1	3.2	3.0
	2	3.1	3.3	3.2	3.2	3.0
	3	3.1	3.3	3.1	3.2	3.0
	4	3.0	3.3	3.2	3.2	3.0
	5	3.0	3.4	3.1	3.2	3.0
	mean	3.1	3.3	3.2	3.2	3.0
	SD	0.03	0.03	0.04	0.03	0.02
	3SD	0.10	0.10	0.13	0.10	0.05
PA/V15-S	1	3.0	3.3	3.1	3.2	3.1
	2	3.0	3.2	3.2	3.3	3.0
	3	3.0	4.6	3.2	3.2	3.1
	4	3.0	3.4	3.2	3.2	3.1
	5	3.0	3.2	3.2	3.2	3.0
	mean	3.0	3.6	3.2	3.2	3.1
	SD	0.03	0.61	0.03	0.02	0.06
	3SD	0.08	1.82	0.09	0.06	0.18
PA/V30-N	1	4.0	4.2	4.1	4.1	3.9
	2	4.1	4.2	4.1	4.2	3.8
	3	4.0	4.2	4.1	4.1	3.8
	4	4.1	4.2	4.1	4.1	3.8
	5	4.0	4.1	4.1	4.1	3.8
	mean	4.0	4.2	4.1	4.1	3.8
	SD	0.05	0.03	0.03	0.05	0.04
	3SD	0.15	0.09	0.08	0.15	0.11
PA/V30-S	1	4.0	4.1	4.0	4.1	3.8
	2	4.0	4.2	4.1	4.1	3.8
	3	4.0	4.0	4.1	4.0	3.8
	4	4.0	4.0	4.2	4.1	3.8
	5	4.0	4.1	4.1	4.2	3.8
	mean	4.0	4.1	4.1	4.1	3.8
	SD	0.03	0.07	0.05	0.04	0.03
	3SD	0.09	0.22	0.14	0.13	0.08
PA/T30	1	7.7	7.6	7.8	7.9	7.7
	2	7.6	7.8	7.8	7.9	7.7
	3	7.7	7.7	7.7	7.9	7.8
	4	7.7	7.6	7.8	7.8	7.8
	5	7.6	7.7	7.6	7.8	7.7
	mean	7.7	7.7	7.7	7.8	7.7
	SD	0.04	0.07	0.09	0.06	0.07
	3SD	0.13	0.20	0.26	0.17	0.21
PA/V15-S/GF15	1	4.7	4.6	4.6	4.7	4.4
	2	4.7	4.6	4.6	4.7	4.5
	3	4.7	4.6	4.7	4.6	4.5
	4	4.7	4.6	4.6	4.7	4.4
	5	4.7	4.7	4.7	4.6	4.4
	mean	4.7	4.6	4.6	4.7	4.4
	SD	0.03	0.04	0.04	0.06	0.07
	3SD	0.09	0.13	0.11	0.19	0.20
PA/GF15	1	5.2	5.4	5.3	5.4	4.8
	2	5.3	5.3	5.4	5.3	4.9
	3	5.2	5.4	5.4	5.3	4.9
	4	5.4	5.4	5.4	5.2	4.9
	5	5.4	5.5	5.3	5.3	5.0
	mean	5.3	5.4	5.3	5.3	4.9
	SD	0.11	0.04	0.02	0.06	0.08
	3SD	0.33	0.13	0.07	0.17	0.23
PA/GF30	1	8.4	8.2	8.5	8.3	8.1
	2	8.3	8.3	8.1	8.3	8.1
	3	8.3	8.1	8.5	8.4	8.1
	4	8.2	8.2	8.6	8.3	8.1
	5	8.4	8.4	8.5	8.2	7.9
	mean	8.3	8.3	8.4	8.3	8.1
	SD	0.05	0.10	0.17	0.06	0.09
	3SD	0.16	0.30	0.52	0.17	0.26

Table C-4 Charpy Impact Strength of composites

Sample	No.	Charpy Impact Strength (kJ m^{-2}) in each exposed time in hour				
		0	100	250	500	1000
PA	1	5.7	1.3	1.3	1.4	1.4
	2	5.3	1.3	1.3	1.4	1.3
	3	5.3	1.3	1.6	1.3	1.4
	4	5.8	1.3	1.5	1.2	1.3
	5	5.8	1.4	1.4	1.3	1.3
	mean	5.6	1.3	1.4	1.3	1.3
	SD	0.26	0.03	0.12	0.09	0.02
PA/V15-N	3SD	0.78	0.08	0.36	0.26	0.07
	1	2.8	1.7	1.6	1.3	1.4
	2	2.5	1.5	1.3	1.3	1.5
	3	2.8	1.7	1.6	1.3	1.4
	4	2.7	1.7	1.2	1.3	1.3
	5	2.9	1.7	1.4	1.3	1.3
	mean	2.7	1.6	1.4	1.3	1.4
PA/V15-S	SD	0.13	0.08	0.18	0.03	0.08
	3SD	0.39	0.25	0.53	0.10	0.25
	1	2.9	1.4	1.3	1.4	1.2
	2	2.8	1.4	1.3	1.3	1.3
	3	2.9	1.3	1.1	1.3	1.4
	4	2.9	1.3	1.4	1.3	1.2
	5	2.8	1.3	1.4	1.3	1.2
PA/V30-N	mean	2.8	1.3	1.3	1.3	1.3
	SD	0.04	0.05	0.10	0.02	0.08
	3SD	0.12	0.14	0.30	0.05	0.23
	1	2.9	2.4	2.4	2.5	2.3
	2	3.0	2.5	2.5	2.7	2.5
	3	2.9	2.5	2.3	2.5	2.2
	4	2.9	2.9	2.6	2.6	2.5
PA/V30-S	5	3.0	2.5	2.7	2.4	2.5
	mean	2.9	2.6	2.5	2.5	2.4
	SD	0.04	0.21	0.17	0.11	0.14
	3SD	0.13	0.62	0.50	0.33	0.42
	1	2.9	2.3	2.9	2.4	2.5
	2	3.0	2.3	2.3	2.4	2.5
	3	3.0	2.4	2.2	2.5	2.2
PA/T30	4	3.0	2.4	2.3	2.4	2.4
	5	3.0	2.3	2.2	2.5	2.4
	mean	3.0	2.3	2.4	2.4	2.4
	SD	0.03	0.05	0.27	0.06	0.12
	3SD	0.08	0.14	0.81	0.19	0.36
	1	2.0	1.9	1.8	1.6	1.5
	2	2.2	2.1	2.1	1.6	1.5
PA/V15-S/GF15	3	2.1	2.2	2.2	1.6	1.6
	4	1.9	1.9	1.9	1.7	1.5
	5	2.1	2.1	1.8	1.7	1.6
	mean	2.1	2.0	1.9	1.6	1.6
	SD	0.09	0.13	0.19	0.05	0.03
	3SD	0.28	0.40	0.56	0.15	0.09
	1	3.2	3.2	2.9	3.1	3.1
PA/GF15	2	3.3	3.2	3.3	3.1	3.0
	3	3.3	3.1	3.2	3.2	3.1
	4	3.3	3.1	3.0	3.1	3.1
	5	3.4	3.2	3.1	3.1	3.2
	mean	3.3	3.2	3.1	3.1	3.1
	SD	0.04	0.06	0.16	0.03	0.05
	3SD	0.13	0.18	0.47	0.09	0.16
PA/GF30	1	7.8	7.7	7.2	7.0	7.1
	2	7.8	7.6	7.6	6.9	7.0
	3	7.8	7.7	7.3	7.7	7.1
	4	6.9	7.4	7.1	7.7	7.2
	5	7.5	7.3	7.5	7.3	6.9
	mean	7.5	7.5	7.3	7.3	7.1
	SD	0.40	0.19	0.19	0.36	0.11
PA/GF30	3SD	1.20	0.58	0.58	1.07	0.34
	1	15.4	14.0	13.6	14.1	15.0
	2	14.5	14.3	15.1	14.7	14.1
	3	14.7	14.9	14.4	14.3	14.1
	4	15.8	14.0	14.6	14.3	15.0
	5	14.3	15.7	14.6	14.4	13.3
	mean	14.9	14.6	14.5	14.3	14.3
SD	0.67	0.71	0.54	0.21	0.70	
3SD	2.00	2.13	1.61	0.64	2.11	

VITA

Mrs. Khanitthakanya Munkid was born on November 19, 1974 at Muang Chiangmai District, Chiangmai Province. She received her Bachelor's Degree of Science (Industrial Chemistry) in Industrial Chemistry Department at the Faculty of Science, Chiangmai University in 1996. She began her master study in polymer science, Program of Petrochemistry and Polymer Science, Faculty of Science, Chulalongkorn University in November 2009 and completed the program in May 2011.

Presentation: "Accelerated weathering effects on mechanical properties and morphology of Vetiver grass fiber/polyamide-6 composites" proceedings of PACCON 2011, Bangkok, Thailand, January 5 - 7, 2011.



ศูนย์วิทยทรัพยากร
จุฬาลงกรณ์มหาวิทยาลัย